MAPPING CROP FIELD PROBABILITIES USING HYPER TEMPORAL AND MULTI SPATIAL REMOTE SENSING IN A FRAGMENTED LANDSCAPE OF ETHIOPIA
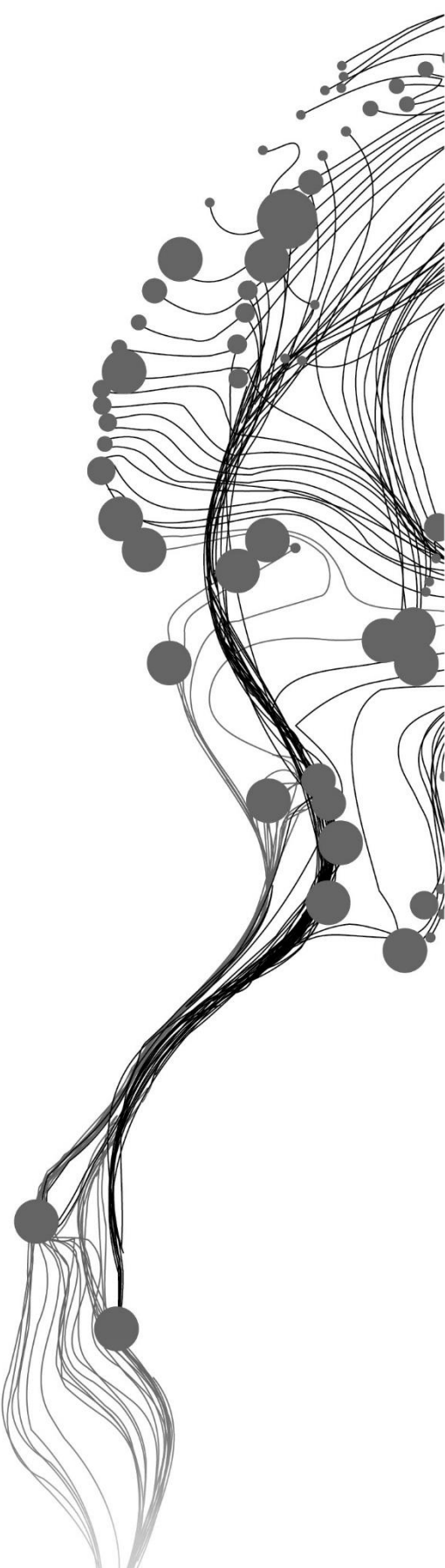
ISSAMALDIN MOHAMMED ALSHIEKH MOHAMMED
February, 2019

SUPERVISORS:
Dr. M.T. Marshall
Dr. C.A.J.M. de Bie

MAPPING CROP FIELD PROBABILITIES USING HYPER TEMPORAL AND MULTI SPATIAL REMOTE SENSING IN A FRAGMENTED LANDSCAPE OF ETHIOPIA

ISSAMALDIN MOHAMMED ALSHIEKH MOHAMMED
Enschede, The Netherlands, February, 2019

Thesis submitted to the Faculty of Geo-Information Science and Earth Observation of the University of Twente in partial fulfilment of the requirements for the degree of Master of Science in Geo-information Science and Earth Observation.
Specialization: Natural Resources Management

SUPERVISORS:
Dr. M.T. Marshall
Dr. C.A.J.M. de Bie

THESIS ASSESSMENT BOARD:
Prof. Dr. A. D. Nelson
Dr. Lyndon Estes (External Examiner, Clark University)

ABSTRACT

Crop production is crucial information for food security analysis. Crop production is defined as a product of crop area (CA) and yield. Therefore, crop area should be estimated accurately to obtain reliable crop production information. Agricultural census contains accurate information about CA but it is costly, and it lacks appropriate temporal and spatial information for reliable frequent crop area estimate. Hyper-temporal remote sensing can capture the general agro-climatic conditions but it is too coarse spatially to capture variability in CA over fragmented landscapes. High-resolution remote sensing can capture the variability of CA but it can not capture the climatic conditions due to its low temporal resolution and subsequently fewer images may be available (i.e. because of persistent cloud cover during crop growing seasons). SPOT-VGT NDVI series (1999-2017) was used to identify agro-ecological zones through ISO-DATA unsupervised classification. Then these zones were integrated with reported crop area statistics through stepwise linear regression to produce coarse field fractions (1km-resolution). Landsat-8 images (2013-2017) were used to extract moderate resolution (30m) long-term average dry and wet seasons NDVI per each agroecological zone. Dry and wet seasons NDVI, elevation, slope, and 1km field fractions were incorporated in a generalised additive model (GAM). Through the Google Earth platform, 271 frames (30mx30m) were visually interpreted to estimate field fractions of these frames for model calibration and validation. The overall deviance explained by the model was 62%. The 1km field fraction was found to be the most important predictor in our model as it explained 24% of the deviance. As many researchers focus on wet season NDVI, our results showed that the dry season NDVI was the second important predictor and explained 16% of model deviance. Elevation added more explanatory power to the model (i.e. explained 15% of the deviance). The field fractions predictions (30m-resolution) produced by our final global model explained 77% of the variation in 81 actual fractions observations. To demonstrate the capabilities of the developed global GAM (i.e. over whole Oromia region), a localised GAM was developed within one agroecological zone and then the global GAM and local GAM were evaluated with an independent test set. The global model performed closely to the local model. These results supports that hyper-temporal remote sensing can be effective in addressing the climatological differences regarding CA estimation. The method can be applied by governments and researchers for further studies and to aid in decision making regarding cropping and food security policies. Future work should consider involving additional predictors to the GAM such as: socio-economic variables, other vegetation indices, and radar images.

ACKNOWLEDGEMENTS

To my first advisor Dr. Michael Marshall, I am really thankful for all what he did and what he offered during this research. Thanks to him for being a mentor and a supervisor. All the way in this research he was advising and motivating me to overcome my weaknesses. His suggestions were always helpful and really opened my eyes to many things even beyond the topic of this research.

To my second advisor Dr. Kees de Bie, for his guidance and valuable inputs in this research. I have learned a lot from such an expert in the field and I found a chance to broaden my thinking.

To the staff of the Natural Resources department, learning is an evolving process and their contribution to building my knowledge since I started studying at ITC helped me to conduct this research.

To my colleagues at ITC, I appreciate all the discussions that we had since our first days at ITC, all that helped in improving my both academic and personal skills.

To my family and my friends, Thanks to them for the kind support. Their support allowed me to finish this journey smoothly and ending it with this research.

TABLE OF CONTENTS

LIST OF FIGURES

LIST OF TABLES

1. INTRODUCTION

1.1. Background and motivation

Food security is one of the major concerns in the future due to global population growth and climate change (Misra, 2014). Agriculture is a main source of food and income particularly in Ethiopia. The contribution of agriculture to the gross domestic product (GDP) in Ethiopia was 37.23% in 2016 (The World Bank, 2018). Agriculture is considered as the largest economic sector in Ethiopia, where approximately 12 million smallholder farming households represent 95% of the agricultural production and 85% of the employment (FAO, 2018).

The policy makers in Ethiopia need to formulate policies and take decisions to secure food and reduce poverty levels. Reliable production estimations help in the determination of the food deficit over a certain area and thus guide further steps to analyse the causes and to develop effective responses (Li, Liang, Wang, & Qin, 2007).

The definition of cropland in this study follows the definition of arable land by FAO (2011). It represents land under temporary crops, meadows, and land temporarily fallow (less than five years). Crop production for a given field or another geographic unit is defined as the product of the crop area (CA) and crop yield (Husak et al., 2008; See et al., 2015). Crop area (i.e. harvested area) is therefore an essential input to food security analysis (Debats, Luo, Estes, Fuchs, & Caylor, 2016; See et al., 2015) in addition to early warning systems for instance FAO Global Information and Early Warning System (GIEWS) (FAO, 2018).

In Ethiopia, the agricultural fields are small and heterogeneous and moreover the landscape characterised to be complex, fragmented (Eggen, Ozdogan, Zaitchik, & Simane, 2016). Therefore, innovative technologies are required for locating and mapping the fields (Jin, Azzari, Burke, Aston, & Lobell, 2017). Due to the inadequate agricultural statistics and reports; accurate and timely information is essential for agricultural field mapping (Carletto, Jolliffe, & Raka, 2013; Li et al., 2007).

The traditional methods for CA estimation that governments rely on include census through ground surveys. Although the census data has its importance as a source of information for CA estimation and food security analysis (Frolking et al., 2002), but it is too generalized (i.e. administrative level) and due to the cost and labour-intensive requirements; census takes place every five or ten years which makes it an inefficient method. The World Bank (2011) reported that developing countries face challenges to collect and report agricultural statistics that are sufficient for agricultural monitoring. They mentioned among other reasons: financial limits, lack of labour and inadequate statistical methodologies. To lower the cost of exhaustive field surveys, the area frame sampling (AFS) method was applied. In AFS, samples of information about agricultural fields collected on different scales; those samples can be collected through field surveys, farmers interviews, very high-resolution imagery and aerial photographs and then generalised over the required area (Husak & Grace, 2016). All the sources of information in the AFS method shared common challenges; they are very also costly, time-consuming and labour-intensive. Moreover, in most of the cases, the samples are too few to be generalised over large areas (Marshall et al., 2011).

Given the mentioned challenges regarding traditional methods, remote sensing has proven to be effective for land cover mapping generally and agricultural mapping particularly. Remote sensing provides large coverage, spatially detailed and continuous information on surface conditions through time. The 'large coverage' minimises the cost efficiently compared to other traditional methods, the 'spatially detailed' information allows for critical spatial analysis for CA, and finally the 'continuous information' facilitate studying the dynamics of the landscape and related factors. Remote sensing is needed most in the developing countries with limited financial resources because it is very difficult to develop a regional or national

monitoring program for agricultural studies since such programs require wide geographic coverage and repetitive information (Wardlow, Egbert, & Kastens, 2007). Remote sensing has been integrated with agricultural statistics for CA estimation in several ways. Remote sensing images have been used for designing sampling schemes for field surveys (Carfagna & Gallego, 2005). Some researchers integrated remote sensing data with agricultural statistics through regression models to estimate spatially explicit CA at coarse resolution (de Bie et al., 2008; Khan et al., 2010).

Many image classification methods have been used to detect the agricultural fields boundaries and CA estimating using satellite images (for an overview on methods see Ozdogan, Yang, Allez, & Cervantes, 2010; Xie, Sha, & Yu, 2008). Examples include: sub-pixel approaches (Verbeiren, Eerens, Piccard, Bauwens, & Van Orshoven, 2008), maximum likelihood technique (Martinez-Beltran & Calera-Belmonte, 2001), K-nearest neighbour classifier (Seetha, Sunitha, & Devi, 2012), fuzzy classification (Murmu & Biswas, 2015), and machine learning methods such as support vector machines (Kuwata & Shibasaki, 2015). Most of the image classification methods utilise only the spectral information of the satellite images. However, ancillary and spatial information (i.e. contextual information) have been used in many studies to improve the accuracy of the crop fields delineation and CA estimation as well (Ruiz, Recio, Fernández-Sarría, & Hermosilla, 2011). The CA estimation of small and heterogeneous fields using remote sensing represents a challenge. The coarse resolution satellite images are available more frequently and over long time periods which allow characterising the long-term trends of climate and landscapes (i.e. agroecological zones) (Tumlisan, 2017; Vintrou et al., 2012). However, the coarse resolution suffers from the mix pixel effect (i.e. different land cover types within a pixel) (Foody, 2000). In contrast, high-resolution images allow to detect the heterogeneity of the landscapes, but this kind of data have less frequent (i.e. longer revisit time) and available over short time frames. In other words, hyper-temporal (i.e. coarse resolution) remote sensing brings the time dimension. Whereas high-resolution remote sensing usually available in a single date or few multi-date images. There is no generally accepted definition for coarse, moderate, and fine resolution, however, for this research purposes coarse resolution is defined as greater than 250m, moderate as 30m and fine resolution as less than 5m.

The accurate estimation of locations and areas of agricultural fields depends on understanding the factors that affect the spatio-temporal distribution of the fields. The main environmental factors that influence the distribution of agricultural fields include terrain and soil properties (Marshall et al., 2011) in addition to climate (Iizumi & Ramankutty, 2015). According to FAO (1978), agroecological zones are geographic units with similar climatic and soil conditions. In large scale CA estimation, the area under study probably consists of different agroecological zones particularly in heterogeneous landscapes in Africa (Hentze, Thonfeld, & Menz, 2016; Vintrou et al., 2012).

In such kind of landscape, the relationships between biophysical variables and CA are complex. Therefore, many studies utilised statistical models and remote sensing to capture these complex relationships. Generalised additive models (GAMs) were used for CA estimation in fragmented landscapes (Grace, Husak, Harrison, Pedreros, & Michaelsen, 2012; Grace, Husak, & Bogle, 2014; Husak et al., 2008; Marshall et al., 2011). GAMs are practical for such relationships because the relationships in the model are data-driven and no prior distribution is assumed (Hastie, Tibshirani, Hastie, & Tibshirani, 2016).

From remote sensing perspective, estimating the probability of an area being cropped can be transformed into CA by handling the probabilities as crop field fractions and hence multiplying the fields extent fractions by the produced cell size (Marshall et al., 2011). In the context of this research, the terms 'fields extent fractions' and 'crop field probabilities' will be used interchangeably.

An improved method that uses a combination of low and medium spatial resolution imagery together with sourcing from reliable tabulated databases (e.g. census) can allow to utilise the advantages of both types of data and fill the data gaps. Hence, this study aimed at combining different Earth observation data with varying spatial and temporal resolution to estimate the fields extent fractions at moderate resolution (30m). Also, it used ancillary topographic and agricultural census data to furthe improve the estimation of fields

extent fractions. The method developed in this research integrates these multi-spatial and hyper-temporal datasets in a generalised additive model (GAM) for estimating field fractions for smallholder farms in a fragmented and complex landscape.

1.2.   Crop area and remote sensing methods

This subsection provides a brief overview of remote sensing techniques used for CA estimation. For each category of methods (e.g. manual methods, pixel-based, object-based), a brief description of the category in addition to common strengths and drawbacks is provided. Under these categories, the methods and popular algorithms are described in addition to examples of previous studies used these algorithms for CA. However, some of these studies inherited CA estimate within the context of land cover mapping.

1.2.1.   Manual methods

The manual method relies on defining crop area based on visual interpretation. These methods used to be applied in earlier stages of remote sensing. The methods under this category usually need high-resolution imagery to facilitate the process of visual interpretation. The common disadvantages of those methods that they are: costly, time-consuming, and biased.

1.2.1.1.   Pixel count:

In the pixel count method, the number of pixels classified as crop will be multiplied by the pixel size to obtain CA. This method requires high-resolution images to be applied since in coarse images the classification will be more difficult. In coarse images, the chance of getting mixed pixels is higher and therefore the classification accuracy will be lower. The major limitation of the pixel count method is that it is subject to the subjectivity of the analyst (Gallego, 2006). The analyst may tune the classification results to a desired number of pixels. The reliability of CA estimation using pixel count depends highly on the classification accuracy. The bias is approximately the difference between commission and omission errors (Carfagna & Gallego, 2005).

Singh et al. (1993) applied pixel count for Wheat acreage in India. The authors used 10x10km sample sites. The authors achieved an accuracy of 90% at 90% confidence level. However, the bias was probably underestimated and these results appeared better than what they actually were (Gallego, 2004).

Fang (1998) found that the spectral mixing issue lowered the accuracy of pixel count method and increased the bias. The author obtained higher accuracy for early planted rice (i.e. 90%) while the semi-late rice was mixed with residential areas and sparse forests. The accuracy dropped to 81% for semi-late rice.

1.2.1.2.   Area frame sampling:

Remote sensing with area frame sampling has been utilised at two stages: at the design stage and the estimation stage (Carfagna & Gallego, 2005). At the design level, remote sensing is used for stratifying the area into different agricultural strata (i.e. approximate agricultural percentage per stratum) through visual interpretation (Cotter & Tomczak, 1994) or existing land cover maps (Carfagna & Gallego, 2005). To elaborate, remote sensing can be used for multi-stage sampling. Stratification based on photo interpretation as a first stage and then concentrate the surveys in agricultural areas. Remote sensing may be used at the design level to define the optimum sample allocation through spatial autocorrelation determination (i.e. to collect spatially uncorrelated samples and reduce the cost) (Carfagna & Gallego, 2005; Gallego, Feunette, & Carfagna, 1999). At estimation level, after collecting the ground samples a statistical relationship is developed between the measurements from the sample and the full coverage of remotely sensed imagery (e.g. regression) (Alonso & Cuevas, 1993). However, the AFS method needs high spatial resolution data and ground surveys to collect those samples which increase the cost significantly.

Additionally, the efficiency of the method depends highly on the complexity of the landscape. The method is less effective in complex landscapes with mixed crops (Carfagna & Gallego, 2005). Whereas in

homogenous landscapes with large fields, the method can be considered efficient (Hanuschak, Hale, Craig, Mueller, & Hart, 2001).

Pradhan (2001) used SPOT-XS images in addition to existing land use data to stratify his study area to produce an effective sampling scheme for CA estimation. Then the author applied remote sensing as a regressor to produce the CA estimate. In spite of the highlighted advantages by the author for using remotely sensed data for sampling optimisation, the high cost of the field data collection remained.

Dong et al. (2017) utilised remote sensing for stratification to exclude non-agricultural areas and a classified image for regression. The study was conducted in a complex landscape in China. The authors achieved an efficiency factor of 2.5. This means the accuracy that they achieved from their 202 ground segments after using classified RapidEye images as a regressor to adjust for bias was equivalent to the accuracy that could be obtained using 505 ground segments. No doubt, area frame sampling aided by remote sensing is more efficient than ground surveys only, however, still high cost for samples collection remains.

1.2.1.3.   Screen digitisation:

This method relies on displaying remotely sensed images (sometimes with other auxiliary data such as soil maps) and interactively (i.e. manually) delineating the fields (Liu et al., 2005). This method should be applied by a good visual interpreter since its accuracy depends on visual interpretation.

Liu et al. (2005) applied on-screen digitisation for CA estimate in China. Their method was applying manual delineation of landcover classes based on visual interpretation of Landsat (TM and ETM). The authors utilised other data sources to aid in visual interpretation (e.g. Soil type, DEM, climate, Roads, rivers). They were able to achieve 94.9% accuracy for the cropland in classification using ground validation data. The authors subtracted the non-agricultural areas -identified using aerial photos- from the agricultural polygons delineated. However, the authors indicated that due to the mixed pixel effect, their CA was overestimated 27.5% compared to the CA after subtracting non-agricultural area within the delineated polygons.

Crowdsourcing is a new concept that evolved under screen digitising. In crowdsourcing, the information about crop area is collected by a network of volunteers (Minet et al., 2017). Many projects have been developed for agricultural land cover mapping through crowdsourcing such as: Collect Earth (Bey et al., 2016), Geo-Wiki (Fritz et al., 2012), DIYlandcover (Estes et al., 2016). In South Africa for example, Estes et al. (2016) showed that overall accuracy of 91% for cropland mapping was achieved through crowdsourcing. The main advantage of crowdsourcing that too many interpreters (i.e. volunteers) can be involved and subsequently large volume of agricultural land use data can be collected in short time (Minet et al., 2017).

See et al. (2013) used crowdsourcing for mapping cropland in Ethiopia. The authors asked users to provide a qualitative measure for agricultural abundance (i.e. none, low, medium, high) by interpreting Google Earth images through Geo-Wiki platform. The authors interpolated the collected crowdsourced data using inverse distance weighted method (IDW) to produce the cropland map for Ethiopia (1km-resolution). The authors used 493 validation points (i.e. crop/non-crop) from different sources (e.g. existing land cover maps, another independent crowdsourcing dataset) for accuracy assessment. The authors showed that the crowdsourced cropland map of Ethiopia had higher accuracy compared to some other existing global land cover datasets (i.e. GLC-2000 and GlobCover). The overall accuracy was 89.3%. However, the authors indicated errors might be due to the interpretation mistakes by the users and the sampling density (i.e. more samples needed for interpolation).

1.2.2.   Pixel-based classification

Pixel-based classification is utilising the spectral information of individual pixels of remote sensing images through classification procedures (Ozdogan et al., 2010). Basically, each pixel will be assigned to a class based on the spectral information of that pixel. The spatial context (i.e. surrounding pixels) is not considered in such methods. The common advantage of the methods under this category that they are easy to implement and more efficient compared to the manual methods. They also utilise the rich spectral

information of moderate resolution EO imagery. The most common methods for CA under this category are: unsupervised classification, supervised classification, fuzzy classification (Murmu & Biswas, 2015), and spectral mixture (Wang & Uchida, 2008). Traditional methods such as supervised and unsupervised classification assume that the individual pixels are homogenous (Smith & Fuller, 2001). Therefore, in complex and fragmented landscapes, these methods are not expected to perform well due to pixel heterogeneity (Murmu & Biswas, 2015; Tran, Julian, & De Beurs, 2014). Another complication for these methods that the pixels within a field parcel may exhibit differences in term of spectra (Forkuor, Conrad, Thiel, Ullmann, & Zoungrana, 2014). The fuzzy and spectral mixture relax the pixel homogeneity assumption. Those two methods were used to address the mixed pixel issue (Lobell & Asner, 2004; Musande, Kumar, & Kale, 2012). In these two methods, the fractions of different land cover types are determined based on training data. However, pixel-based methods suffer from an issue called 'salt' and 'pepper' effects (i.e. sparse pixels) (Belgiu & Csillik, 2018).

1.2.2.1. Unsupervised classification:

In unsupervised classification, statistical algorithms are used for partitioning the image into distinct clusters based on error function (Enderle & Weih, 2005). In this method, the user should determine the number of desired clusters and criteria for ending the aggregating of pixels into clusters (i.e. stop merging clusters). Then later the analyst will assign classes of land cover to the clusters. The advantage of unsupervised classification appears when no prior knowledge about the study area is available. In other words, in some cases the analyst may not be able to identify the different classes in the area. Thus, the software will identify automatically the possible classes in the area. For example, in fragmented landscapes with small farms it is difficult to identify classes due to the heterogeneity of the landscape. Unsupervised classification requires very little user interaction in the stage of clustering but it requires a lot of field work or visual interpretation in the stage of assigning labels to the clusters (Xiong, Thenkabail, Gumma, et al., 2017). The most common algorithms of unsupervised classification are: K-means and ISO DATA clustering.

In remote sensing applications, usually multisource data are integrated to fill the gaps in the data. Gumma et al. (2011) applied K-means unsupervised classification for rice area estimate in a fragmented landscape in Nepal. They clustered MODIS images (250m) using K-means and then the clusters were labelled using field data and visual interpretation of high-resolution images (through Google Earth platform). The authors used intensive field data to handle the mixed pixel effect and determine the field fractions. They indicated that to label the clusters, intensive field data and a large volume of high-resolution images are needed. However, the authors achieved an overall accuracy of 82% validated through ground truth data. The rice area derived in that study explained 99% of the variation in the reported national crop statistics.

In West Africa, Vintrou et al. (2012) used ISO-DATA clustering of MODIS NDVI series (250m-resolution) for crop area estimation. They produced 20 clusters and then crop/non-crop classes were assigned to the clusters through visual interpretation (using Landsat-ETM+) and field data. The field fractions that they produced were not quantitative. The authors assigned 1 and 0.5 as field fractions for pure and mixed pixels respectively. For validation, they classified SPOT images (2.5m) acquired in November 2007 to estimate the CA. In addition, they collected ground data in 2009 and 2010 at six validation sites to check the accuracy of the interpretation of SPOT images. They reported that their CA estimate assessed the overall CA in five sites out of six. The results showed that the MODIS product gave more accurate CA estimation than some global products such as: GLC2000 and GLOBCOVER land cover. The MODIS product resulted in less than 6% difference in CA compared to the reference data that they obtained from SPOT classification. However, they mentioned that their CA product doubled the reported CA by FAO. However, the authors indicated that the accuracy of CA estimate was affected by the complexity of the landscape (and the input coarse resolution).

A study by Shen et al. (2015) proposed using moderate resolution imagery to guide a stratified sampling by UAV for CA in China. They used unsupervised classification and visual interpretation over SPOT 5 image to determine the rice areas, then they developed a sampling frame based on the classified image to determine

the distribution of the transects of the UAV. They achieved an accuracy of 95% in CA estimation at 95% confidence interval when 2% of the population was sampled.

1.2.2.2. Supervised classification

Supervised classification is based on developing training samples either from field work or visual interpretation. In both cases, the process is time-consuming and costly (e.g. cost of high-resolution images). In this process, training data is used to extract the statistical measures of the samples and then assigning each pixel to a class using certain classifier such as: Maximum Likelihood, Minimum Distance, Mahalanobis, and kNN (Nearest Neighbour) (Richards, 2012).

Maximum likelihood (ML) method relies on assigning probabilities (i.e. probability of belonging to certain class) to the pixels based on a statistical model (i.e. variance and covariance calculations). The main problem with this method is that it assumes the probability density function for a class is normally distributed. In the real world, distributions are more complex (Choodarathnakara, Kumar, & Koliwad, 2012).

Supervised classification is difficult to be repeated over time (Zhong, Gong, & Biging, 2014) which limit its use for monitoring programs. In fragmented landscapes such as in Africa, supervised classification can lead to high uncertainty (Xiong, Thenkabail, Gumma, et al., 2017).

Kerdiles et al. (2014) used maximum likelihood classifier for estimating crop area in North China Plain. The authors used Spot-5 images to estimate CA for maize and soybean. Their product explained 62% of the variation in 83 ground segments. However, the authors indicated the cost of field surveys needed in such approaches is high.

Delrue et al. (2013) applied maximum likelihood classifier for crop mapping in central Ethiopia. The authors used Disaster Management Constellation (DMC) (32m-resolution) images and Landsat 7 (30m-resolution) for classification. They used ground surveys data and delineated segments through the Google Earth platform to train and validate the model. The authors achieved an overall accuracy of 49% and 37% using only Landsat 7 collection and using only DMC collection respectively. Merging the two collections the authors achieved 44% overall accuracy. The authors concluded that the small size of the farms and the complexity of the landscape represented a challenge to achieve satisfactory results. However, the authors in another experiment applied climatological zones stratification using ISO-DATA clustering to improve accuracy. They trained a neural network model (discussed below) per strata and they found that the accuracy ranged from 65% to 91% for the four strata that they produced. The authors concluded that the small size of farms remained a challenge to achieve good results over the whole study area.

Some studies utilise multitemporal information from remote sensing in addition to the multispectral information. Arvor et al. (2011) applied the maximum likelihood classifier over MODIS enhanced vegetation index (EVI) time series from 2005 to 2008. The authors achieved 85.5% accuracy for an agricultural mask that they developed in Amazonia in Brazil. They concluded that the vegetation index time series with maximum likelihood classifier showed high ability to determine cultivated areas. The authors showed that a post-classification process was needed to handle the 'salt' and 'pepper' effect resulted from using a pixel-based classifier.

With the evolution in computers technology, machine learning methods became more popular. Image machine learning is a branch of artificial intelligence, in which the heuristic and expert knowledge are used to train the computer to automatically extract the objects of interest (Yang & Li, 2012). The most common supervised machine learning algorithms are artificial neural network (ANN), support vector machines (SVM), decision trees (DT) and random forest (RF). These learning methods are non-parametric. Unlike parametric classifiers, such as maximum likelihood, non-parametric classifiers are data-driven and they overcome the issue of distribution assumptions (Rogan & Chen, 2004).

In ANN technique, the neural network learns from the training data set to extract the classification rules and then those rules will be applied over the whole input image (Civco, 1993; Mondal, Kundu, Chandniha, Shukla, & Mishra, 2012). ANN has many advantages in image classification. It can handle complex pattern relationships for rules extraction and it can handle noisy data (Mas & Flores, 2008). However, ANN can

suffer from overfitting with small size training set and moreover it is complicated and computationally intensive technique (Mas & Flores, 2008).

Kussul et al. (2015) used ANN for regional CA estimate in Ukraine. The authors used multitemporal Landsat 8 images (30m-resolution) from April to August 2013. The authors achieved an overall accuracy of 85% for classification. Then they compared their CA estimate to official statistics. Their results showed the error was ±28% compared to official statistics.

SVM algorithm builds a hyperplane that separates the dataset into a predefined number of classes utilising training data (Huang, Davis, & Townshend, 2002). The hyperplane represents the decision boundaries that produces the minimum misclassification over the training data (i.e. an iterative process) (Mountrakis, Im, & Ogole, 2011).

Lambert et al. (2016) applied SVM for cropland mapping over Sahelian and Sudanian agroecosystems. The authors used multispectral ProbaV (100m) time series of 11 months. The authors trained the model over four spectral bands and five temporal features. The temporal features that they used were maximum of the red band, minimum and maximum of NDVI and the decrease and increase of the slope of NDVI profile. They achieved an overall accuracy of 84% and F-score for cropland of 74%. Validation samples were developed using high-resolution images through the Google Earth platform. The authors concluded that the errors were due to data availability and the fragmented landscape.

Decision tree is an algorithm to classify image pixels through sequential decisions. Decision tree algorithm consists of a root node, intermediate nodes, and terminal nodes. Using training data, a decision is made at each intermediate node to determine the next step in the hierarchical process. Until the pixel reaches a terminal node and then it will be classified into certain class (Friedl & Brodley, 1997).

In India, Sharma et al. (2013) applied the decision tree method for land cover mapping including agricultural landscape. The authors used a single date image of Landsat TM (30m-resolution). For agricultural land, the authors achieved 96% producer's accuracy and 75% user's accuracy. However, the authors indicated that the method needs a large volume of ground data and finer spatial resolution to capture the variability at fine scales. In their study, DT was compared to ISO-DATA algorithm and maximum likelihood classifier. DT was found to be superior to those other traditional algorithms. The overall accuracy of DT classifier was 90% compared to 76.7% and 57.5% for maximum likelihood and ISO-DATA respectively.

Shao and Lunetta (2012) used MODIS NDVI series from 2000 to 2009 for land cover mapping (including agriculture) in North Carolina in the US. Although the landscape is homogenous compared to the landscape in Ethiopia, the authors showed that the purity of training pixels affected the classification accuracy significantly. The authors compared the accuracies of DT, SVM, and neural networks using pure pixels for training and using heterogeneous pixels (i.e. dominant cover >75% was assigned to the pixel). They found that the overall accuracy was 91%, 89%, and 85% for SVM, neural network, and DT. Whereas using heterogenous pixels, the accuracy dropped to 64%, 58%, and 55% for SVM, neural network, and DT. This indicates much more challenges if these methods applied in a complex and fragmented landscape.

Some methods are designed to group several weak learners to form a strong learner. Such methods are called ensemble methods. One of the most common ensemble methods is Random Forest. It is an ensemble learning method which can be used to solve both classification and regression problems although it has been used rarely for regression issues in the agronomical applications (Jeong et al., 2016). In the case of the RF, these weak learners are the individual decision trees. RF method has been proved that it works well in heterogeneous landscapes (Tatsumi, Yamashiki, Canales Torres, & Taipe, 2015). Random forests method is more common in crop classification and yield prediction more than crop area estimation (Crnojevic, Lugonja, Brkljac, & Brunet, 2014; Nitze, Schulthess, & Asche, 2012; Ok, Akar, & Gungor, 2012; Tatsumi et al., 2015). Recently, RF is rarely used in pixel-based for CA and instead it is usually combined in an object-based classification framework (see subsection 1.2.3.2 below)

Mutanga et al. (2014) compared the performance of RF and SVM for identifying land cover types in a fragmented landscape. They used RapidEye (5m-resolution) images to identify the landcover types. The

authors achieved an overall accuracy of 93% and 91% for RF and SVM respectively. The authors concluded that these methods are powerful for mapping in fragmented landscapes but high-resolution images are needed which increase the cost. However, the number of user's defined parameters required for RF is less than SVM (Pal, 2005).

1.2.2.3. Fuzzy classification

Compared to the hard classification methods mentioned above, the fuzzy classification handles the sub-pixel heterogeneity. This method allows for multiple classes per pixel. The multiple classes are expressed in terms of probabilities or membership of the land cover types per pixel (Zhang & Foody, 1998). This method consists of two stages: fuzzy parameters determination from training data and fuzzy partition of pixels (Wang, 1990). The membership functions (i.e. functions to identify the fractions) are defined through maximum likelihood function. More details about the calculations are provided by Wang (1990).
Arora and Ghosh (2003) compared the fuzzy classifier to crisp classifiers for areal extent of land cover classes including cropland in a fragmented landscape in India. They found that the fuzzy classifiers produced higher accuracy than the crisp classification. The difference between estimated areas and actual extent was 13% using fuzzy classifiers compared to 34% using crisp classifier.

1.2.2.4. Spectral mixture classification

In addition to fuzzy methods, spectral mixture analysis was developed to handle mixed pixel effect (Adams, Smith, & Johnson, 1986). The basic concept of this method that assumes the spectral reflection received by the sensor is a linear combination of spectra from all landcover types per pixel (Adams et al., 1994). The result of the spectral mixture is different fractions of land cover that form the pixel. Spectral mixture method is more accurate than conventional methods for area estimation of land cover (Lu & Weng, 2007). In a study by Batistella et al. (2004), the authors applied the spectral mixture method for estimating land cover proportions (i.e. including agriculture class) in a moist tropical area in Brazil. They used Landsat-TM images for classification and ground truth data for training and validating their product. The authors were able to achieve 87% and 90% for user's accuracy and producer's accuracy respectively. The authors implied that in a large complex landscape, the endmembers needed to be developed every time to apply the method. This suggests difficulties in repeating the method for monitoring studies for example.

1.2.3. Object-based classification

With the evolution in recent remote sensing data sources (particularly high-resolution), object-based methods have been developed. Unlike pixel-based classification, object-based classification uses the contextual (i.e. neighbouring pixels) information in addition to the spectral information to perform the classification (Li, Yang, & Wang, 2017). Object-based classification consists of two stages: segmentation and classification. In the segmentation stage, the study area will be partitioned into homogenous clusters (i.e. objects) (Wulder, White, Hay, & Castilla, 2008) based on some contextual information such as compactness and shape. In the classification stage, the objects will be assigned to classes based on the statistical properties of the object (Yeom, 2014). Compared to pixel-based methods, object-based can handle within the field variability better. In a complex and heterogeneous landscape, object-based provides more accurate results than pixel-based (Blaschke, 2010; Hussain, Chen, Cheng, Wei, & Stanley, 2013; Peña-Barragán, Ngugi, Plant, & Six, 2011). Moreover, dividing the area into objects solves the issue of 'salt' and 'pepper' that pixel-based suffers from (Belgiu & Csillik, 2018, Liu & Xia, 2010) However, object-based classification requires high-resolution images which increase the cost considerably. The accuracy of the segmentation process depends heavily on the predefined parameters by the users (e.g. scale, shape, colour, compactness, smoothness) (Rahman & Saha, 2008). Therefore, the accuracy of segmentation affects the accuracy of the results (Liu & Xia, 2010). Over-segmentation (one object portioned to many) and under-segmentation (i.e. many different objects merged) are issues related to object-based methods (Rao, Stephen, & Phanindra, 2012).

1.2.3.1. Edge detection:

In edge object-based classification, the image is segmented into objects described by their boundaries. The boundaries are produced through an edge filter (e.g. Prewitt, Canny detectors) and then the objects are closed using a contouring algorithm (Schiewe, 2002). This algorithm is highly affected by noise in input data (Schiewe, 2002). Edge detection for image classification was used in many studies, and it is more common to be used with radar images (Carvalho et al., 2010; Gambotto, 1993; Moigne & Tilton, 1995; Yang, Yang, Li, Yin, & Qin, 2008).

Rydberg and Borgefors (2001) used an integrated method of edge detection and image clustering over multispectral imagery for CA delineation. They applied edge filters on Spot image in Sweden, then they matched the resulted edges with a segmented image. For clustering they used ISODATA method. They found that the clustering process produced too many segments. The authors achieved 87% accuracy when they compared the clustered image with manually digitised segments within an error of one pixel. The main advantage of their method that it is fully automated but an expert knowledge to determine the suitable edge filter to be used.

1.2.3.2. Image segmentation:

In image segmentation, the process is bottom-up meaning it starts from a single pixel as an object and merging pixels into objects. The merging process is based on predefined criteria regarding the spectral and contextual aspects. The percentages of the contribution of spectra and context into defining the homogeneity objects should be determined (Castillejo-González et al., 2009).

In a study aimed at producing nominal cropland extent for Africa, pixel-based machine learning and segmentation were combined (Xiong, Thenkabail, Tilton, et al., 2017). The authors integrated Landsat 8 images to fill gaps in Sentinel 2. They composited five bands from Landsat 8, Sentinel 2 and additionally slope layer. Random forest showed overfitting and therefore the combined it with SVM. Then the authors applied a method called Hierarchical Segmentation (HSeg) for identifying objects for cropland and non-cropland. The authors achieved 85.9% and 68.5% for producer's accuracy and user's accuracy respectively. The authors indicated big challenges due to the complexity of the African landscape. Particularly, the authors showed there were difficulties in discriminating croplands from seasonal vegetation.

Eggen et al. (2016) applied SVM over time series of Landsat 5 and Landsat 7 from 2000 to 2011 to identify land cover classes in Ethiopia Highlands. The authors used the spectral bands and NDVI in addition to digital elevation model as predictors in SVM. To overcome the salt and pepper issue, the authors applied image segmentation as post-processing. They validated their product using 200 validation segments per class developed through the Google Earth platform. The authors achieved an overall accuracy of 55%. However, for the agricultural category the producer's accuracy was 51% whereas the user's accuracy was 85%. The authors indicated that the main reasons for the low producer's accuracy for cropland are the fragmentation of the landscape and cloud contamination of the images.

Vogels et al. (2017) used object-based RF classifier to estimate CA in two regions in Ethiopia and The Netherlands. They used panchromatic WorldView-1 images (0.5m) for Ethiopia and aerial photos (0.3m) for The Netherlands. They applied object-based segmentation on the high-resolution images to produce homogeneous segments. Then they used texture variables, shape variables, brightness, slope, and difference between neighbouring pixels as predictors to train their RF model. Then they performed visual interpretation to add a label to their sample points (crop or other land cover), they achieved an overall accuracy of 90% and 96% for CA in Ethiopia and Netherlands respectively.

Vogels et al. (2019) applied RF and image segmentation for irrigated smallholder farms mapping in a complex landscape in Central Rift Valley in Ethiopia. The authors used Spot-6 images (6m-resolution) during the dry season of 2013-2014. They used multi-resolution segmentation over extracted NDVI from Spot-6 images to produce the objects. Then random 3000 segments out of all segments were interpreted visually (i.e. using Spot-6, Google maps, Worldview in ArcMap) and divided into training set and validation set for RF classifier. For classification, they used 17 spectral variables, 8 shape variables, 22 texture variables,

8 neighbour variables and coordinates as predictors for the model. The authors achieved an overall accuracy of 95%. They concluded that this method could be used for mapping irrigated agriculture in complex landscapes.

In a fragmented landscape in Madagascar, Lebourgeois et al. (2017) combined RF and object-based segmentation for smallholders farms mapping. They indicated that due to the complexity of the landscape, multi-source data should be integrated to achieve good accuracy. The authors integrated Sentinel 2 images, very high-resolution images (0.5m-resolution), DEM, Spot images and Landsat 8 images. The authors applied the segmentation over the very high-resolution image. Then they developed 4 types of variables based on their data: reflectance variables, spectral indices, textural indices and ancillary variables. By utilising ground truth polygons, the RF classifier was trained using the variables values of ground samples. They achieved 91.7% accuracy for crop/non-crop determination. At sub-level classification (i.e. different crops), the accuracy dropped to 64.4%. Despite the high resolution and ancillary data that the authors used, they indicated difficulties in detecting the rain-fed agricultural fields. They attributed that to the small size of the farms and the mixed cropping system in the study area.

1.3.   Hyper temporal NDVI

NDVI is one of the most widely used vegetation indices in natural resources management. The NDVI reveals a lot of information about vegetation health. The healthy vegetation has high reflectance in Near Infra-red (NIR) wavelength and low reflectance in red wavelength which means the healthy vegetation has high NDVI values (NASA, 2000). From an agricultural perspective, the temporal profile of NDVI starts rising with the growth of the crops until peak productivity and then starts decreasing during senescence (Soudani et al., 2012). Image classification methods perform better using multi-date imagery than single date imagery for vegetation monitoring. The temporal variation (i.e. phenological cycles) includes important information to help in discriminating between different features (Gómez, White, & Wulder, 2016; Langley, Cheshire, & Humes, 2001). In a single date image, many features may exhibit similar reflectance properties while using multi-date images allow capturing the distinct phenological patterns of the features (Viña et al., 2004).

Applications of multi-temporal remote sensing in agriculture faced by the challenge of suitable acquisition imagery dates. The images are needed during or near the growing seasons for crop identification and CA estimation. Those times usually are during the wet season which usually is too cloudy (Belgiu & Csillik, 2018; Petitjean, Inglada, & Gancarski, 2012). The clouds reduce the values of NDVI due to the aerosols and water vapour effect which will affect the subsequent analysis procedures (Kaufman, Tanré, Markham, & Gitelson, 1992). Hyper temporal satellites are characterized by very high temporal resolution (i.e. short revisit time) usually between one to two days. The short revisit time increases the probability of cloud-free pixels, but at the expense of spatial resolution due to the altitude of the sensors (Lefsky & Cohen, 2003).

Although the long-term records of AVHRR data (since 1979); it is not widely used for vegetation monitoring due to the coarse resolution (i.e. 8km), the radiometric and spatial characteristics were designed for atmosphere studies and not vegetation monitoring (Yin, Udelhoven, Fensholt, Pflugmacher, & Hostert, 2012). Nevertheless, some studies used AVHRR imagery for crop monitoring (Granados-Ramírez, Reyna-Trujillo, Gómez-Rodríguez, & Soria-Ruiz, 2004). Due to the higher spatial resolution compared to AVHRR; MODIS vegetation series became more popular for land cover mapping and agricultural applications (Yin et al., 2012). MODIS NDVI series characterised by spatial resolution of 250m and the product is 16-days composite (USGS, 2014).

In a study by Victoria et al. (2012), the authors found that using unsupervised classification over hyper temporal NDVI series gave very promising results when compared to agricultural statistics. They used 16-day composite MODIS NDVI from 2005 to 2009 and applied a Fourier transformation to extract the seasonality of crop phenology. The Fourier transformation gives amplitude, the first harmonic (i.e. first cosine wave) of the temporal profile represents one cycle over the year, and the second harmonic represents

two cycles over the year. Then they classified the amplitude images into ten clusters. Utilising the information from temporal profiles, clustered images, and higher resolution images they were able to define the CA. They concluded that the method is suitable for large crop areas because in the municipalities with CA more than 10% they achieved R² of 0.89, the municipalities with CA less than 10% they achieved only R² of 0.41. However, this study was applied over agricultural lands characterised by large and mechanised fields. The coarse resolution yields lower results for smallholder farms as mentioned before.

SPOT-ProbaV was launched in May 2013 mainly to fill the gap of SPOT-VGT sensor (March 1998 – May 2014), thus, the product continuity is stable over time with a maintained interval of 10-days between consecutive products, and it is available at resolutions from 100m to 1km (Dierckx et al., 2014). Since the data of Proba-V of dates before 2013 are compensated from SPOT-VGT, there are some concerns about the orbital drift of SPOT-VGT between 2013 and 2014, the orbital drift has impacts on the reflectance but less significant impacts on the NDVI (Swinnen, Verbeiren, Deronde, & Henry, 2014).

Toté et al. (2017) found that ProbaV has a high correlation with other NDVI products such as MODIS and AVHRR. Chen et al. (2006) achieved better results for identifying corn growth using SPOT-Vegetation series rather than MODIS. They concluded that MODIS was highly affected by the soil background. Zhang et al. (2016) Compared the 300m ProbaV and MODIS vegetation series for crop mapping, in one site they found that ProbaV is slightly better than MODIS but for another site it was significantly better by 26%.

1.4.   Terrain and agriculture

Terrain has effects on micro-climate and soil characteristics such as soil temperature which subsequently affect where and what crops are planted (Kumhálová, Matějková, Fifernová, Lipavský, & Kumhála, 2008). According to Kaspar et al. (2003), elevation and slope have direct effects on the infiltration rate due to their effect on the water flow. Additionally, elevation and slope affect the water storage and infiltration indirectly through their influence on soil characteristics and soil erosion. Based on that, the terrain has significant influence in CA distribution and yield.

In a study by Recio et al. (2010), the authors tested the effect of incorporating the contextual information, elevation, slope, aspect, lithology, and distance to rivers into hierarchical decision trees on the accuracy of agricultural parcels classification. The accuracy of the classification results decreased when some data were added. However, they found that using the textual information, elevation, and slope increased the accuracy by 5%.

Mukashema et al. (2014) applied a method using Bayesian inference to estimate the CA for coffee in Rwanda. Their method required very high-resolution images; they used aerial photos (0.25) and a Quick-Bird image (2.44m for multispectral bands and 0.61m for a panchromatic band). However, using only spectral data in their model they were able to achieve 50% overall accuracy in CA estimation of coffee. After incorporating a digital elevation model and a forest map in their model, the accuracy improved to 87%. They achieved an R² value of 0.92 with agricultural statistics when the results aggregated to district level. Thus, incorporating terrain in CA estimations is promising in improving the accuracy of the CA products.

1.5.   Problem statement

The issues related to crop area estimate in a fragmented landscape are mainly due to gaps in the different data sources (i.e. agricultural statistics and remote sensing) that have been used for CA estimation. Agricultural statistics are usually obtained using AFS method which based either on ground surveys or remote sensing (Gallego, 1999; Husak & Grace, 2016; Pradhan, 2001). Agricultural statistics are too generalised spatially (i.e. into districts or national level) (Marshall et al., 2011) which limit their use for critical food security analysis. Location, extent and distribution of cropland are often unavailable from agricultural statistics (Lunetta, Shao, Ediriwickrema, & Lyon, 2010). Additionally, the agricultural statistics data are inconsistent over time (Ramankutty, 2004) which limit their use for agricultural monitoring programs. Collecting data for agricultural statistics is expensive, time-consuming and labour intensive.

Regarding the use of remote sensing sensors for CA estimation, usually there is a trade-off between the spatial resolution and temporal resolution due to design restrictions (Chen, Huang, & Xu, 2015). The coarse resolution images have a very high temporal resolution which allows capturing the general agroclimatic conditions necessary for crop growth. However, the accuracy of detecting the CA in fragmented landscapes using coarse resolution is low due to the heterogeneity of the landscapes particularly in areas with smallholders farms (typically ≤2 ha) (Estes et al., 2016; Jain, Mondal, DeFries, Small, & Galford, 2013; See et al., 2015).

On the other hand, the high, as well as moderate resolution images, can provide high accuracy results for CA estimation in smallholder farms areas (Neigh et al., 2018) but at the expense of the temporal resolution which will affect the data availability due the clouds effects during crops growing season (Chen et al., 2018; Estes et al., 2016; Reiche, Verbesselt, Hoekman, & Herold, 2015). High-resolution images usually characterised by relatively small coverage which will require mosaicking process, this process may result in spectral differences due to the vegetation phenology, atmospheric effects, and bidirectional effects (Estes et al., 2016; McCarty, Neigh, Carroll, & Wooten, 2017). Additionally, high-resolution images are often available at high cost.

To test the possibility of coming over these issues, in this study a method for crop probabilities estimation was developed and evaluated. The method used the temporal characteristics of coarse resolution images for capturing the different climatological trends in the study area (i.e. defining agroecological zones). The spatial characteristics of moderate spatial resolution images integrated with coarse resolution images to improve the spatial resolution and the accuracy of crop probabilities. In addition to assessing inclusion of other terrain auxiliary data to improve the prediction of crop probabilities in a study area characterised by having small farms, complex climate and ecosystems. Inputs derived from these different sources were involved in a generalised additive model (GAM) as an attempt to address the gaps mentioned above in estimating crop field probabilities in a complex landscape with smallholder farms.

1.6. Research objectives and questions

The main aim of the research is to develop a new method to estimate the fraction (probability) of crop area in topographically complex and highly fragmented landscapes of Ethiopia integrating coarse and moderate resolution remote sensing with agricultural census data. To achieve this aim, the underlying objectives are:

1. To identify agroecological zones using hyper-temporal NDVI.

    a) Can hyper-temporal (1km spatial resolution) NDVI effectively stratify topographically complex and highly fragmented landscapes into agroecological zones, i.e. homogenous regions exhibiting similar phenological patterns?

2. To evaluate the use of agroecological zones coupled with agricultural statistics for coarse probabilistic crop mapping.

    a) Can agroecological zones effectively disaggregate agricultural statistics to 1km spatial resolution pixels?

3. To establish and evaluate GAMs to estimate crop field probabilities using moderate (30m) resolution NDVI and terrain data in addition to coarse field fractions.

    a) Do moderate resolution NDVI for both dry and wet season improve the predictions of crop field probabilities?

b) Do moderate resolution topographic predictors improve the predictions of crop field probabilities?

c) Do coarse filed fractions produced using coarse spatial resolution hyper temporal NDVI improve the moderate resolution GAM?

4. To evaluate the inclusion of coarse field fractions as a predictor in a global GAM for whole Oromia versus developing localised GAMs for each agro-ecological zone.

a) Are there differences between using global GAM incorporating the coarse field fractions from agroecological zones and using separated GAMs for each agro-ecological zone in terms of model performance?

2. STUDY AREA AND DATA

2.1. Study area

2.1.1. Geography:

Oromia region located in the middle and extends to the south of Ethiopia, it is situated between 3º 30' and 10º 23'N latitude 34º 7'E and 42º 55'E longitude (Figure 1). The Ethiopia Rift which is part of The Great African Valley passes through the central part of Oromia. The total area of Oromia is approximately 353,690km², and it consists of 12 administrative zones (Ethiopian Government, 2018). Oromia is one of the biggest regions in Ethiopia; the capital Addis Ababa is located in the region. The landscape in Oromia is characterised to be heterogeneous and fragmented in addition to the smallholder farming systems (Eggen et al., 2016) which make Oromia attractive to test the proposed methodological framework. Moreover, Oromia consists of 188 districts (i.e. the largest in Ethiopia). A large number of districts is preferable for our method because it guarantees that the statistical models used to derive crop area a high degree of freedom (Pandey & Bright, 2008).

2.1.2. Topography and climate:

The altitudes vary a lot in the study area, it ranges from 298m to 4385m above the mean sea level. The landscape in Oromia has diverse structures including rugged mountain ranges, undulating plateaus, panoramic gorges and deeply incised river valleys, and rolling plains (Ethiopian Government, 2018).
Oromia consists of three climatic zones: tropical (49.8%), sub-tropical (42.2%), and temperate (7.5%) climate. The average annual rainfall in Oromia is between 200-2400mm, and the average annual temperature ranges between 7.5 – 27.5ºC (Embassy of the Kingdom of the Netherlands Ethiopia, 2015).
In Ethiopia, there are two growing seasons: the Meher (major season with 96% of total production) and the Belg (mainly by smallholders) (Alemayehu, Paul, & Sinafikeh, 2012).

2.1.3. Population and agricultural activities:

According to a census that was held in 2007, the population in Oromia region is 26,993,933 (Central Statistical Agency of Ethiopia, 2010) which makes Oromia is the most populous region in Ethiopia.
Agriculture is the main source of livelihood for most of the people in Oromia, it represents 56.2% of the regional economy (Embassy of the Kingdom of the Netherlands Ethiopia, 2015). The farming system in Oromia is mixed of livestock and crops. The main crop types that cultivated in the region are maize, teff, wheat, barley, peas, bean and oilseeds (Ethiopian Government, 2018).
In the Meher season, rains start in June-July and end in September-October. Meher is considered as the main season in Oromia. The main crops grown during Meher season in Oromia are: Pulses, Cereals, Teff, Wheat, Barley, Maize and Sorghum (FAO, 2007b).
The Belg season is shorter and less intensive; it receives rains start in February and end in April-May. The short cycle crops usually harvested in April-May by the end of the rainy season (FAO, 2007b). The dominant crops during this season are: Potatoes and Yams (Husak et al., 2008).
The climatic conditions for the major crops as indicated by Chamberlin & Schmidt (2011): Teff is grown in areas with altitudes between 1800-2100m, average annual rainfall in range 750-1000m, and temperature between 10-27 ºC. Maize is grown in areas lower than 2400m and rainfall between 800-1500mm. The Maize produced by Oromia represents 60% of the total production of Ethiopia. Sorghum is usually grown in relatively low areas with altitude less than 2400m and drier areas with annual average rainfall less than 250mm. Wheat is grown in altitudes between 1600-3200m, rainfall between 400-1200mm, and temperature between 15-25 ºC.
Climatic conditions affect farming systems and therefore different farming systems follow different climatic zones. Seed farming complex can be found in dry to wet areas with altitudes between 500 – 3200m; seed

farming has large range of moisture conditions since it accommodates cereals, oilseeds and pulses. Shifting cultivation and pastoral complexes are found in tropical areas. In low altitude arid and semi-arid regions, rain-fed crops are limited due to the lack of rainfall (Chamberlin & Schmidt, 2011). For details about farming systems and climatic zones in Ethiopia see (Amede et al., 2017).
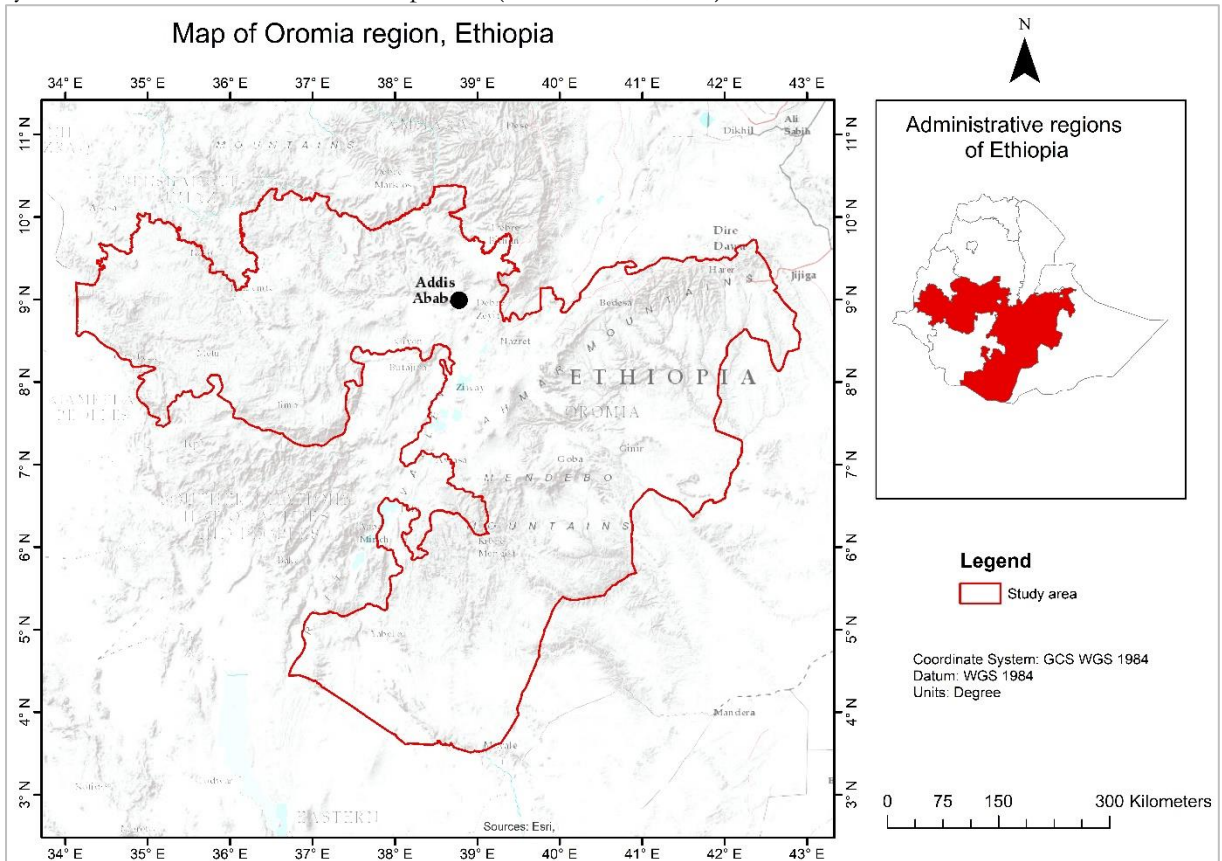

Figure 1: Study area location

2.2.   Data used

In this research, data from different sources have been used to estimate the field fraction. The data included: SPOT-ProbaV NDVI, Landsat 8 NDVI, Shuttle Radar Topography Mission (SRTM), DigitalGlobe images through Google Earth platform, and agricultural census data.

2.2.1.   Agricultural Census data

The district agricultural census data (September 2001- August 2002) was used for this study. To the limit of our knowledge, this is the most recent census data available at district (i.e. woreda) level. The annual survey is done in Ethiopia by the Central Statistics Agency (CSA) but that data is at regional or zonal level (Wolaita) level (Cochrane & Bekele, 2018). As indicated by (Hazell & Wood, 2008), the global growth of arable land was 9% (i.e. around one mha) from 1961 to 2002. Thus, an assumption was made that the production can change rapidly but the extent of the fields is stable through a period less than 20 years. Therefore, using this data and the below remotely sensed data (with different temporal windows) was feasible. The survey was done by the Ethiopian Central Statistical Authority (CSA) and the data was provided by the second supervisor of this study. The data was provided in tables format, the tables contained the districts and the crop areas in hectares. For the present study, the census data used included the total of both seasons (i.e. Meher and Belg) for temporary crops.

2.2.2. SPOT-ProbaV NDVI

The method used coarse SPOT-ProbaV NDVI series (between 1999 and 2017). The SPOT-ProbaV sensor has a revisit time of one day (i.e. daily images) and spatial resolution of 1 km spatial, however, the NDVI product is a 10-day maximum value composite (Wolters et al., 2018). SPOT-ProbaV NDVI was presented as values (0-255) as that was the native representation of the data by the providers (Wolters et al., 2018). Omitted pixels in SPOT-ProbaV (i.e. missing, cloud, snow, sea, and background) contain data flags (Wolters, Dierckx, Dries, & Swinnen, 2015) which help to process the data based on this quality information.

2.2.3. Landsat 8

The study area is covered by seven Landsat-8 scenes, thus, for each scene coverage, a pair (i.e. dry season and wet season) of Landsat-8 images per year from 2013 to 2017 were obtained. The images from 2013 to 2017 were used because of the availability of Landsat data. Landsat 7 has issues of black lines since 2003 due to the failure of the scan line corrector (U.S. Geological Survey, 2018). Landsat 5 was decommissioned since 2013 and therefore it does not provide recent data to produce updated maps. This should not be mixed with the assumption above (subsection 2.2.1). The field extent is stable but discriminating active fields from fallow lands at certain date of time depends on the dates of the Landsat images because dry and wet seasons will be extracted from Landsat-8 images. To avoid the spectral differences can appear by fusing Landsat 8 with old Landsat 5; only Landsat 8 was used. The images are freely available at Earth Explorer platform (https://earthexplorer.usgs.gov/), due to the huge data size, the Landsat data was obtained and preprocessed through the Google Earth Engine platform.

2.2.4. SRTM

The Shuttle Radar Topography Mission (SRTM) was used to get the terrain information. SRTM is a digital elevation model with 30 meters spatial resolution, the data can be gathered freely at the United States Geological Survey (USGS) website. A slope layer was derived from the DEM using ArcGIS software.

2.2.5. Training and validation set

For training and validating our model 271 area frames sized 30mx30m were distributed randomly over the study area (Figure 2). Each area frame contained a grid of 16 points with a distance of 9 meters between the points. The choice of 16 points grid considered a balance between representative coverage and the amount of visual work that would be required to conduct the interpretation. Those points were interpreted visually using Google Earth into field and non-field then the percentage of the field per frame was obtained by dividing the number of field points by the total number of points within the frame.

The study area was mainly covered by 'DigitalGlobe' constellation in which all sensors have a sub-meter resolution (DigitalGlobe, 2019). This dataset was used to develop and validate the produced field fraction at 30m through the global models for whole Oromia.

Google Earth has been used in many studies for collecting reference data, particularly for land cover mapping (Defourny et al., 2009; Fritz et al., 2011) and urban land use mapping (Malarvizhi, Kumar, & Porchelvan, 2016). Regarding the positional accuracy of Google Earth, Potere (2008) concluded that Google Earth images could be used with other moderate resolution remote sensing, the author assessed the positional accuracy based on global 436 ground control points to reach that conclusion.
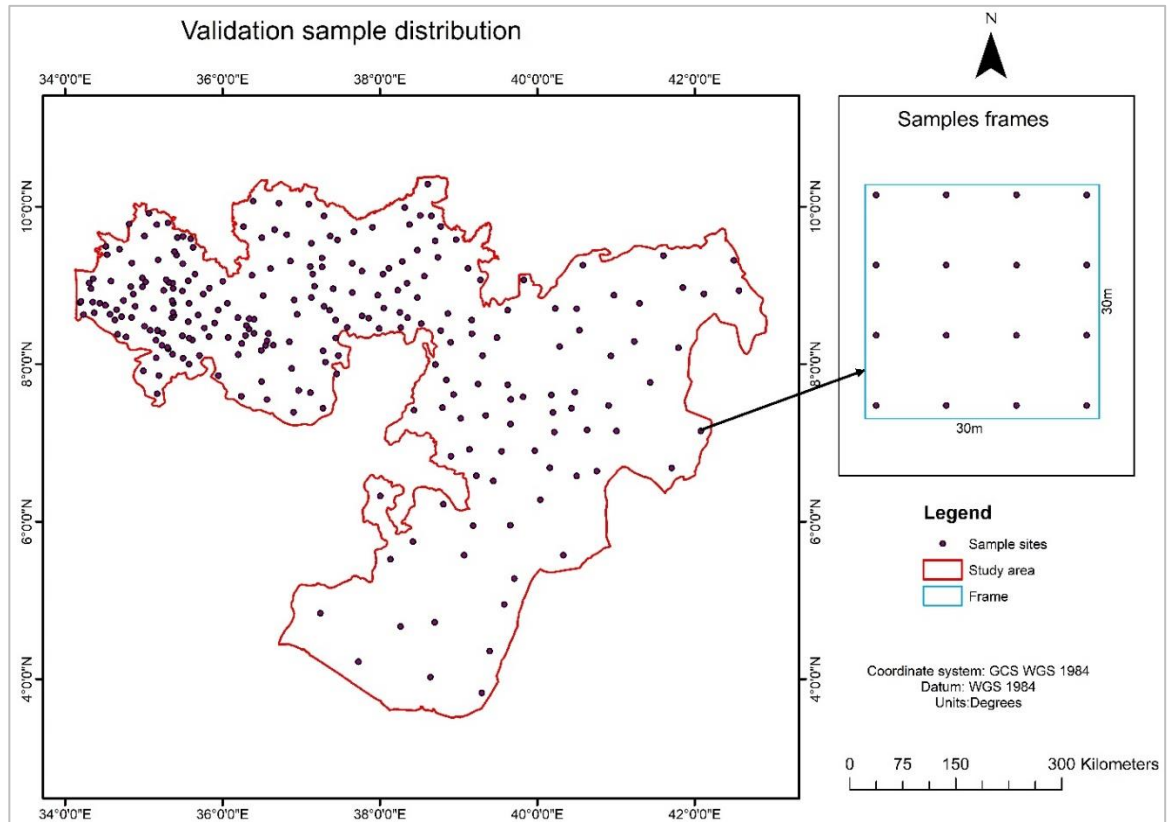
Figure 2: The distribution of the validation sample observations

3. METHOD

The method outlined as producing 1km field fractions by incorporating agricultural census data with hyper temporal NDVI, developing and evaluating two global GAMs for predicting crop field probabilities (i.e. using only moderate resolution dry and wet season NDVI, elevation and slope, the other model added the 1km fractions as a categorical predictor (Figure 3). In other words, the two global models (with and without 1km field fractions input) were compared. Moreover, an experiment was carried out to demonstrate the differences between the better global model (i.e. from the previous comparison) and a local GAM developed within one agroecological zone differ to elaborate on the global model capabilities (not shown in the flowchart).
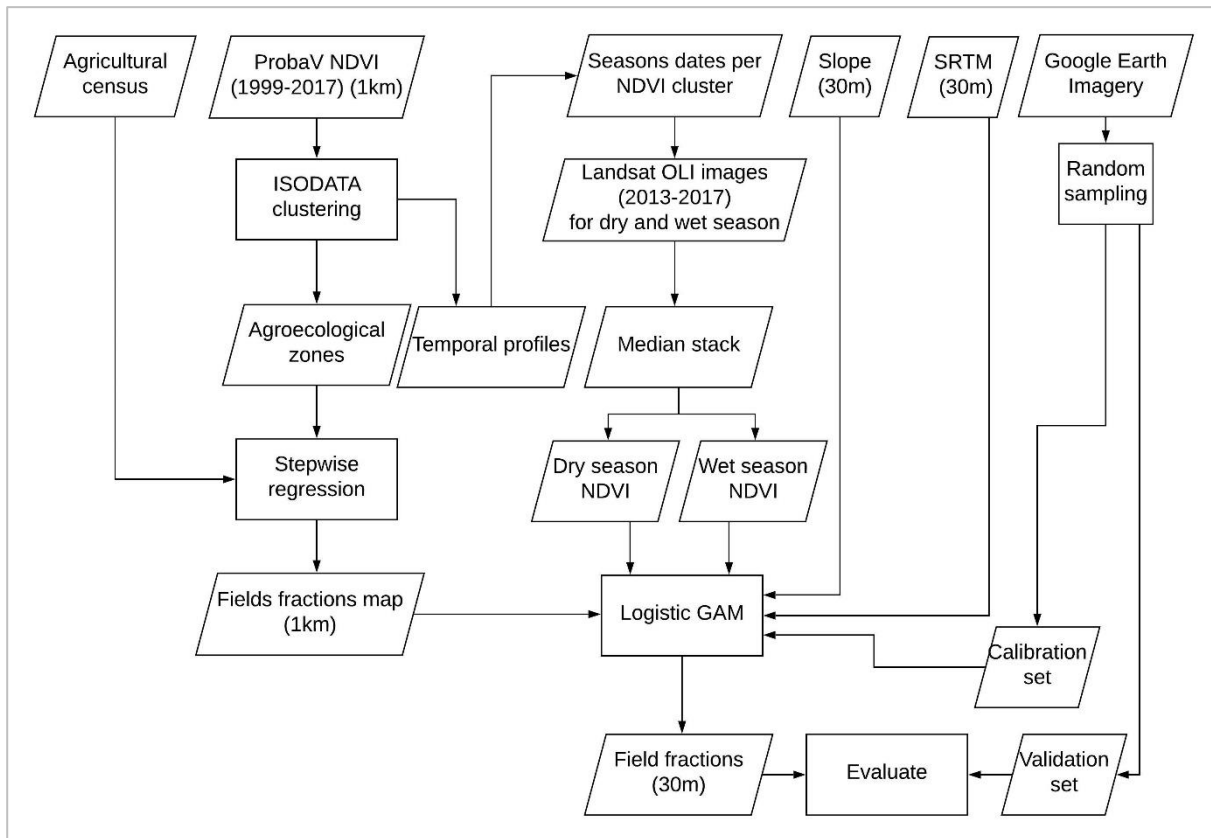

Figure 3: Flowchart of the research method

3.1. Estimation of field fraction at coarse resolution (identify agroecological zones)

3.1.1. SPOT-ProbaV NDVI preprocessing:

Using hyper-temporal NDVI series such as SPOT-ProbaV allows for feasible clouds compensation and capturing the long-term trends in the vegetation (see subsection 1.2.4). Flagged pixels (see subsection 2.2.2) were replaced by zero value. Then those pixels have been compensated using Savitzky –Golay filter (Savitzky & Golay, 1964) through TIMESAT software. In this method, a piecewise regression will be fitted within a temporal window (i.e. NDVI multi-date observations) to reconstruct the series. Defining too small window can overfit the series while too large value may over smooth (Chen et al., 2004). Regarding the software, half window size should be defined by the user. In the present study, 4 was defined as a half window size as suggested by Chen et al. (2004) that size is appropriate.

3.1.2. NDVI stratification:

After preparing the Proba-V NDVI series, all the time series images were stacked. Then the ISO data unsupervised clustering method (Dhodhi, Saghri, Ahmad, & Ul-mustafa, 1999) was used to produce mixtures of land covers exhibiting similar surface responses to climate (i.e. agroecological zones). The unsupervised classification was used since the design of the method relies on minimising the user's interaction. One hundred fifty clusters were produced since a hierarchical clustering analysis was planned to be done then the number of produced clusters was not a critical parameter. The number of iterations was defined as 50 iterations with convergence threshold 0.95. The hierarchical clustering method identifies the groups within the dataset to reduce the number of clusters without losing the structure of the data (Gonçalves, Netto, Costa, & Zullo Junior, 2008). In other words, the cluster analysis merges the clusters into new groups based on certain statistics (e.g. mean) without dissolving the variability of the data. Minimising the number of clusters (i.e. independent variables) increases the degree of freedom. Regression models become more robust with higher degrees of freedom (Pandey & Bright, 2008).

Therefore, the median of each cluster (for the whole time series) has been extracted and then SPSS software was used to run the hierarchical cluster analysis. The median is less sensitive than the mean (Hippel, 2005). After that the resulted clustered image was converted into shapefile to be integrated with the agricultural census data.

3.1.3. Regression analysis:

The data from agricultural census tables have been attached to the administrative shapefile of Oromia region, then an intersection was performed between the NDVI clusters shapefile and the agricultural census data and new areas based on the intersection were calculated. As a result, the new attribute table contained the areas of the NDVI clusters within each district. Then the cropped area from the agricultural census was related to the NDVI clusters using a step-wise regression to produce the field fraction at 1km resolution. This process was based on the fact that agricultural fields show distinctive temporal NDVI profiles (i.e. phenological cycles) compared to other types of land cover (Sakamoto et al., 2005). Step-wise regression is an automated procedure that eliminates uncorrelated or redundant data. The regression model was used can be expressed by:

$$Y = \beta_1 C_1 + \beta_2 C_2 + \beta_3 C_3 + \ldots + \beta n Cn$$

Where Y is the cropped areas from agricultural statistics, β_1, β_2, β_3, …, β_n are the coefficients, C_1, C_2, C_3, …, C_n is the NDVI clusters areas within district. The model was forced through origin because not every pixel contains agricultural fields. The regression model was carried on SPSS software environment. The regression model distributed the cropped areas over the study area at 1km resolution based on the occurrences of the different NDVI clusters within each district. Thus, the coefficients represented above are the proportion of the agricultural fields within the NDVI clusters (i.e. field fractions at 1km). This regression method to downscale agricultural census data from the district level to 1km resolution was developed by de Bie et al. (2008). The authors achieved adjusted R^2 of 45% using a validation set of 3272 segments for rainfed wheat. However, Khan et al. (2010) also illustrated the method in southern Spain, their 1km field fraction map explained 68% of the variation in 1415 validation samples of wheat fields which supported the use of the method.

3.2. Estimation of field fraction at fine resolution (30m)

3.2.1. Landsat NDVI selection and pre-processing:

Before starting downloading the Landsat 8 scenes, the phenology (i.e. temporal behaviour) of the NDVI clusters were used to determine the dry season and wet season windows Landsat 8 images per each cluster. The wet season and the dry season were determined both because they explain different variations regarding the land cover types. For example, cropland tends to have low dry season NDVI and high wet season NDVI

while forests and other natural vegetation tend to have high NDVI values throughout the year. In contrast, bare lands tend to have low NDVI throughout the year.

A simulation of a year temporal profile was produced per cluster by extracting the median of each decade through the years which resulted in 36 observations (i.e. three observation per month) time series for a year simulation. The delayed moving average method (Reed et al., 1994; Verdin et al., 2000) was used to extract the start and the end of the wet season. Reed et al. (1994) suggested using nine observations for biweekly series (i.e. four months interval) in the United States. Taking into consideration the Meher season extends for three months, thus, taking less interval would allow capturing the changes in the trend. Therefore, nine decades (i.e. three months interval) were used as a moving window. To apply the method, the edge of the series (i.e. last nine decades in the year) was padded by the same values of the first nine observations in the year. Then the moving average was calculated from the beginning of the year up to observation 36th. In the delayed moving average method, the start of the season is when the original temporal NDVI profile crosses the smoothed profile in the upward direction, in contrast, the end of the season is when the original profile crosses the smoothed profile in the downward direction (Figure 4). This process was carried using Excel software.
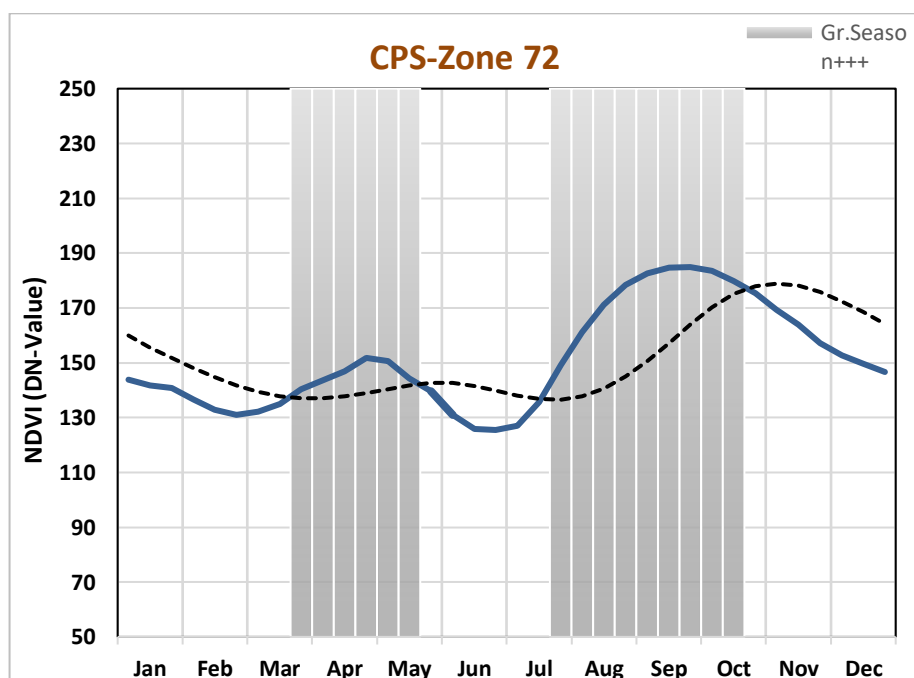

Figure 4: An example of the delayed moving average method on one of the NDVI clusters. Grey shaded area denotes the wet season windows.

After the start and the end of the season have been extracted for each cluster, Google Earth Engine was used to prepare and download the Landsat 8 NDVI images. A built-in function was used to mask out the clouds from the reflectance images between 2013 and 2017. Then the median of the wet season and the median of the dry season within each year and then among all the years were extracted. All the extracted images were mosaiced using ArcGIS software to cover the whole study area.

3.2.2.   Global GAMs development and evaluation:

GAMs were developed by Hastie and Tibishirani (1986), it represents a relationship between supporting data (i.e. predictors) and a target or a response variable. GAMs can be explained through the generalised linear models (GLMs) and the additive models (AMs). GLM is a class of linear models; they are used to predict a mean of a response variable based on many explanatory variables (i.e. predictors). GLMs establish a linear relationship between the response variable and the predictors (Khuri, Mukherjee, Sinha, & Ghosh,

2006). GLMs consist of three components: the response variable, the linear function of the predictors and the link function. It can be written as following:

$$f(\mu) = \beta_0 + \beta_1 X_1 + \beta_2 X_2 + \beta_3 X_3 + \ldots + \beta_n X_n$$

where $f(\mu)$ is the link function and β_0 is intercept, β_1, β_2, β_3, …, β_n are the coefficients and X_1, X_2, X_3, …, X_n are the predictors. In the case of a binomial response variable, the most common link function is the logit link which predicts the probability of the occurrence of the response variable. This kind of model called logistic regression (Bewick, Cheek, & Ball, 2005). The logit function for a probability (p) is expressed as:

$$logit \ (p) = log \ [p/ \ (1- \ p)]$$

In AMs, the coefficients are replaced by smoothing functions such as splines. The AMs can be expressed as:

$$Y = \beta_0 + S_1 X_1 + S_2 X_2 + S_3 X_3 + \ldots + S_n X_n$$

where Y is the response variable, S_1, S_2, S_3, …, Sn are the smoothers (i.e. smoothing functions).
The combined models of GLMs and AMs give the GAMs which can be written as following:

$$f(\mu) = \beta_0 + S_1 X_1 + S_2 X_2 + S_3 X_3 + \ldots + S_n X_n$$

In GAMs, instead of using slope coefficients to capture the impact of the predictors on the response variable, local smoothing functions for each predictor are used.

Despite that logistic GLM can be used to model binomial response variables, the rationale for using GAM was the expected nonlinear relationships between the crop field probabilities and both NDVI and terrain since GAM relaxes the linearity assumption of GLM (Hastie et al., 2016). For example, the agricultural fields are expected to have a nonlinear relationship with elevation (i.e. crop field probability increases with elevation then decreasing with very high altitudes) (Husak et al., 2008). The crop field probabilities are expected to be negatively correlated with slope and dry season NDVI. On the other hand, they are expected to increase with the increase of wet season NDVI. All these relationships were found to be nonlinear in fragmented and complex landscapes (Grace, Husak, Harrison, Pedreros, & Michaelsen, 2012; Kathryn Grace, Husak, & Bogle, 2014; Husak et al., 2008; Marshall et al., 2017). Therefore, using fixed slopes in regression (i.e. linear relationships) is impractical. In contrast, GAMs have two main limitations: GAMs produce graphical function forms between the response and the predictors instead of explicit equations (Liew & Forkman, 2015), and overfitting (Maloney, Schmid, & Weller, 2012).

To summarise that, logistic GAM was preferred to logistic GLM to relax the linearity assumption and capture the complex non-linear relationships between agroclimatic drivers and crop area. The distribution and nature of the variables used in any model affect the type of the model. The independent subframe points that were absence/presence of agricultural fields; and the goal was to predict crop field probabilities. Thus, logistic GAM (with logit function) was used. A typical logistic model usually used to model binary response variables, however, in the present study the response variable is field fractions resulted from dividing the proportion of crop subframe points by the total number of points within the frame (i.e. 16 points). In such a case, field fractions would show greater variation than just binary, therefore, quasibinomial distribution was applied (Consul, 1990).

Before developing the GAM, the independent data set (see subsection 2.2.5) was divided into calibration set and validation set by 70% and 30% respectively (i.e. 190 and 81 observations).

Then a logistic GAM model was developed (globally over whole Oromia) in R software using 'mgvc' package (Wood, 2013) between the 30m frames with the following covariates: dem, slope, dry and wet season NDVI. Splines smoothers were used as smoothing functions (Wood, 2013). The model was forced through the origin because not every pixel contained agricultural fields. Another GAM model included the 1km fractions as a categorical predictor was developed to assess the effect of including the potential agroecological zones. Our estimated field fractions at 1km resolution is a semiquantitative variable which

means it is quantities (i.e. field fraction) based on a categorical variable (i.e. NDVI clusters). This kind of variables has limited outcomes (i.e. too many pixels with a same value). Therefore, it was included as a categorical variable to be used as a predictor in GAM in the context of the present study. To elaborate, all the zero fractions represented by one category and each fraction greater than zero represented by a category. Both models were evaluated using out of sample validation (i.e. the 81 observations). Based on that, the highest-performing model was applied over the whole of Oromia to produce 30m-resolution field fractions.

3.2.3.   Global GAM and local GAM

To achieve objective 4, new binary 508 area frames sized 30mx30m were distributed randomly over one of the produced agroecological zones, the chosen stratum had the largest value in terms of fields extent fraction at 1km resolution. The 508 area frames were classified through Google Earth imagery to crop/non-crop, crop areas appeared in 389 observations (all sampled area frames contain more than 90% crop area), and 119 area frames were non-crop. This sample was created as only binary observations because the objective was to compare the previously developed GAM (global) to a localised GAM within one agroecological zone and not to relate the predicted fractions to actual field fraction like the previous case.

The dataset was divided into a training set and a testing set with 70% and 30% respectively (i.e. 356 and 152 observations) with considering the representativeness of both binary classes within both training and testing sets.

To make the global model comparable to the local model (i.e. local model uses binary response); the global model was redeveloped using binary response (i.e. crop/no-crop). The training fractions data in section (3.2.2) (i.e. the 190 frames) was converted into binary (1 for values greater than 0).

Then, a local GAM within only the chosen zone was developed through R software between the training binary area frames and the four predictors. The resulted predictions were evaluated using the testing set (i.e. the binary 119 frames). Finally, the predictions that produced using the binary global GAM were evaluated against the same testing set to determine how important to develop localised GAMs per each agroecological zone.

Basically, this experiment was done as a demonstration of the capabilities of the global model to compete with the local model in predicting field fraction. In other words, comparing a model that uses agroecological zones as a predictor (i.e. global) and one that uses it to categorise the model (i.e. localised). The local model is expected to perform better but the purpose of the experiment is to assess the differences between the two models and evaluate our global model. In case the global model performed close to the local, that supports the use of the global model developed in (section 3.2.2).

4. RESULTS

4.1. Field fractions at coarse resolution

4.1.1. NDVI clustering (agroecological zoning):

After the filtering process of NDVI series, a stack of the whole series from 1999 to 2017 was clustered into 150 clusters using ISODATA classification algorithm. An optimum number of clusters to stratify the area into appropriate agroecological zones is unknown. Therefore a hierarchical cluster analysis was performed to merge relatively similar clusters. As a result, 60 clusters were created, Figure 5 shows the spatial distribution of the merged clusters.
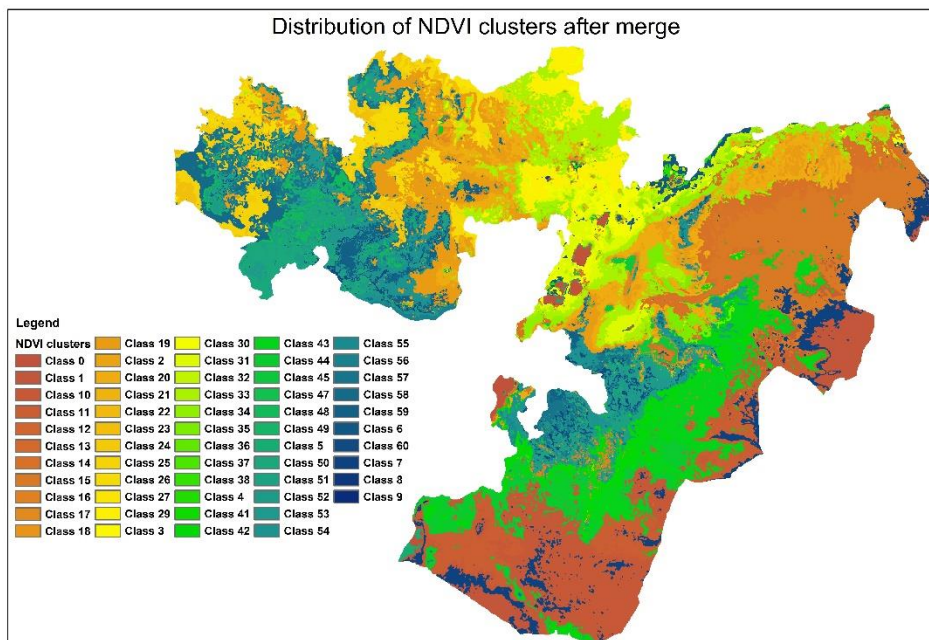

Figure 5: Merged NDVI clusters (60 clusters)

To elaborate on the meaning of relatively similar clusters mentioned above, some examples of the temporal behaviour of NDVI long term median among different clusters are shown in Figure 6.

NDVI long time series can be used to provide indications about dominant land cover types, each temporal profile (i.e. profile line) in Figure 6 represents a cluster before the merge (i.e. out of the initial 150 clusters). Figure 6-a shows three initial classes were merged to form cluster 33. The figure indicates presence of agriculture with monomodal distribution. Some parts of cluster 33 located west to the rift valley and some parts located east to the valley. That zone is a relatively hot zone in drier areas. The amount of rainfall in this zone is not sufficient for crop growing in two seasons. By checking rainfall data (not shown here), this cluster located in relatively dry areas (i.e. <350mm). The season starts around decade 19 (beginning of July) and ends around decade 30 (beginning of October); this is a typical Meher season. Some examples of crops perhaps grown within that cluster are: Maize and Horse beans.

Figure 6-b indicates agricultural land mixed with other land cover types with bimodal rainfall (I.e. two growing seasons). Cluster 35 was not merged with any other initial cluster and remained as single cluster before and after the hierarchical analysis (just the number of the cluster changed). The first season starts around decade 9 (end of March) is shorter than the second season which starts around decade 25 (beginning of August). Also the amount of greenness is different between the two seasons as can be seen from Figure

6-b. The two seasons for this cluster match the start for both Belg and Meher seasons in Ethiopia (Alemayehu, Paul, & Sinafikeh, 2012). As mentioned before Belg is shorter than Meher and less intense which justify the less amount of greenness in the first season showed in the figure. Examples for crops perhaps grown within this cluster during the Belg season are Sweet Potatoes and Yams. While crops perhaps grown during Meher within cluster 35 are: Teff and other cereals, grains and pulses. In this cluster, the Meher season starts slightly late. Most parts of this cluster located in areas wetter than the previous cluster (i.e. >450), however, some small parts located within relatively drier areas. That indicates this cluster falls within tropical and sub-tropical climatic zones.

a)   b)

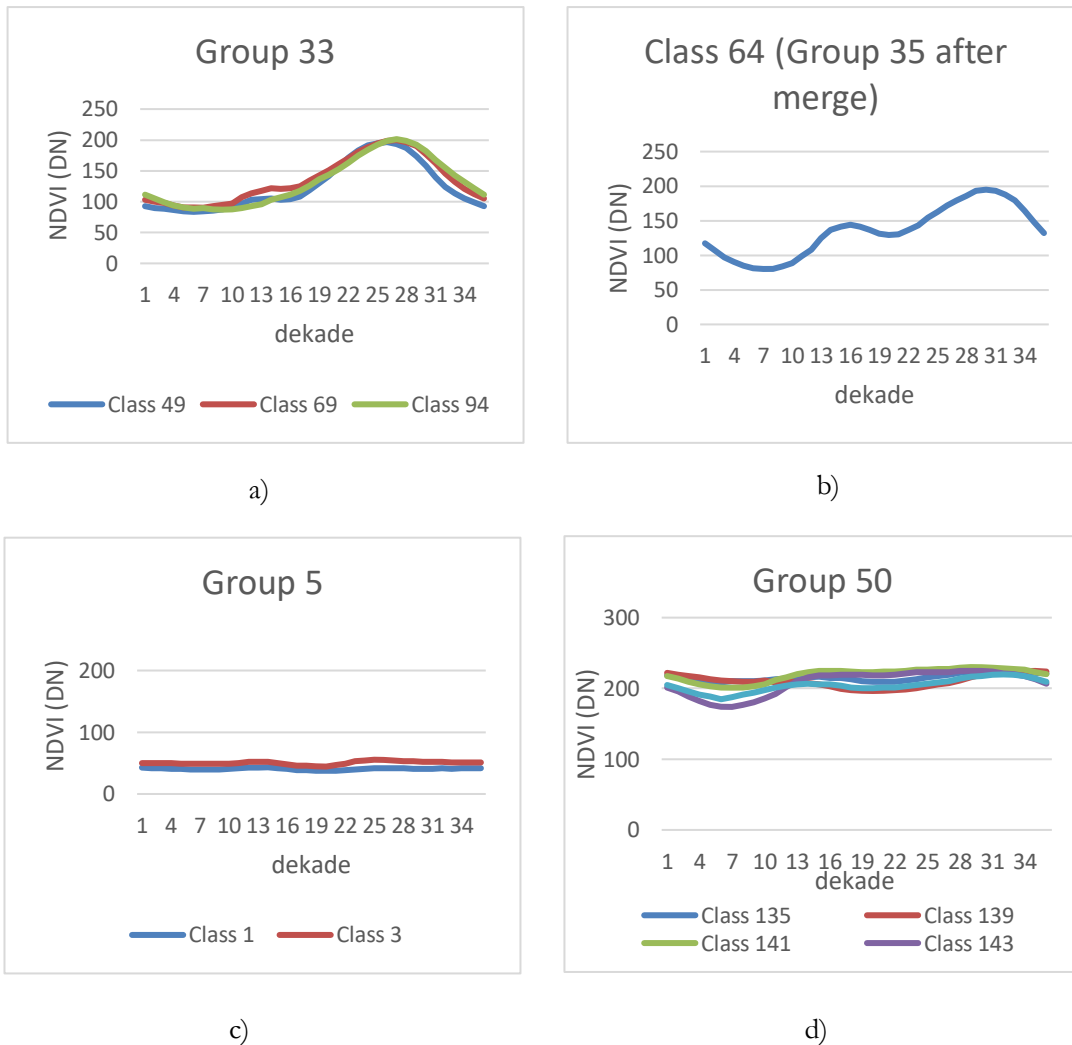c)   d)

Figure 6: Some examples of the grouped clusters through hierarchical clustering, profiles (lines) denotes the initial classes behavior, titles named groups denote the cluster number after merge

Regarding non-agricultural clusters, Figure 6-c represents temporal behaviour for initial clusters 1 and 3 which have been merged to form cluster 5 after the hierarchical clustering. The behavior of these clusters can be described as stable (i.e. no abrupt change in greenness) and low through the year which indicates bare land or water dominance within clusters 1 and 3 and because of very low value more likely to be water. On the other hand, the behaviour in Figure 6-d characterised to be stable also but high greenness amount. Clusters in Figure 6-d are dominant by forested areas with an increase of greenness around May and again around August. The increase of greenness in these clusters related to rainfall since the date of increase

coincide with dates of seasons in some other clusters (for example cluster 35 in Figure 6-b). The interpretations of these examples have been confirmed visually using Google Earth imagery.

4.1.2. Regression for 1km field fraction estimations

To prepare the data for regression, the agricultural census data was related to the spatial districts and then intersected with NDVI clusters (Figure 7). The table within Figure 7 displays an example of legend construction. Legend construction -in this context- is a process of determining the occurrence of NDVI clusters within each cluster in terms of area in hectares.
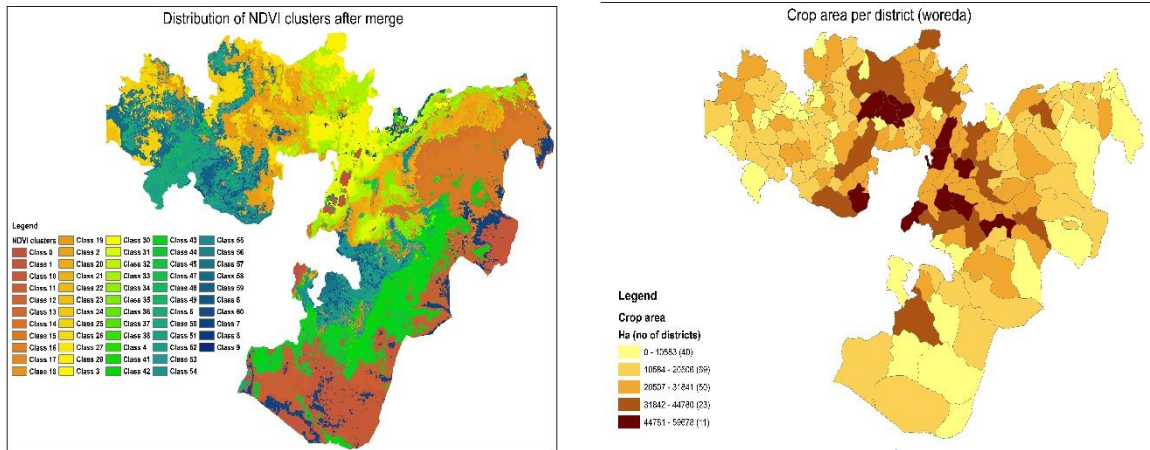
Woreda	Crop area (ha)	Class 48 (ha)	Class 50 (ha)	Class 53 (ha)	Class 54 (ha)	...
Mana Sibu	23,029	1,611	0	23,907	283	...
Nejo	14,390	279	0	8,536	0	...
Gimbi	9,085	4,845	0	37,467	272	...
Lalo Asabi	5,645	275	0	17,621	0	...
Boji	12,739	3,329	0	22,512	0	...
Ayra Guliso	16,761	3,744	0	15,922	0	...
Jarso	18,238	302	0	10,349	0	...
Gidami	13,953	23,962	1,707	11,899	2,105	...
Hawa Welele	19,894	2,222	569	8,988	3,251	...
Gawo Dale	22,139	7,855	2,023	21,577	1,785	...
Dale Sadi	10,583	4,065	0	7,409	0	...
Ganji	5,784	112	0	9,170	0	...
...	...	...	...	...	...	...

Figure 7: The process of legend construction (NDVI clusters cross with agricultural census) and example of the output legend

The relationship between occurrences of NDVI clusters (i.e. proportional areas within the district) and crop area was investigated through a stepwise linear regression model (Khan et al., 2010). In other words, the predictors are the proportional areas of NDVI clusters within each district, and the response is the crop area per district in hectares. The results of the regression model are shown in Table 1, the coefficient column in the table represents the field fraction within each cluster. Cluster 54 and cluster 11 were less significant than the rest of the clusters. Three NDVI clusters contained more than 50% crop per km2, 11 clusters contained between 50% and 10% crop per km2, and 3 clusters with crop forms less than 10% per km2. This regression model was able to explain 91.4% (adjusted R2) of the variation in the agricultural census data. The cluster values in Figure 5 were replaced by the intensities (coefficients) from Table 1 to produce the 1km field extent fractions map Figure 8. The total CA based on the 1km field fractions produced was 3,954,067 while the reported CA in Oromia was 4,077,968. This suggests the method performed well in terms of relating agroecological zones to the reported statistics, but this should not be mixed with the accuracy of reported data. The agreement does not necessarily indicate high quality reported statistics.

Table 1: Results of the regression model between district crop area and NDVI clusters

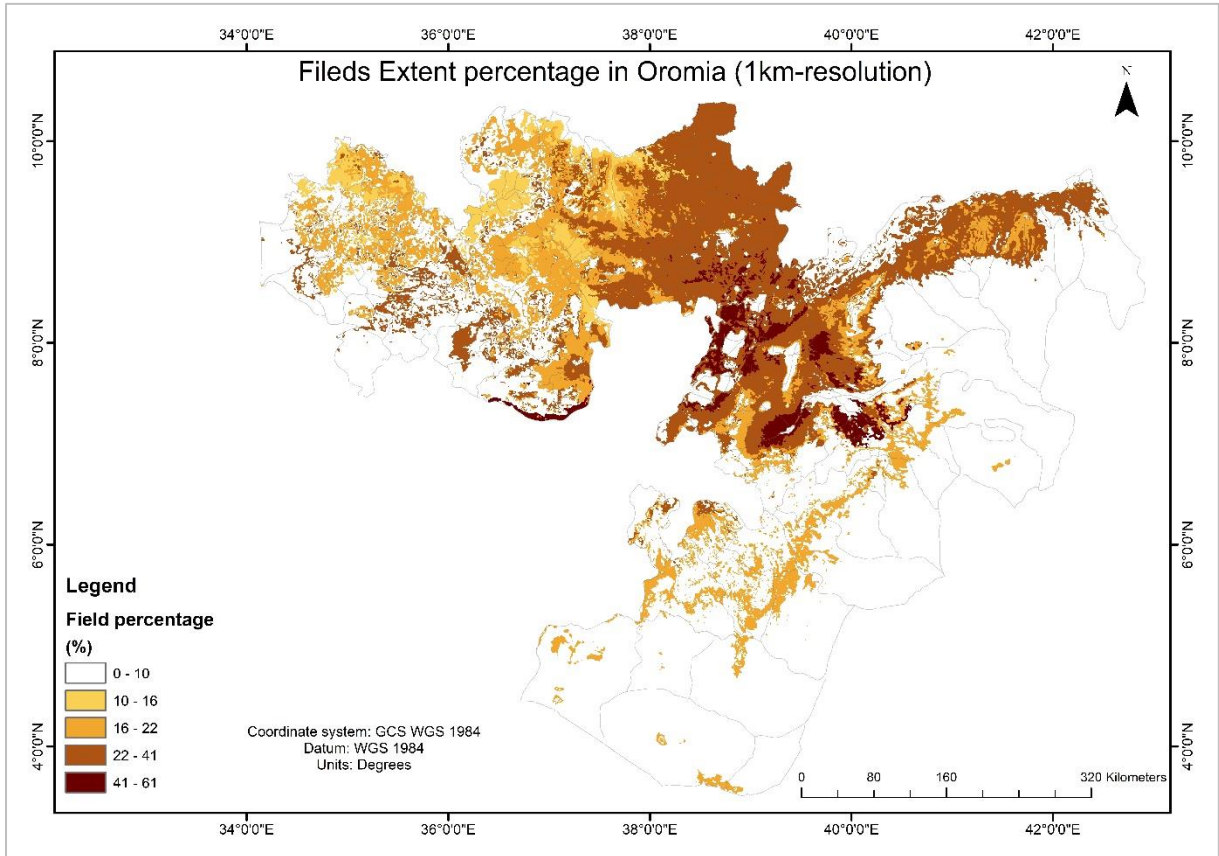| NDVI cluster	Coefficient	Sig.
20	0.301	0.000
30	0.342	0.000
33	0.307	0.000
19	0.203	0.000
54	0.039	0.146
57	0.219	0.000
35	0.614	0.000
31	0.525	0.000
29	0.276	0.000
34	0.328	0.000
11	0.023	0.113
48	0.405	0.000
56	0.503	0.000
42	0.165	0.000
59	0.411	0.000
15	0.028	0.003
26	0.114	0.012

Figure 8: Fields extent percentage per km²

4.2. Field fraction estimations at 30m

4.2.1. Global GAMs

Two global GAMs were developed in this study to evaluate the effect of including the 1km field fraction to predict field fraction at 30m-resolution. Both models applied four environmental predictors: elevation, slope, dry and wet season NDVI. The two models were evaluated using threshold-independent metrics to assess the model performance. To assess the performance and the predictive power of the models; independent 81 frames (i.e. actual fractions) were used. The overall deviance of the binomial distribution explained by each model and the area under the curve (AUC) were obtained. AUC indicates the goodness of fit. A perfect model would have AUC equal to 1 and a random model (chance model) would have a value of 0.5 (Ormerod, Manel, & Williams, 2001). Since our response variable is not binary and it has many levels, thus, instead of the normal AUC, a multiclass AUC (Landgrebe & Duin, 2007) was used in the present study. To assess the predictive power of the two models; an independent validation set was used. The field fractions predicted by both models were compared to the actual fractions of the 81 frames.

The AUC and overall deviance explained before including the 1km field fraction were 0.73 and 38.5% while after adding that variable the AUC and overall deviance explained improved to 0.83 and 62.2% respectively. The relationship between the predicted field fraction by both models and the actual fractions are shown below. The figure shows points in a form of vertical lines because the distribution of the sample was binomial with systematic grid at sub-frames level. The predicted fractions explained only 69% of the variations in the actual fractions when the 1km field fractions were not included (Figure 9). Including the 1km field fractions allowed the predicted fractions to explain 77% of the variation in the actual fractions (Figure 10). Based on all these performance and accuracy metrics; it is very clear including the 1km field fractions improved the model massively.

The model included the 1km field fractions improved the low extremes predictions compared to the other model. Even though the model including the 1km field fractions improved the predictions significantly; the model was weak in capturing the extremes.
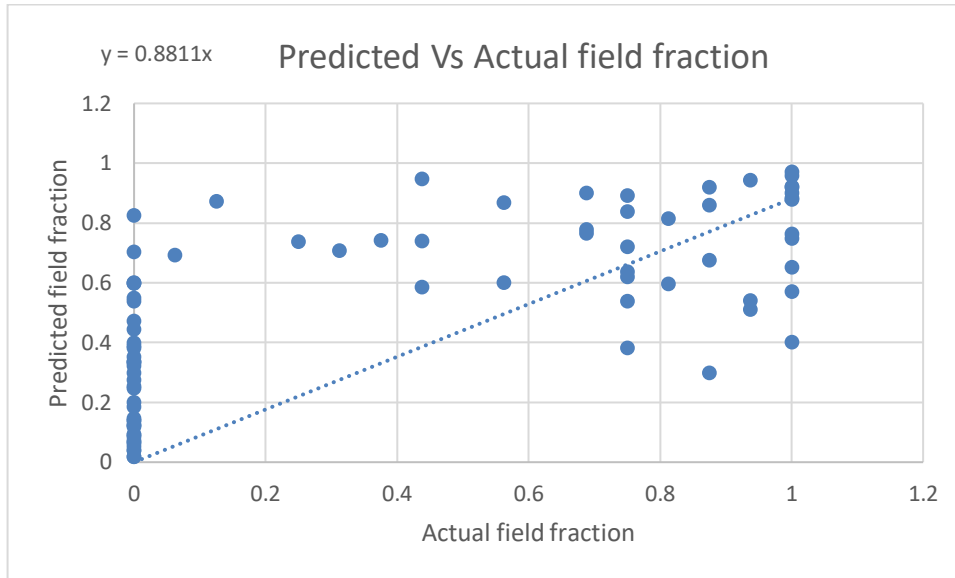

Figure 9: The relationship between actual field fractions and predicted field fractions without including the 1km field fraction in the model
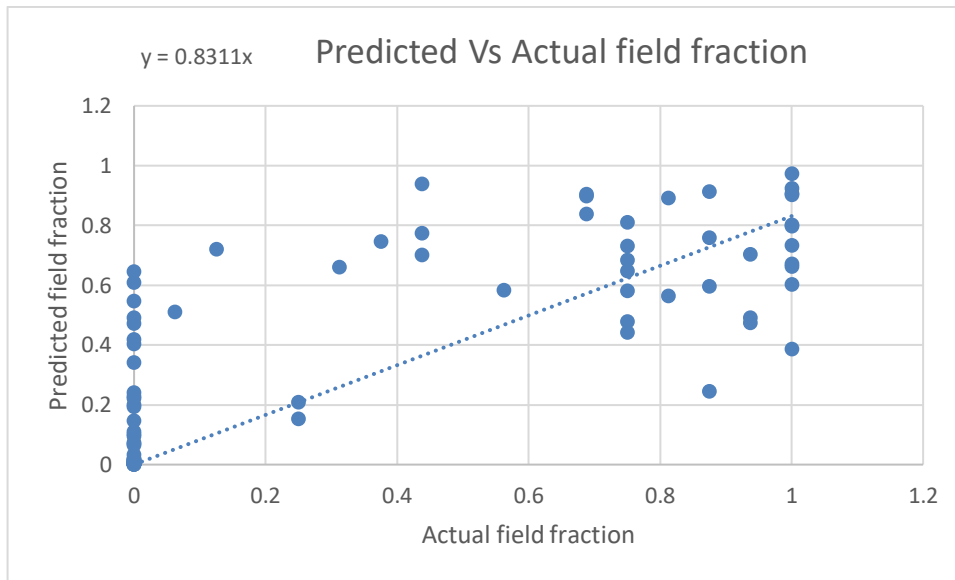

Figure 10: The relationship between actual field fractions and predicted field fractions after including the 1km field fraction in the model

Table (2) shows the p-values for each predictor in both models to illustrate how adding the categorical predictor affected the significance of each predictor. In the model without including the 1km field fractions, the most significant predictor was the dry season NDVI, followed by elevation. Slope was the third significant predictor and wet season NDVI was the least significant predictor. All predictors in this model were found to be significant ($p<0.001$) except wet season NDVI (i.e. $p<0.01$). Similarly, in the model included the 1km field fractions the relative importance remained the same as in the other model (i.e. the order of importance). Since the 1km field fraction variable was produced based on long term NDVI clustering, that variable inherits information about climatology thus it lowered the significance of all the

environmental predictors (i.e. multicollinearity). Out of 17 categories of 1km field fractions, 8 categories were found to be significant.

Table 2: The p-values of the environmental predictors before and after adding the categorical variable

Predictor	Without 1km fractions	With 1km fractions
Elevation	1.75e-08	6.95e-05
Slope	0.000108	0.000142
Dry season NDVI	1.33e-10	4.97e-08
Wet season NDVI	0.003176	0.096137

Based on that, the final model included: elevation, slope, dry season NDVI, wet season NDVI, and the 1km field fractions was investigated in detail. The individual relationships (i.e. partial correlation) between each predictor and the field fraction (i.e. crop field probabilities). Moreover, the partial deviance explained by each predictor was explored. Figure 11 shows the deviance explained of the binomial distribution by each predictor in the improved model, among the predictors, the 1km field fractions was the most important predictor with deviance explained 24%. Followed by dry season NDVI with deviance explained 16%. While elevation explained 15%, slope explained 6% of the deviance. Wet season NDVI was the least important predictor with 0.6% deviance explained.
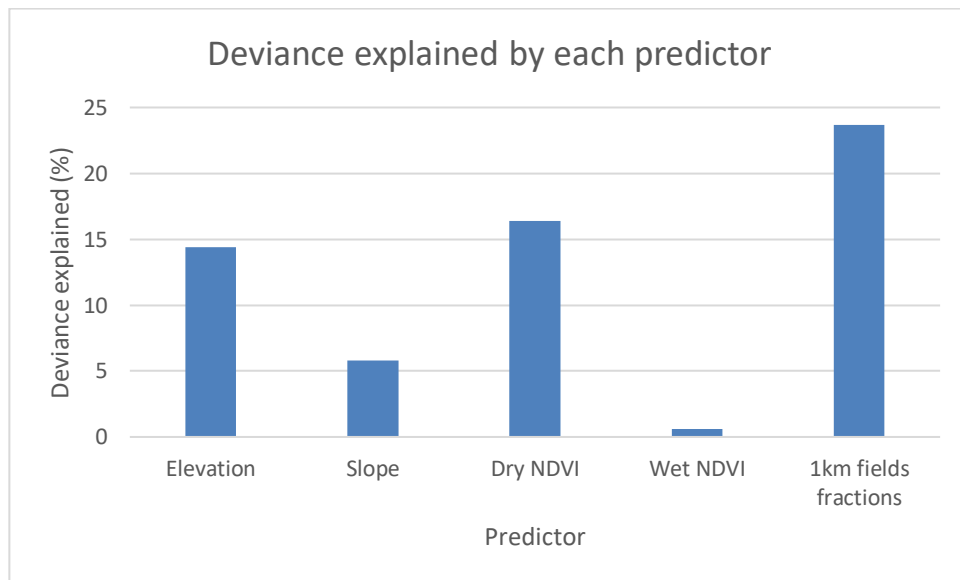

Figure 11: Deviance explained by each predictor

The following figures show the relationship between each predictor and the response values which in this case the crop field probabilities expressed as log of odds ratios. However, the log of odds ratios can be used to explain the relationships because those ratios are proportionally related to the probabilities (Bland & Altman, 2000).

In Figure 12-a, the relationship between crop field probabilities and the elevation characterised as a nonlinear relationship. It can be seen that areas with elevation between 1500m and 2500m are very likely to be cropped. Areas lower or higher are expected to have less cultivated areas. This can be due to the preference of the farmers to plant on those areas and/or due to suitable landscape characteristics within these altitudes. The model shows more certain predictions in moderate elevation values. In contrast, the model shows wider confidence values (i.e. less certain predictions) at high altitude areas with low capability of discriminating field fractions (i.e. semi-flat line).

Figure 12-b shows the relationship between slope and occurrences of agricultural fields. The crop field probabilities are negatively correlated with slope, areas steeper than 20% are expected to have less cropped areas. The model shows high uncertain predictions on very steep areas (i.e. >40%) due to the small number of observations (i.e. the small lines along the x-axis) having very high slope values.

Figure 12-c shows a negative correlation between the probability of an area being cropped and dry season NDVI. Overall, a form of exponential relationship can be seen in the figure. As dry season NDVI increases (i.e. most likely forest, or grass, or any other green vegetation) there is less chance of cropland. In areas with dry season NDVI higher than 0.51, the probability of agricultural fields declines drastically.

In Figure 12-d, the crop field probabilities are proportional to the wet season NDVI. The graph shows that the model faced difficulties in discriminating agricultural fields within low wet season NDVI values, the curve was flatter compared to the curve of dry season NDVI. This is related to the significance and deviance explained. The wide confidence values at lower wet season NDVI values probably due to few samples at that range of NDVI. From the figure, most of the cropped areas had wet season NDVI values higher than 0.75.
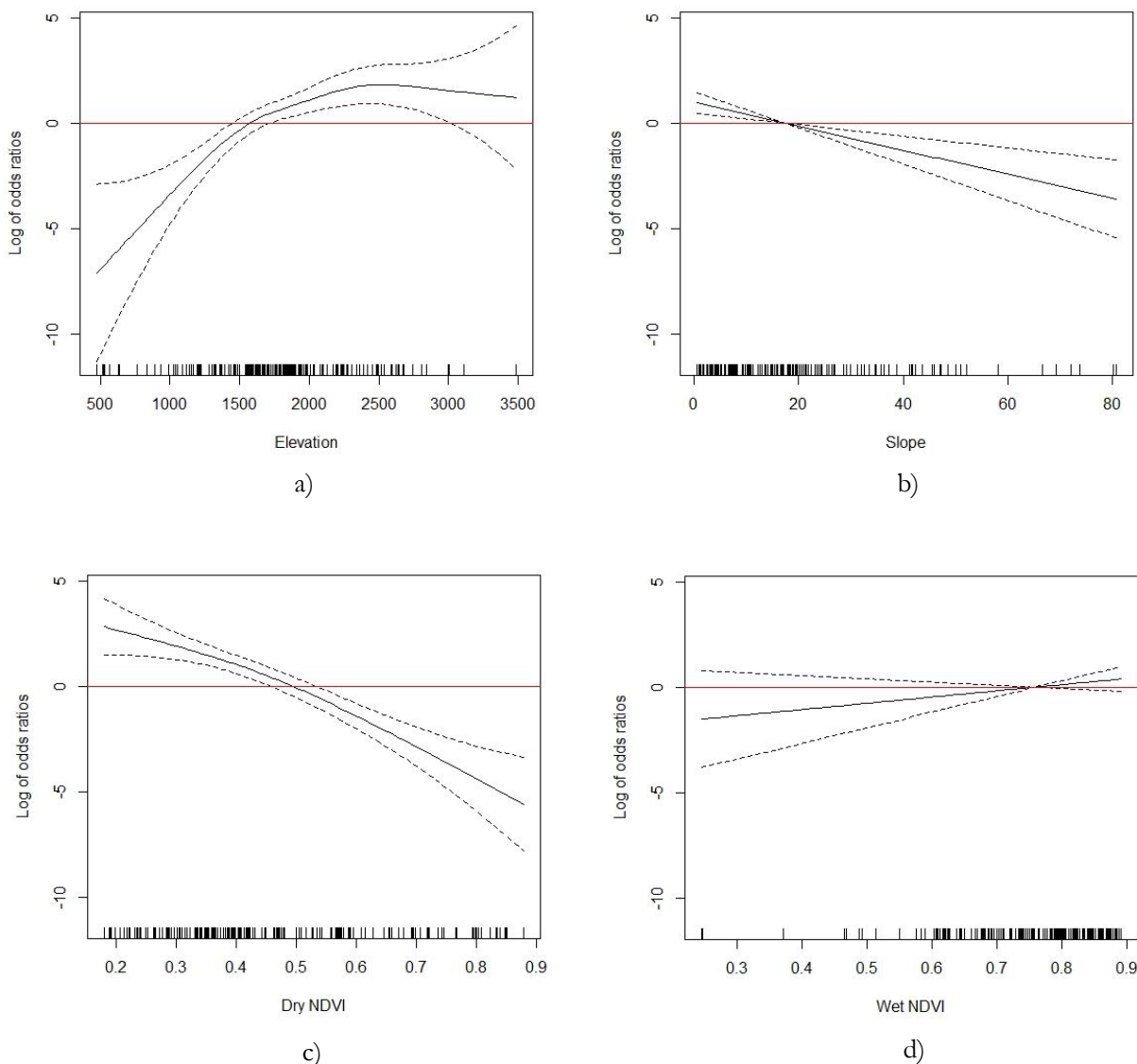

a)

b)

c)

d)

Figure 12: Relationship between crop field probabilities expressed as log of odds ratios and smoothing term of: a) Elevation, b) Slope, c) Dry NDVI, d) Wet NDVI. The red line represents 0.5 field probability (zero odd ratio). The small lines along the x-axis are predictor's values at sample locations. Dot lines are 2 standard error above and below.

The final global model was applied over the whole Oromia to produce 30m-resolution field fractions (Figure 13). The 30m map showed an overall agreement with the 1km map in terms of detecting fields. However, the30m map showed more agricultural areas due to the extremes issue shown in the above figure. Due to the change in the pixel size (i.e. smaller), very high values appeared (even 99.8% fields at pixel level) in the map. The total agricultural area in Oromia according to our model was 10,109,174 hectares (31% of Oromia region) while the total area reported by agricultural census data was 4,077,968 hectares. Our model showed a large crop area estimation compared to the reported agricultural areas by the agricultural census, our model is suspected to overestimation taking into consideration the complexity of the landscape. But at the same time, agricultural census data is suspected to underestimate. Some areas were checked just visually to get an insight about the estimation, for example the southern areas in Figure 13 with dense agricultural areas, those areas contain large natural pastoral lands with some agricultural fields, while the agricultural census reported less agricultural areas in those parts (i.e. from the 1km field fractions).
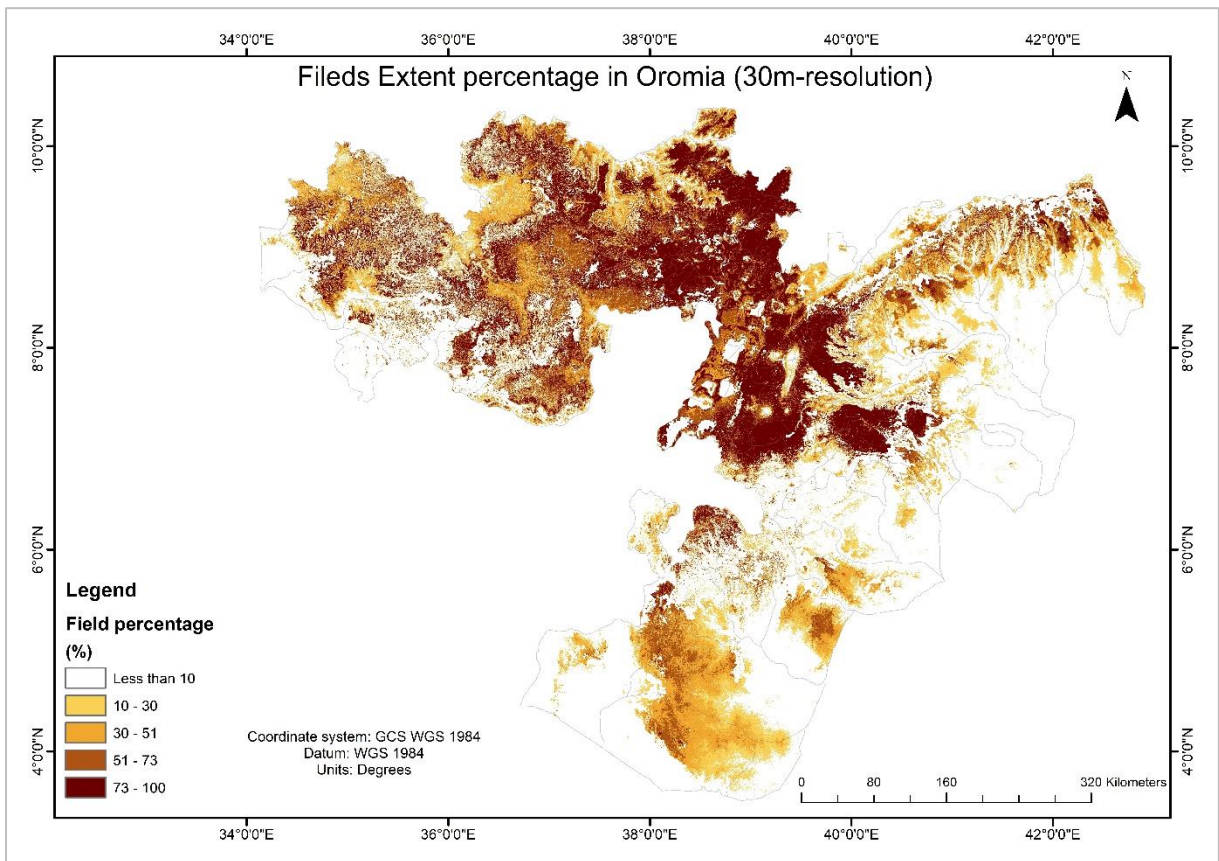
Figure 13: Map of the predicted field fraction (30m resolution) in Oromia

4.2.2. Global GAM and local GAM

The described global GAM above is easy to be developed since the process of creating the categorical predictor can be fully automated. On the other hand, developing separate models at each agroecological zone may result in better predictions but it can be a tedious task. Therefore, a localised GAM model was developed within cluster 35 (Figure 14) to be compared with the final global model produced above to demonstrate the differences. This cluster was chosen because it was the smallest cluster captured after incorporating agricultural census data to hyper temporal NDVI. Thus, less time can be consumed to run the experiment.

An independent data set within cluster 35 was used to develop the model and to test it later (Figure 14), the sample contained 507 binary 30x30m frames, 356 observations were used to develop the model, and 152 observations were used to test the model later to be compared to the global model. Cluster 35 is a relatively topographically homogenous unit. Therefore, elevation was found to be insignificant (p-value = 0.79). It explained nothing of the deviance of the binomial distribution. Thus, a model including slope, dry season NDVI and wet season NDVI was developed. The AUC for the model was 0.96 and the deviance explained was 64.2%.
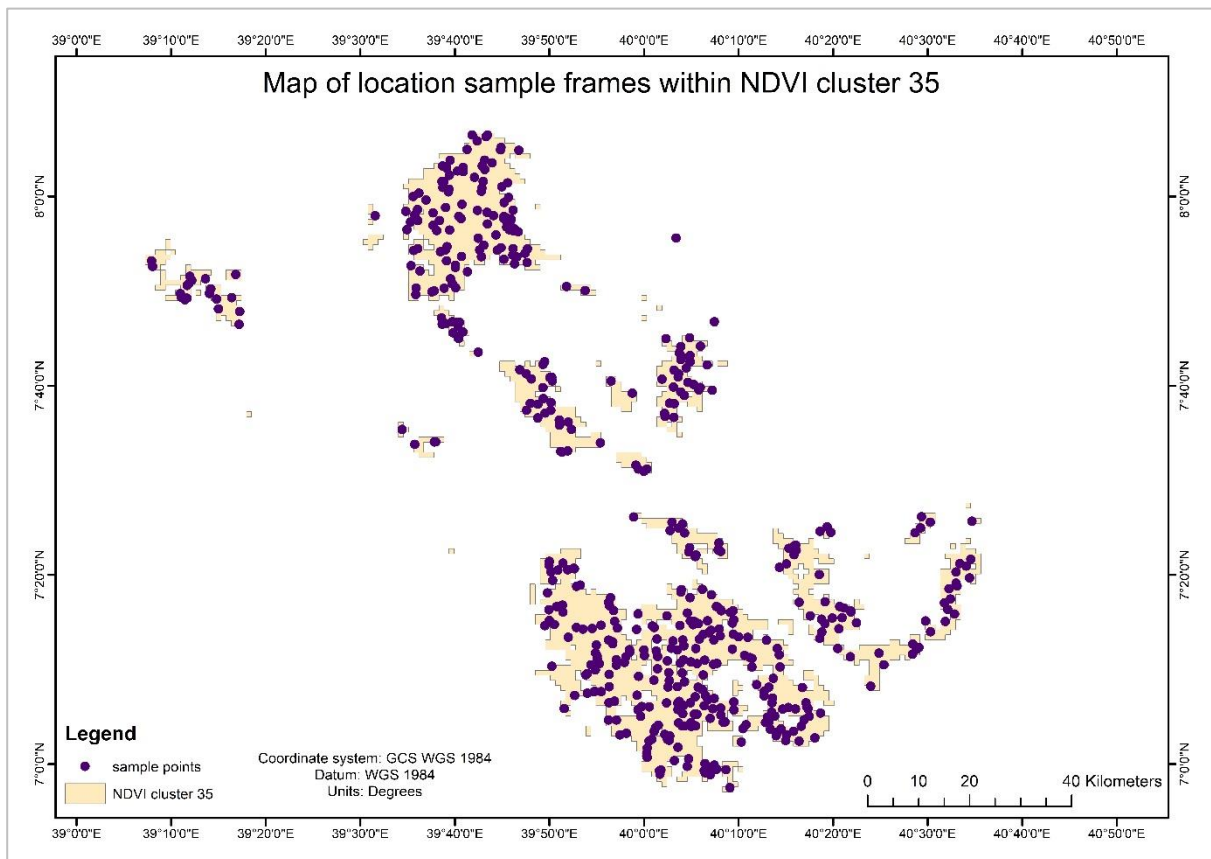
Figure 14: Sample locations within NDVI cluster 35

Table (3) lists the p-values and the deviance explained by each predictor, all variables were highly significant (p<0.001). However, the deviance explained by each variable differed, slope was found to be the most important variable in terms of deviance explained 27%. That was basically due to the presence of very steep areas at some edges of the cluster (Figure 15) meaning slope was the most discriminant factor between agricultural areas and non-agricultural areas within that zone. Dry season NDVI was the second important variable with deviance explained 24%. Similar to the global model, wet season NDVI was found to the least significant predictor with deviance explained 16%.

Table 3: p-values and deviance explained by each predictor in the stratified GAM

Predictor	p-value	Deviance explained (%)
Slope	4.97e-11	27
Dry season NDVI	2.60e-11	24
Wet season NDVI	0.000391	16

Figure 15: Estimated field fraction and the effect of the edge steep areas

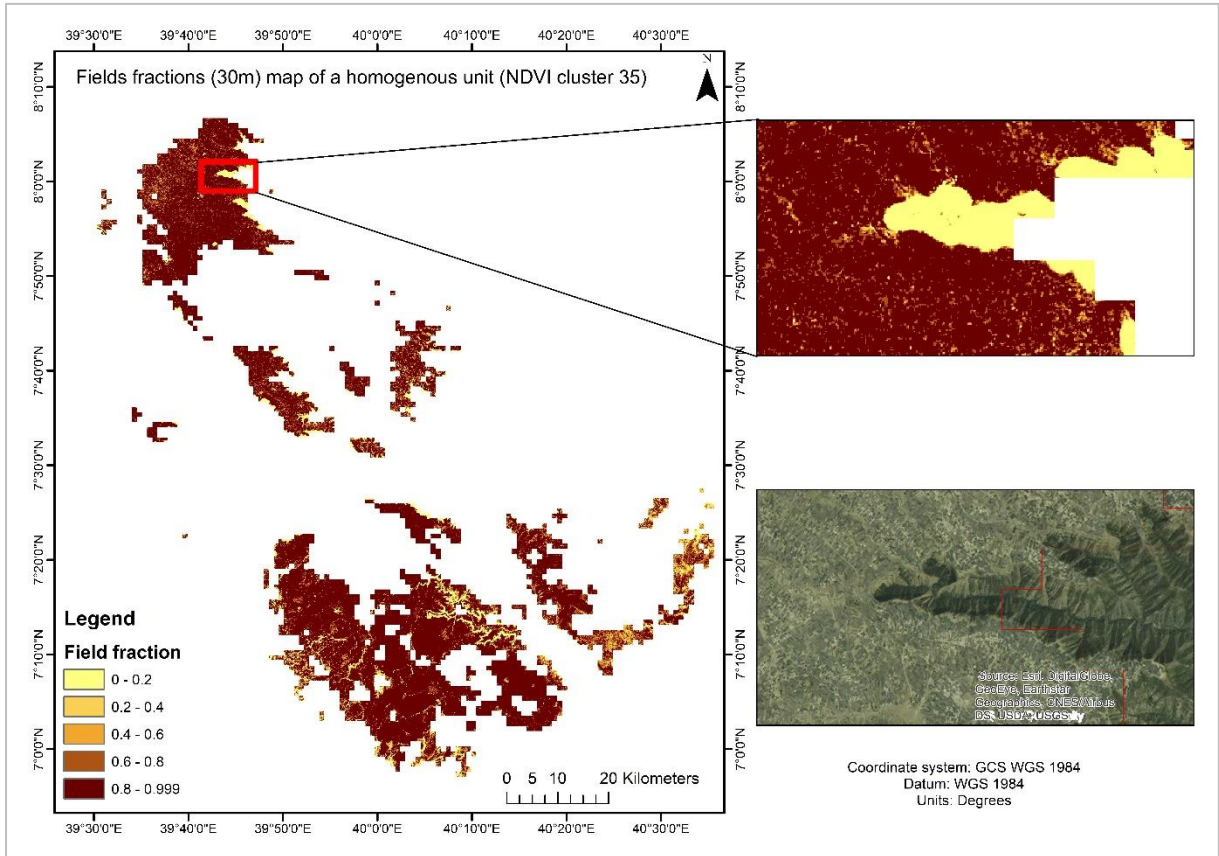Figure (16-a) shows that the relationship between crop field probabilities and slope, the relationship is a negative nonlinear relationship. The crop field probabilities decrease drastically in steeper areas (steeper than 20%) meaning areas steeper than 20% are unlikely to be cropped.

From Figure (16-b), dry season NDVI is showing almost semi flat behaviour which means the model suffered in discriminating fields from non-fields areas based on dry season NDVI. Even though the partial deviance explained by dry season NDVI was high. The model showed that areas with dry season NDVI above 0.35 are less likely to be cropped.

In Figure (16-c), it can be seen that the crop field probabilities increase with the wet season NDVI. Unlike the global model, the stratified model was able to discriminate crop and no crop areas up to a value of 0.55. However, the model showed high uncertainty in those areas due to the few observations at that range. Between 0.55 and 0.85 wet season NDVI values, the model became flat which indicates difficulties in discriminating different levels of field fractions. However, this part of the model showed highly certain predictions as can be seen from the narrow confidence bands. The model showed highly uncertain predictions in areas with wet season NDVI values above 0.87. The fluctuations seen in mid values (e.g. at value 0.68) probably due to the existence of natural vegetation in the zone.
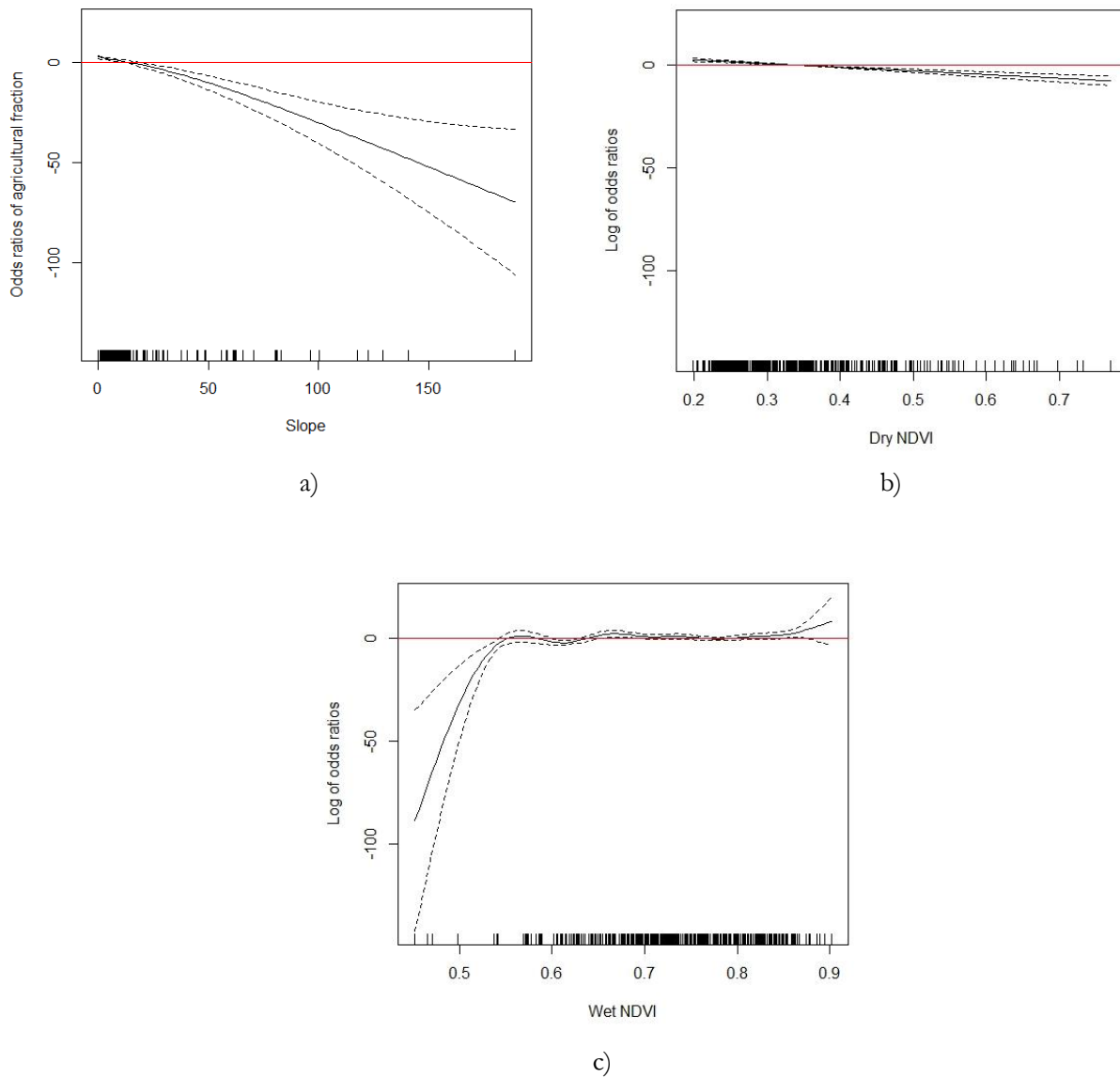
Figure 16: Relationship between crop field probabilities expressed as log of odds ratios and smoothing term of: a) Slope, c) Dry NDVI, d) Wet NDVI. The red line represents 0.5 probability (zero odd ratio). The small lines along the x-axis are predictor's values at sample locations

Finally, to assess the performance of the local GAM to the global GAM, both models were used to predict the agricultural fractions over the independent 156 binary frames. The stratified GAM was found to be slightly better than the global model, the AUC values were 0.90 and 0.89 for the stratified GAM and global GAM respectively. That indicates a need for other predictors at local scale, and at the same time, it indicates that the global GAM compensated for the information about climatology. The global model showed great performance compared to a local GAM developed only within only one agroecological zone.

5.   DISCUSSION

5.1.   On estimating field fraction at coarse resolution (1km)

Agroecological zones require several types of information to be identified properly such as: topography, climate, soil and land use (Quiroz et al., 2000; de Bie et al., 2008; de Bie et al., 2008; de Bie, Nguyen, Ali, Scarrott, & Skidmore, 2012; Usman, Liedl, Shahid, & Abbas, 2015). Hyper-temporal NDVI stratification was found to be appropriate in identifying the spatial climatological patterns based on the fact that the greenness of distinct zones differs (Ali et al., 2013).

Using ISODATA clustering algorithm 150 clusters were produced, the result showed that long term NDVI could be used for capturing the different agroecological zones. The strata showed homogenous patterns which can be due to many factors, for example, there was a clear pattern following the terrain changes (i.e. topographic uplift). The implications that can be driven from such temporal profiles of NDVI support the argument of the advantage of using hyper temporal NDVI stratification for delineating different mixtures of land cover. Different dominant land cover types can be identified through the profiles as explained in (section 4.1.1). The agro-ecological zones that showed bimodal phenology (i.e. two seasons) are located mostly in tropical areas. The crop field probabilities are expected to be high in such zones. Among these zones, the zones with higher rainfall amounts have a higher probability of agriculture. Compared to zones with bimodal phenology (i.e. one season), crop field probabilities are expected to be less in such zones. Monomodal behaviour of NDVI profile indicates drier areas and less rainfall amount. Stable (i.e. no peak) NDVI profile with low values indicates bare lands in arid or semi-arid regions. Due to lack of rainfall, less crop field probabilities (i.e. possibility of zero crop field probability). The stable NDVI temporal profile with high values indicates forested areas or green vegetation. Although such zones are located in areas with a high amount of rainfall, low crop field probabilities are expected within such areas. Other reasons may lead to low cropping areas in these zones can be inappropriate soil type for cropping, slope (i.e. very steep), proximity to other infrastructure (i.e. too far), protected forests. The capabilities of the stratification of long NDVI series to discriminate between different land cover types was shown in a study by (Ali et al., 2013).

Regarding the number of clusters, the initial number of clusters was determined randomly just as a relatively large number to avoid merging clusters that supposed to be separate. That was followed by using hierarchical cluster analysis to merge the clusters without losing the structure (Gonçalves, Netto, Costa, & Zullo Junior, 2008). This can be considered as a simple and time efficient approach for optimising the number of clusters which in this study was 60 clusters. However, de Bie et al. (2008) suggested the use of separability values (i.e. minimum and average separability) to determine the optimal number of meaningful ecological units. For future studies, separability analysis can be a better alternative to determine the optimal number of clusters, in this context, it is an iterative process in which several runs with different numbers of clusters are used and then based on divergence statistics the optimum number of clusters can be determined. The minimum and average separability values can be used to determine appropriate options for the number of clusters.

The NDVI ecological zones explained 91.4% of the variation in the reported crop areas. The value of adjusted R^2 was comparable to another study applied using the same method. In a study by Khan et al. (2010) in southern Spain, the authors achieved adjusted R^2 of 98.8%, 97.5%, and 76.5% for rainfed wheat, rainfed sunflower, and barley respectively. A major difference between their study and the current study was that they applied the method for specific types of crops, while in the current study the objective was to estimate the field fraction regardless the crop type. The authors in that study found that the method was capable of capturing the variation between different zones (i.e. relative determination of field fractions). This finding supported accepting the produced 1km fractions maps in the present study. However, the effect of applying the method for all crops together or separately still undetected. To elaborate, the relatively lower adjusted R2 achieved in the current study perhaps due to including all crops. Another reason perhaps is the

quality of agricultural census data. More import reason could be that the landscape in Ethiopia is more complex and fragmented (i.e. topographically heterogenous and climate is more variable) compared to southern Spain. In line with that, the size of the farms in Ethiopia is probably smaller than in southern Spain. The distinct phenology of the agro-ecological zones are related to certain crops mixed with other land cover types (Waine, Taylor, & Juniper, 2014) in addition to cropping systems (Wu et al., 2010). Perhaps relating the temporal behaviour of agroecological zones to all crops led to an over-generalization of the relationship and therefore lower R2. Due to time limits, no validation set at 1km was produced to validate the product. For future studies validation frames of 1x1km can be developed through free cost Google Earth images to validate the method more critically when applied for all fields regardless of the crop type. For the present study what is critical is that prior probabilities of crop area were generated and significantly improved the estimation at higher spatial resolution. The coarse field fractions variable was included in the GAM as a categorical predictor which was represented in terms of levels. In other words, this variable was not included as a continuous predictor. Thus, the absolute value of field fraction is less important. This variable brings in hyper temporal data over a long time. Therefore, it captures some of the long-term agroclimatic conditions for agriculture which can compensate for the complexity of mapping over large scale areas (i.e. over different climatological conditions). As previously mentioned, there was no validation set developed and therefore no guarantee that if the 1km fractions produced fulfilled the relative determination aspect which leaves a degree of uncertainty. The high adjusted R^2 resulted in this study should not be taken as an assurance of high quality of the agricultural census data. Basically it showed that there was a linear relationship between the agroecological zones occurrences and the reported district statistics.

In the present research, the 1km field fraction product was used to develop the fine resolution model, but this product reveals very useful information that can be applied differently. The downscaled agricultural census data can be useful for policy-makers because it allows them to develop policies based on critical spatial analysis of agricultural fields. Moreover, applying the regression model for different crops separately can allow for food security analysis at large scales but for more critical food security analysis, more detailed product is needed.

5.2. On estimating field fraction at moderate resolution (30m)

5.2.1. Global GAMs:

In this study, two GAMs for crop area estimation over Oromia region were evaluated. A model used four environmental predictors at 30m-resolution: elevation, slope, dry season NDVI and wet season NDVI. Whereas another model added downscaled crop area district data (i.e. 1km field fractions). The results showed that inclusion of the 1km field fractions improved the global model (i.e. the explanatory and predictive power) to estimate field fractions at 30m-resolution. Most of the researchers in crop-related applications focus on collecting EO imagery over the wet season. However, our results showed that dry season NDVI was more important than NDVI for field fractions estimate. In fact, the dry season NDVI was the most important predictor out of the four environmental predictors. Elevation was found to be important in explaining the deviance of the field fractions and subsequently predicting the field fractions over Oromia.

The produced 1km field fractions added 24% to the overall deviance explained (i.e. 62%) by the model. Among the other predictors, the 1km field fractions was the most important predictor. Our model utilised information about the relationship between agro-ecological zones (i.e. derived from hyper temporal NDVI) and the reported crop area. This predictor was important because agricultural field abundance is affected by different climatological conditions. In reality, the relationships between landscape characteristics (e.g. elevation, slope) and agriculture can be different among the different agroecological zones (Brink & Eva, 2009; Grace et al., 2014). That can be explained by taking elevation as an example. In Oromia, most of the regions contain highlands. In such regions, farmers may plant more areas due to the high rainfall and low

temperature. So high field fractions can be found in many ranges of high altitudes. Whereas, in low altitude areas, farmers may plant different types of crops and in fewer areas. The functional form of the relationship will differ compared to highlands. It can be that the field fractions are high in some low altitude areas then continue to increase without dropping (i.e. no extreme highlands). The model based on only the four environmental predictors ignores such differences and subsequently showed low overall deviance explained. Therefore, the importance of this predictor comes from that it utilised the reported agricultural statistics and agroecological zones to determine the agricultural abundance at coarse level. In other words, agroecological zones consider the differences in landscape characteristics (i.e. terrain, climate, soil, geology) between the zones while the reported statistics show which agroecological zones have higher field fractions. In the model, the general forms of the relationships are assumed to be same among the zones, but the differences are captured implicitly through fulfilling fifth criterion related to the 1km field fractions. In zones with higher field fractions at coarse resolution, the higher proportions of moderate resolution field fractions occur at those zones. To summarize, the combinations of the four predictors values for high crop probabilities are not same for all agroecological zones. Similarly, the combinations values are not same for low crop probabilities among different zones. The 1km field fractions variable allows compensating for these differences through explaining a large part of deviance that left after using the four predictors.

The overall explained deviance by our final model (i.e. including the 1km field fractions) was comparable to other studies applied to GAMs in complex and fragmented landscapes. Grace et al. (2012) incorporated demographic data in addition to biophysical variables in a GAM for CA. They achieved overall deviance explained 43% and 55% in Guatemala and Haiti respectively. Grace et al. (2014) achieved 41.9% and 81.4% deviance explained in 2011 and 2012 in an agricultural productive zone in Kenya. In Ethiopia, Husak et al. (2008) achieved 33.6% deviance explained. However, their model considered cultivated land in addition to grassland and shrubland for CA. Marshall et al. (2011) applied GAM for CA estimation in Niger; their model explained 75% of the overall deviance in CA. In all these studies, the produced CA maps were at coarse resolution (>2km). Unlike those studies, the present research produced the field fractions at 30m-resolution. This is indicating good explanatory power by our model because getting overall deviance explained value comparable to those previous studies but at 30m-resolution can be considered as a big step forward in CA mapping. The predicted field fractions by the global model included the 1km fractions showed a better relationship with the actual fractions. The value of R2 improved from 70% to 77% after including the 1km field fractions. Among the previous studies under consideration, only Marshall et al. (2011) compared their predicted fractions to actual fractions, and they achieved R^2 of 73%.

Regarding the relationship between the environmental predictors and probability of agricultural fields, dry season NDVI was found to be the most important factor. The dry season NDVI showed a negative correlation with cropping probabilities. The model showed an exponential relationship with a drastic decrease in cropping probabilities at areas with dry season NDVI greater than 0.51. As mentioned before, areas with high dry season NDVI represent dense vegetated areas and trees. The steepness of the relationship and the narrow confidence band indicated that the dry season NDVI had high capability to discriminate between different field fractions. It was important to use dry season NDVI due to the different behaviour of cropland and other green vegetation during the dry season. These land cover types are difficult to be discriminated through only wet season NDVI (i.e. they show high wet season NDVI values). The importance of dry season NDVI in the current model suggests that Oromia has large areas of forests, pastoral lands, or any other green vegetation.

The second most important biophysical predictor was elevation. Based on our model, at low altitude areas there was less probability of cropping. Low altitude areas are expected to have high temperature and low precipitation relatively. Therefore, farmers avoided cropping in such areas in Oromia. According to Alemayehu et al. (2012), most of the smallholder farms are located in semi-humid highlands (i.e. 70% of the total crop area) and 26% located in relatively drier highlands. Only around 4% of the total crop area was in semi-humid lowlands. Our model showed that the probability of a location being cropped became high in

areas with altitudes between 1500-2500m. In a good agreement with Husak et al. (2008) in central Ethiopia, the range found by them was 1500m to little more above 2000m. Taking into consideration that their study area was part of central Ethiopia which is a portion of Oromia region (i.e. their study area was smaller). Therefore, the range showed a difference between the current study and their study. The power of GAM it is that it allows capturing such complex relationships on different study areas and at different scales. For example, Grace et al. (2014) found that in two zones in Kenya (i.e. marginal mixed zone and high productive zone) the crop field probabilities were higher at low altitudes. Marshall et al. (2011) in part of Niger found the range of altitudes for high probabilities of agriculture was 300-400m. Therefore, using GAM allows determining the exact ranges of altitudes for high field probabilities.

The model showed the flat areas are more likely to be cropped. The effect of the slope in CA variations comes from its direct effect on soil characteristics and infiltration rate (Kaspar et al., 2003). Infiltration rate would affect CA massively particularly in rain-fed agricultural systems such as in Oromia region. Steep areas have lower infiltration rate and higher runoff rate (Mu et al., 2015). Thus, the water storage capacity of the soil is low and subsequently crops may not find enough water in the soil. Farmers avoid farming in steep areas because soil is shallower (Mehnatkesh, Ayoubi, Jalalian, & Sahrawat, 2013), less fertile (Selassie, Anemut, & Addisu, 2015) and harder to work (i.e. to crop) compared to flatter areas. Shallow soils are more prone to soil erosion and landslides (FAO, 1999). According to the model, the cropping probability decreased with the steepness with extremely low cropping probability in areas steeper than 20%. This finding supported by FAO publication about land evaluation; the report stated the areas with slope greater than 20% are not suitable for agricultural activities (FAO, 2007a). Similarly, Husak et al. (2008) found that in Ethiopia that the cropping probability decreased drastically in areas steeper than 20% slope. In a good agreement with Eggen et al. (2016), they found that the largest category of agricultural lands (45% of the total agricultural land) in Ethiopia Highlands were located in areas with slope less than 5% and two medium categories (28% and 21.9%) located in slope areas between 5% to 20%. Areas with a slope between 20% and 40% contained 5% of the total farmland. In area steeper than 40% slope, they found only 0.1% of the farmland located there.

Wet season NDVI was the least important predictor. The model showed semi-flat behaviour for the relationship between wet season NDVI and crop field probabilities after the other predictors were accounted for in the model. This indicates the wet season NDVI was not a helpful predictor in determining field fractions. As indicated above, in dense vegetative areas dry season NDVI tends to have high explanatory power, on the other hand, in those areas wet season NDVI tends to have low explanatory power (Marshall et al., 2011). Wet season NDVI was positively correlated with crop field probabilities. However, a typical form of this relationship is positive correlation up to a certain range and then the cropping probabilities start decreasing (due to forest areas or other densely vegetated areas) as found in these studies (Grace et al., 2014; Marshall et al., 2011). In the present research, the model showed a continuous increase for CA with wet season NDVI due to the inclusion of dry season NDVI in the model. The deviance explained by wet season NDVI was largely unexplained by dry season NDVI. Dry season NDVI identified forested and other naturally vegetated areas (i.e. negative correlation), thus, wet season NDVI in the present study did not show a decrease of CA in high wet season NDVI areas. That was tested by excluding the effect of dry season NDVI from the model. In that experiment wet season NDVI showed the typical form of relationships with CA. However, the model showed that areas with wet season NDVI greater than 0.75 are very likely to be cropped. Wet season NDVI can be important in crop-specific area estimation due to its ability to capture different phenological stages.

Comparing the two global models, the difference in terms of R^2 was not very high compared to the deviance explained by the two models. With a larger testing set, the difference is expected to be higher and the model including the 1km field fractions is expected to perform much better than the other model. Despite our model showed a high value of R^2, the value was leveraged by the extremes. It can be taken as an indicator for the good quality of our model, but it does not reflect the actual correlation (i.e. actual correlation is

expected to be lower). Compared to the model developed by Marshall et al. (2011), our model was weak at capturing the extremes in actual field fractions. The samples that showed low actual fractions and high predicted fractions (i.e. lower extremes) represented densely vegetated areas (including flooded areas and large streams) and dense trees (including dense trees between fields). Both classes sometimes act like cropland in terms of dry and wet season NDVI (i.e. low and high respectively) following rainfall events. This weakness in discriminating those areas can be due to the small size of the sample, in other words, the model needed more data to be calibrated. Basically, with small training sample the wet and dry season NDVI may not be able to discriminate between fields and dense trees or vegetation. That means those areas had elevation ranged between 1500-2500m, slope less than 20% and fell within non-zero 1km field fractions category. Those are the ranges for high crop field probabilities based on our model. Therefore, elevation and slope in addition to the 1km field fractions were not able to assist the model in discriminating them. The sample size is not the only factor that affects the model but also the range of observations (i.e. for field fractions and predictors). Regarding observations for predictors, the difficulties that our model faced in discriminating crop field probabilities at very high altitudes because very few observed values were at that high range (i.e. perhaps outliers). This effect was clear at low wet season NDVI values where the model showed high uncertainty.

On the other hand, upper extremes (i.e. low predictions and high actual fractions) can be attributed to fallow lands (i.e. without natural grass). In Google Earth imagery, the identified fields can be fallow lands at the date of the extracted median of dry and wet seasons. In that particular year, our model will define the frame as low crop probability due to the similar characteristics between bare land and the field which was left as fallow land at that year (i.e. low dry and wet season NDVI). Another possible cause perhaps errors in defining wet and dry seasons. These errors can be due to errors by analyst or the temporal window identified for the delayed moving average algorithm. The relationship between errors in identifying seasons and upper extremes can be explained through an example. Assuming the dry season NDVI was identified wrongly for one of the agroecological zones, cropland and evergreen trees within that zone may both have high dry season NDVI and subsequently low predicted fractions. Similarly if wet season NDVI was identified wrongly for one of the zones, cropland and bare land may have low wet season NDVI values and subsequently low predicted fractions. The delayed moving average algorithm was used in the current study because it is simple and time efficient.

The issue of both extremes can be attributed to misregistration errors. Google Earth images and the moderate resolution predictors may have alignment errors at pixel level taking into consideration the different sources of this data. In the present study, the native resolution of the predictors was used (i.e. 30m). This can be improved through aggregating the predictor to coarse resolution (Grace et al., 2012; Grace et al., 2014; Marshall et al., 2011). However, that comes at the expense of the product spatial resolution. A suggestion for further studies would be aggregating into 90x90m for example.

The abovementioned issues resulted in over-estimation of the total CA in Oromia compared to the reported statistics by the Central Statistics Authority (CSA). This comparison is difficult to be conducted due to the different definitions of CA between our product and reported statistics. Our method estimated cropland area including both active and fallow land (i.e. fields identified through Google Earth). Whereas in reported statistics only active crop land at 2001-2002 was reported. In Ethiopia, agricultural statistics are produced by both CSA and the Ministry of Agriculture and Rural Development (MoARD) and their estimates differed significantly (Carletto, Jolliffe, & Raka, 2013). Those findings were similar to the findings by Husak et al. (2008) in Ethiopia. The authors compared their CA estimation through remote sensing to the reported statistics by CSA for nine districts. They found that the remotely sensed total estimation was higher by 74% while for the present study our model overestimated the reported statistics by 148% (taking into consideration different study area size in the two studies). That was because of the extremes issues in our model compared to their model. However, the authors indicated a high positive correlation between the estimations which can be understood as an indicator of systematic bias. Another reason for the differences

between our product and the reported statistics is the shifting cultivation. Shifting cultivation is common in Ethiopia; the timely remote sensing information as used in this study can allow for capturing the changes while the reported statistics lack enough temporal information. Similarly, the changes in intercropping strategies by framers in different years my contributed to those differences. However, the agricultural census data in the present study was not used for validation. The method incorporated the agricultural statistics to determine the relative agricultural abundance with each agroecological zone at a coarse resolution to improve the CA estimation at finer resolution. Other data sources are available at global and regional scales but they are characterized with high uncertainty (Fritz et al., 2011; See et al., 2015; Vintrou et al., 2012). Official agricultural statistics data by CSA was considered to be the most accurate available data.

The method showed great performance in terms of predicting moderate resolution field fractions taking into consideration all the issues discussed above in addition to the fragmentation of the landscape. The method relied on using existing and freely available data. The only time-consuming part is developing the calibration set. However, compared to collecting data through field surveys, the method outlined in this study can save massive time. The method can be used by researchers and governments for applications related to CA such as: environmental studies, food security analysis and crop modelling. In a country such as Ethiopia which lacks quality information about crop area mapping and estimate, this method can produce good quality crop area information for any particular year by extracting dry and wet season NDVI for that particular year. A possibility of utilising free Sentinel-2 images (10m resolution) for a particular year to aid in visual interpretation with Google Earth can be explored for further improvements. Utilizing such data on the same year for dry and wet season NDVI would enhance the discrimination between fallow land and active fields. Sentinel-2 offers higher spatial, spectral, and temporal resolution compared to Landsat-8 (Forkuor, Dimobe, Serme, & Tondoh, 2018). Sentinel-2 has three bands in red-edge (20-m resolution). Red-edge bands represent a steep transition in the wavelength from red portion to near-infrared portion (i.e. sharp increase in vegetation reflectance) (Delegido, Verrelst, Alonso, & Moreno, 2011). Those bands were found to help improve the accuracy agricultural mapping (Ezzahar et al., 2018; Forkuor et al., 2018; Griffiths, Nendel, & Hostert, 2019; Immitzer, Vuolo, & Atzberger, 2016; Lambert, Traoré, Blaes, Baret, & Defourny, 2018). Useful indices can be extracted using these bands such as red-edge normalised index and then used as a predictor in GAM. Other vegetation indices -in which atmospheric and soil background effects are less than NDVI- can be useful to improve the accuracy of CA estimate. Examples of such indices that can be considered as potential predictors: enhanced vegetation index (EVI) and soil adjusted vegetation index (SAVI) (Sonobe et al., 2018). The capabilities of radar remote sensing can also be useful to be used in future studies. Radar systems are independent of weather conditions and they can penetrate clouds (Chen, Lasaponara, & Masini, 2017). This makes radar systems suitable for agricultural monitoring (Bargiel, 2017; Canisius et al., 2018; Jiao et al., 2014; Steele-Dunne et al., 2017) due to the ability to get cloud-free images during the growing season (Brisco, 2004). For example, Sentinel-1 radar system has spatial resolution ranges from 5m to 40m for different instruments and revisits time of 12 days which makes it appropriate for detecting temporal behaviour for crops (Veloso et al., 2017). Additionally, Sentinel-1 data can be used to retrieve soil moisture (Gao, Zribi, Escorihuela, Baghdadi, & Segui, 2018). Such data can be used as a predictor within the context of the GAM to explore its capability to improve the overall deviance of agricultural fields.

For future studies, to enhance the model in detecting extremes more extreme fractions (i.e. both low and high) should be collected to calibrate the model. In addition to the improvements mentioned above, there is an alternative worthy to be explored for further studies. The agro-ecological zones can be used only for defining wet and dry seasons per zone or it can be used as a categorical predictor. Based on that, NDVI data can be extracted for a particular year or two following years. However, other temporal windows can be explored in the delayed average algorithm and even other algorithms to extract seasonality such as peak NDVI method (Sakamoto et al., 2005) can be used. By developing a lot of samples using Google Earth images and Sentinel-2 images and adding some potential other predictors, the method is expected to

improve significantly. Due to time constraints related to this study, few samples were obtained while a sample size of thousands can be developed easily using the same way outlined in the current method. Other potential predictors to consider can be: livelihood zones (Marshall et al., 2011), demographic data (Grace et al., 2012), soil characteristics and population pressure (López, 2014). Socio-economic factors (e.g. population density, age of farmers, education, number of households) affect the agricultural distribution (Abah & Petja, 2015; Dang & Kawasaki, 2017; Teshome, 2014). Including such predictors to the GAM can improve the results significantly (Marshall et al., 2017).

5.2.2. Global GAM and local GAM

In a study area with fragmented landscape and high variations in climatic conditions, defining different homogenous zones and apply separate GAMs for each zone is expected to improve the estimations. Grace et al. (2014) suggested the use of separate GAMs for two different zones in Kenya named 'Marginal Mixed Zone' and 'High Potential Zone'. Their suggestion was based on the differences (e.g. climatology, terrain, land use practices) between the zones and separate GAMs would allow for improved estimation of CA. Therefore, in the present research a local GAM within one agroecological zone was developed to be compared to our final global model. Due to the homogeneity of the zone, elevation was found to be insignificant. Contradictory to that, slope was found as the most important predictor. That was due to the effect of steep areas at the edge of the zone. Those steep areas were non-agricultural areas; thus, slope was the main variable in discriminating fields from non-fields taking into consideration the zone was dominated by agricultural areas. Like the global model, areas steeper than 20% are very less likely to be cropped. Despite ISO DATA clustering divided the study area into relatively homogenous zones but issues related to edges remained. That can be due to running large initial number of clusters and then merging them. As mentioned above, an improvement would be to use the separability analysis to determine the optimal number of zones. The zone was dominated by agricultural areas (i.e. highest 1km field fractions zone) and some trees including trees between fields. Moreover, the steep areas at the edges contained shrubs and grass. Therefore, although dry season NDVI showed a semi-flat negative relationship (i.e. weak discrimination) but it explained 24% of the binomial deviance. Dry season NDVI was used to help in differentiating fields from trees and green vegetation and since those classes were abundant, dry season NDVI explained a large part of the deviance. On the other hand, wet season NDVI was important to discriminate between fields and bare land. That can also be seen from the steepness of the relationships. Wet season NDVI showed great performance in discriminating fields and non-fields even though the model became flat above an NDVI value of 0.55. However, areas with dry season NDVI less than 0.35 are more likely to be cropped. In another zone dominated by fields and bare areas, wet season NDVI would become more important than dry season NDVI since both these land cover types have high dry season NDVI.

Our global model was redeveloped using a binary response variable instead of fractions (crop/no-crop) to be compared to the local model. The comparison between the two models showed that the global model included the 1km field fractions was able to predict the crop field probabilities within that zone. The comparison showed very close results and the local model was not superior to the global model. However, there is a degree of uncertainty in this experiment. Although the two models were evaluated using the same testing set, different calibration sets were used to develop the models. Additionally, in the local model more one predictor was excluded (i.e. elevation).

In the local model, the different forms of the relationships between the crop probabilities and the predictors are explicitly addressed through developing separate GAM for each agro-ecological zone. Whereas in the global model, the forms of the relationships are considered to be same and the differences are captured implicitly through the 1km field fractions (i.e. the added partial deviance explained). Based on the results, including the agroecological zones from hyper temporal NDVI compensated for the differences in climatological conditions. The process of developing a global GAM is much easier and more time efficient than developing separate GAMs per zone. That makes our global model a vital tool for governments and researchers in applications related to crop area estimation.

6.   CONCLUSION

In this research, a method for crop field probabilities mapping (at 30-m resolution) in a fragmented landscape was developed and evaluated. In this study, agroecological zones (i.e. derived from hyper-temporal NDVI) were integrated with reported agricultural statistics to estimate coarse field fractions (at 1km-resolution). Since the study aimed at estimating crop field probabilities at moderate resolution (i.e. 30-m), four moderate resolution environmental factors were involved. The coarse field fractions, elevation, slope, dry season NDVI, and wet season NDVI were used as predictors in a generalised additive model (GAM). In the model, the predictors were able to explain 62% of the overall deviance in field fractions. The predicted field fractions by the model explained 77% (R^2 value) of the variations in the actual fractions of 81 validation observations. The 1km field fraction was found to be the most important variable (i.e. partial deviance explained value of 24%). Among the four environmental predictors, dry season NDVI was the most important predictor (i.e. 16% deviance explained) followed by elevation (i.e. 15% deviance explained). In other words, the inclusion of moderate resolution NDVI and terrain improved the explanatory and the predictive power of the model. This global GAM (i.e. over whole Oromia) was compared to a local GAM (i.e. within one agroecological zone) in terms of model performance. The area under curve values were 0.89 and 0.90 for the global model and the local model respectively. Thus, including a predictor related to the different climatic conditions (using hyper-temporal remote sensing) in a global model can replace developing separate GAMs per each homogenous zone. Taking into consideration the complexity of the landscape, GAM was able to capture the complex relationships between field fractions and the predictors. GAM has this capability since it relaxes linearity assumptions compared to other models which subsequently allow capturing complex nonlinear relationships. The method is easy and time efficient to be applied. Most importantly, all the data used to conduct this study were free of cost. Therefore, this method may contribute to providing timely, good accuracy, moderate resolution field fractions even in fragmented landscapes for food security and environmental studies. Thus, the method outlined can be used effectively by governments (i.e. particularly in developing countries with limited funds) to produce crop area maps and subsequently estimate the crop production. Accurate and timely information about crop production aids governments in decision and policy-making process to secure food. In future studies, using the agroecological zones as a categorical predictor in the model without incorporating the reported statistics can be explored. Other sources of remotely sensed data can be utilised to derive potential predictors to improve the crop field probabilities estimate. The red edge bands provided by Sentinel-2 can be used to derive red-edge normalised index. Moreover, using radar data (e.g. Sentinel-1) may improve the model due to its capabilities (i.e. cloud penetration and weather-independent). Additionally, some other vegetation indices such as enhanced vegetation index (EVI) and soil adjusted vegetation index (SAVI) can be explored as potential predictors. In addition to biophysical variables, including socio-economic variables (e.g. population density, number of households, income) is a valuable option to consider for applying the method in future.

LIST OF REFERENCES

Abah, R. C., & Petja, B. M. (2015). The Socio-economic Factors affecting Agricultural Development in the Lower River Benue Basin. *Journal of Biology*, *5*(24), 84–94. Retrieved from www.iiste.org

Adams, J. B., Sabol, D. E., Kapos, V., Almeida Filho, R., Roberts, D. A., & Gillespie, A. R. (1994). Classification of Multispectral Images Based on Fractions of Endmembers: Application to Land-Cover Change in the Brazilian Amazon. *REMOTE SENS. ENVIRON*, *52*, 137–154. Retrieved from http://www.geog.ucsb.edu/viper/viper_pubs/Adams_et_al95.pdf

Adams, J. B., Smith, M. O., & Johnson, P. E. (1986). Spectral mixture modeling: A new analysis of rock and soil types at the Viking Lander 1 Site. *Journal of Geophysical Research: Solid Earth*, *91*(B8), 8098–8112. https://doi.org/10.1029/JB091iB08p08098

Alemayehu, S., Paul, D., & Sinafikeh, A. (2012a). *Crop Production in Ethiopia : Regional Patterns and Trends. ESSP II Working Paper 16. International Food Policy Research Institute (IFPRI)*. Retrieved from http://www.edri.org.et/.

Alemayehu, S., Paul, D., & Sinafikeh, A. (2012b). *Crop Production in Ethiopia : Regional Patterns and Trends. ESSP II Working Paper 16. International Food Policy Research Institute (IFPRI)*. Retrieved from http://www.edri.org.et/.

Ali, A., de Bie, C. A. J. M., Skidmore, A. K., Scarrott, R. G., Hamad, A., Venus, V., & Lymberakis, P. (2013). Mapping land cover gradients through analysis of hyper-temporal NDVI imagery. *International Journal of Applied Earth Observation and Geoinformation*, *23*(1), 301–312. https://doi.org/10.1016/j.jag.2012.10.001

Alonso, F., & Cuevas, J. M. (1993). Remote sensing and agricultural statistics: Crop area estimation through regression estimators and confusion matrices. *International Journal of Remote Sensing - INT J REMOTE SENS*, *14*, 1215–1219. https://doi.org/10.1080/01431169308904405

Amede, T., Auricht, C., Boffa, J., Dixon, J., Mallawaarachchi, T., Rukuni, M., & Teklewold-deneke, T. (2017). A Farming System Framework for Investment Planning and Priority Setting in Ethiopia, (June), 52pp.

Arora, M. K., & Ghosh, S. K. (2003). An evaluation of fuzzy classifications from IRS 1C LISS III imagery: A case study AU - Shalan, M. A. *International Journal of Remote Sensing*, *24*(15), 3179–3186. https://doi.org/10.1080/0143116031000094791

Arvor, D., Jonathan, M., Simões, M., Meirelles, P., Dubreuil, V., & Durieux, L. (2011). Classification of MODIS EVI time series for crop mapping in the state of Mato Grosso, Brazil. *International Journal of Remote Sensing*, *32*(22), 7847–7871. https://doi.org/10.1080/01431161.2010.531783

Bargiel, D. (2017). A new method for crop classification combining time series of radar images and crop phenology information. *Remote Sensing of Environment*, *198*, 369–383. https://doi.org/10.1016/j.rse.2017.06.022

Batistella, M., Moran, E., & Mausel, P. (2004). Application of spectral mixture analysis to Amazonian land-use and land-cover classification AU - Lu, D. *International Journal of Remote Sensing*, *25*(23), 5345–5358. https://doi.org/10.1080/01431160412331269733

Belgiu, M., & Csillik, O. (2018). Sentinel-2 cropland mapping using pixel-based and object-based time-weighted dynamic time warping analysis. *Remote Sensing of Environment*, *204*(September 2017), 509–523. https://doi.org/10.1016/j.rse.2017.10.005

Bey, A., Sánchez-Paus Díaz, A., Maniatis, D., Marchi, G., Mollicone, D., Ricci, S., … Miceli, G. (2016). Collect Earth: Land Use and Land Cover Assessment through Augmented Visual Interpretation. *Remote Sensing* . https://doi.org/10.3390/rs8100807

Bland, J. M., & Altman, D. G. (2000). The odds ratio. *BMJ*, *320*(7247), 1468. https://doi.org/10.1136/bmj.320.7247.1468

Blaschke, T. (2010). Object based image analysis for remote sensing. *ISPRS Journal of Photogrammetry and Remote Sensing*, *65*(1), 2–16. https://doi.org/https://doi.org/10.1016/j.isprsjprs.2009.06.004

Brink, A. B., & Eva, H. D. (2009). Monitoring 25 years of land cover change dynamics in Africa: A sample based remote sensing approach. *Applied Geography*, *29*(4), 501–512. https://doi.org/https://doi.org/10.1016/j.apgeog.2008.10.004

Brisco, B. (2004). The application of C-band polarimetric SAR for agriculture: a review AU - McNairn, H. *Canadian Journal of Remote Sensing*, *30*(3), 525–542. https://doi.org/10.5589/m03-069

Canisius, F., Shang, J., Liu, J., Huang, X., Ma, B., Jiao, X., … Walters, D. (2018). Tracking crop

phenological development using multi-temporal polarimetric Radarsat-2 data. *Remote Sensing of Environment*, *210*, 508–518. https://doi.org/10.1016/j.rse.2017.07.031

Carfagna, E., & Gallego, J. F. (2005). Using Remote Sensing for Agricultural Statistics. *International Statistical Review*, *73*(3), 389–404. https://doi.org/10.1111/j.1751-5823.2005.tb00155.x

Carletto, C., Jolliffe, D., & Raka, B. (2013). *Agricultural S tatistics in Sub - Saharan Africa*. Retrieved from http://mortenjerven.com/wp-content/uploads/2013/04/Panel-3-Carletto.pdf

Carvalho, E. A., Ushizima, D. M., Medeiros, F. N. S., Martins, C. I. O., Marques, R. C. P., & Oliveira, I. N. S. (2010). SAR imagery segmentation by statistical region growing and hierarchical merging. *Digital Signal Processing: A Review Journal*, *20*(5), 1365–1378. https://doi.org/10.1016/j.dsp.2009.10.014

Castillejo-González, I. L., López-Granados, F., García-Ferrer, A., Peña-Barragán, J. M., Jurado-Expósito, M., de la Orden, M. S., & González-Audicana, M. (2009). Object- and pixel-based analysis for mapping crops and their agro-environmental associated measures using QuickBird imagery. *Computers and Electronics in Agriculture*, *68*(2), 207–215. https://doi.org/https://doi.org/10.1016/j.compag.2009.06.004

Central Statistical Agency of Ethiopia. (2010). *Population and Housing Census 2007 Report. Population and Housing Census 2007 Report, National*. Retrieved from http://www.csa.gov.et/surveys/Population and Housing census/ETH-pop-2007/survey0/data/Doc/Reports/National_Statistical.pdf

Chamberlin, J., & Schmidt, E. (2011). Ethiopian Agriculture : A Dynamic Geographic Perspective. Ethiopia Strategy Support Program II (ESSP II) ESSP II Working Paper No. 017, (April). Retrieved from http://ebrary.ifpri.org/utils/getfile/collection/p15738coll2/id/124850/filename/124851.pdf

Chen, B., Huang, B., & Xu, B. (2015). Comparison of spatiotemporal fusion models: A review. *Remote Sensing*, *7*(2), 1798–1835. https://doi.org/10.3390/rs70201798

Chen, F., Lasaponara, R., & Masini, N. (2017). An overview of satellite synthetic aperture radar remote sensing in archaeology: From site detection to monitoring. *Journal of Cultural Heritage*, *23*, 5–11. https://doi.org/https://doi.org/10.1016/j.culher.2015.05.003

Chen, J., Jönsson, P., Tamura, M., Gu, Z., Matsushita, B., & Eklundh, L. (2004). A simple method for reconstructing a high-quality NDVI time-series data set based on the Savitzky-Golay filter. *Remote Sensing of Environment*, *91*(3–4), 332–344. https://doi.org/10.1016/j.rse.2004.03.014

Chen, P.-Y., Fedosejevs, G., Tiscareno-LOPEZ, M., & Arnold, J. G. (2006). ASSESSMENT OF MODIS-EVI, MODIS-NDVI AND VEGETATION-NDVI COMPOSITE DATA USING AGRICULTURAL MEASUREMENTS: AN EXAMPLE AT CORN FIELDS IN WESTERN MEXICO. *Environmental Monitoring and Assessment*, *119*(1–3), 69–82. https://doi.org/10.1007/sl0661-005-9006-7

Chen, Y., Lu, D., Moran, E., Batistella, M., Dutra, L. V., Sanches, I. D., … de Oliveira, M. A. F. (2018). Mapping croplands, cropping patterns, and crop types using MODIS time-series data. *International Journal of Applied Earth Observation and Geoinformation*, *69*(November 2017), 133–147. https://doi.org/10.1016/j.jag.2018.03.005

Choodarathnakara, A. L., Kumar, T. A., & Koliwad, S. (2012). Mixed Pixels: A Challenge in Remote Sensing Data Classification for Improving Performance. *International Journal of Advanced Research in Computer Engineering & Technology (IJARCET)*, *1*(9), 2278–1323. Retrieved from https://pdfs.semanticscholar.org/63b9/7ce83281e012da96d7be39d84a1739fae67c.pdf

Civco, D. L. (1993). Artificial neural networks for land-cover classification and mapping AU. *International Journal of Geographical Information Systems*, *7*(2), 173–186. https://doi.org/10.1080/02693799308901949

Cochrane, L., & Bekele, Y. W. (2018). Average crop yield (2001–2017) in Ethiopia: Trends at national, regional and zonal levels. *Data in Brief*, *16*, 1025–1033. https://doi.org/10.1016/j.dib.2017.12.039

Consul, P. . (1990). On some properties and applications of quasi-binomial distribution AU - Consul, P. C. *Communications in Statistics - Theory and Methods*, *19*(2), 477–504. https://doi.org/10.1080/03610929008830214

Cotter, J., & Tomczak, C. (1994). An Image Analysis System to Develop Area Sampling Frame for Agricultural Surreys. *Photogrammetric Engineering and Remote Sensing*, *60*(3), 299–306. Retrieved from https://pubag.nal.usda.gov/pubag/downloadPDF.xhtml?id=21452&content=PDF

Crnojevic, V., Lugonja, P., Brkljac, B., & Brunet, B. (2014). Classification of small agricultural fields using combined Landsat-8 and RapidEye imagery: case study of northern Serbia. *Journal of Applied Remote Sensing*, *8*(1), 083512. https://doi.org/10.1117/1.JRS.8.083512

Dang, A. N., & Kawasaki, A. (2017). Integrating biophysical and socio-economic factors for land-use and land-cover change projection in agricultural economic regions. *Ecological Modelling*, *344*, 29–37.

https://doi.org/https://doi.org/10.1016/j.ecolmodel.2016.11.004

de Bie, C. A., Khan, M. R., Toxopeus, A. G., Venus, V., & Skidmore, A. K. (2008). Hypertemporal image analysis for crop mapping and change detection. *The International Archives of the Photogrammetry, Remote Sensing and Spatial Information Sciences. Vol. XXXVII. Part B7. Beijing 2008*, *2*, 803–814. Retrieved from www.VGT.vito.be.

Debats, S. R., Luo, D., Estes, L. D., Fuchs, T. J., & Caylor, K. K. (2016). A generalized computer vision approach to mapping crop fields in heterogeneous agricultural landscapes. *Remote Sensing of Environment*, *179*, 210–221. https://doi.org/10.1016/j.rse.2016.03.010

Defourny, P., Schouten, L., Bartalev, S., Bontemps, S., Caccetta, P., De Wit, A. J. W., … Arino, O. (2009). Accuracy assessment of a 300 m global land cover map: The GlobCover experience. *33rd International Symposium on Remote Sensing of Environment, ISRSE 2009*, 400–403. https://doi.org/10.1016/j.molcata.2005.07.030

Delegido, J., Verrelst, J., Alonso, L., & Moreno, J. (2011). Evaluation of sentinel-2 red-edge bands for empirical estimation of green LAI and chlorophyll content. *Sensors*, *11*(7), 7063–7081. https://doi.org/10.3390/s110707063

Delrue, J., Bydekerke, L., Eerens, H., Gilliams, S., Piccard, I., & Swinnen, E. (2013). Crop mapping in countries with small-scale farming: a case study for West Shewa, Ethiopia. *International Journal of Remote Sensing*, *34*(7), 2566–2582. https://doi.org/10.1080/01431161.2012.747016

Dierckx, W., Sterckx, S., Benhadj, I., Livens, S., Duhoux, G., Van Achteren, T., … Saint, G. (2014). PROBA-V mission for global vegetation monitoring: standard products and image quality. *International Journal of Remote Sensing*, *35*(7), 2589–2614. https://doi.org/10.1080/01431161.2014.883097

DigitalGlobe. (2019). Satellite Information - DigitalGlobe. Retrieved January 29, 2019, from https://www.digitalglobe.com/resources/satellite-information

Dong, Q., Liu, J., Wang, L., Chen, Z., & Gallego, J. (2017). Estimating crop area at county level on the North China plain with an indirect sampling of segments and an adapted regression estimator. *Sensors (Switzerland)*, *17*(11). https://doi.org/10.3390/s17112638

Eggen, M., Ozdogan, M., Zaitchik, B. F., & Simane, B. (2016). Land cover classification in complex and fragmented agricultural landscapes of the Ethiopian highlands. *Remote Sensing*, *8*(12). https://doi.org/10.3390/rs8121020

Embassy of the Kingdom of the Netherlands Ethiopia. (2015). *HANDS-ON INVESTMENT GUIDE Horticulture Floriculture and Dairy Oromia Regional State Ethiopia*. Retrieved from http://edepot.wur.nl/359503

Enderle, D., & Weih, R. (2005). Integrating supervised and unsupervised classification methods to develop a more accurate land cover classification. *Journal of the …*, *59*, 65–73. https://doi.org/10.1080/10810730903460526

Estes, L. D., McRitchie, D., Choi, J., Debats, S., Evans, T., Guthe, W., … Caylor, K. K. (2016). A platform for crowdsourcing the creation of representative, accurate landcover maps. *Environmental Modelling and Software*, *80*, 41–53. https://doi.org/10.1016/j.envsoft.2016.01.011

Ethiopian Government. (2018). Oromia Regional State - Ethiopia. Retrieved January 5, 2019, from http://www.ethiopia.gov.et/oromia-regional-state

Ezzahar, J., Miao, Z., Defourny, P., El Harti, A., Nicola, L., Traore, P. S., … Savinaud, M. (2018). Near real-time agriculture monitoring at national scale at parcel resolution: Performance assessment of the Sen2-Agri automated system in various cropping systems around the world. *Remote Sensing of Environment*, *221*(November 2018), 551–568. https://doi.org/10.1016/j.rse.2018.11.007

Fang, H. (2010). Rice crop area estimation of an administrative division in China using remote sensing data, *1161*. https://doi.org/10.1080/014311698214073

FAO. (1978). *Report on the agro-ecological zones project*. Rome.

FAO. (1999). *New concepts and approaches to land management in the tropics with emphasis on steeplands FAO SOILS BULLETIN*. Rome. Retrieved from https://vtechworks.lib.vt.edu/bitstream/handle/10919/65385/316_FAO_75_soil_management_on_steeplands.pdf?sequence=1&isAllowed=y

FAO. (2006). *Independent External Evaluation of the FAO*. ROME.

FAO. (2007a). *Land evaluation : Towards a revised framework*. Rome. https://doi.org/10.1016/j.geoderma.2008.11.001

FAO. (2007b). *S P E C I A L R E P O R T FAO/WFP CROP AND FOOD SUPPLY ASSESSMENT MISSION TO ETHIOPIA*. Rome. Retrieved from http://www.fao.org/giews/

FAO. (2011). *The state of the world's land and water resources for food and agriculture (SOLAW) – Managing systems at risk*. Rome: Earthscan.

FAO. (2018). FAO,GIEWS, Earth Observation,METOP, NDVI, ASIS, VHI, VCI,ECWMF, Agricultural Stress Index, NDVI Anomaly,Vegetation Condition Index,Vegetation Health Index,Estimated Precipitation,Precipitation AnomalyMap. Retrieved January 24, 2019, from http://www.fao.org/giews/earthobservation/index.jsp?lang=en

Foody, G. M. (2000). Estimation of sub-pixel land cover composition in the presence of untrained classes. *Computers and Geosciences*, *26*(4), 469–478. https://doi.org/10.1016/S0098-3004(99)00125-9

Forkuor, G., Conrad, C., Thiel, M., Ullmann, T., & Zoungrana, E. (2014). Integration of Optical and Synthetic Aperture Radar Imagery for Improving Crop Mapping in Northwestern Benin, West Africa. *Remote Sensing* . https://doi.org/10.3390/rs6076472

Forkuor, G., Dimobe, K., Serme, I., & Tondoh, J. E. (2018). Landsat-8 vs. Sentinel-2: examining the added value of sentinel-2's red-edge bands to land-use and land-cover mapping in Burkina Faso. *GIScience and Remote Sensing*, *55*(3), 331–354. https://doi.org/10.1080/15481603.2017.1370169

Friedl, M. A., & Brodley, C. E. (1997). Decision tree classification of land cover from remotely sensed data. *Remote Sensing of Environment*, *61*(3), 399–409. https://doi.org/https://doi.org/10.1016/S0034-4257(97)00049-7

Fritz, S., McCallum, I., Schill, C., Perger, C., See, L., Schepaschenko, D., … Obersteiner, M. (2012). Geo-Wiki: An online platform for improving global land cover. *Environmental Modelling & Software*, *31*, 110–123. https://doi.org/https://doi.org/10.1016/j.envsoft.2011.11.015

Fritz, S., See, L., McCallum, I., Schill, C., Obersteiner, M., van der Velde, M., … Achard, F. (2011). Highlighting continued uncertainty in global land cover maps for the user community. *Environmental Research Letters*, *6*(4), 044005. https://doi.org/10.1088/1748-9326/6/4/044005

Gallego, F. J. (2004). Remote sensing and land cover area estimation. *International Journal of Remote Sensing*, *25*(15), 3019–3047. https://doi.org/10.1080/01431160310001619607

Gallego, F. J. (2006). Review of the main remote sensing methods for crop area estimates. *Proceedings of the Workshop Remote Sensing Support to Crop Yield Forecast and Area Estimates Vol. 36*, 1–6.

Gallego, F. J., Feunette, I., & Carfagna, E. (1999). Optimising The Size of Sampling Units in an Area Frame BT - geoENV II — Geostatistics for Environmental Applications. In J. Gómez-Hernández, A. Soares, & R. Froidevaux (Eds.) (pp. 393–404). Dordrecht: Springer Netherlands.

Gallego, J. F. (1999). IRC-SP-62-2004 Construction Of Cement Concrete Pavement For Rural Roads. *Conference on Ten Years of the MARS Project*, (April), 1–11. Retrieved from http://citeseerx.ist.psu.edu/viewdoc/download?doi=10.1.1.561.678&rep=rep1&type=pdf

Gambotto, J.-P. (1993). A new approach to combining region growing and edge detection. *Pattern Recognition Letters*, *14*(11), 869–875. https://doi.org/https://doi.org/10.1016/0167-8655(93)90150-C

Gao, Q., Zribi, M., Escorihuela, J. M., Baghdadi, N., & Segui, Q. P. (2018). Irrigation Mapping Using Sentinel-1 Time Series at Field Scale. *Remote Sensing* . https://doi.org/10.3390/rs10091495

Gómez, C., White, J. C., & Wulder, M. A. (2016). Optical remotely sensed time series data for land cover classification: A review. *ISPRS Journal of Photogrammetry and Remote Sensing*, *116*, 55–72. https://doi.org/10.1016/j.isprsjprs.2016.03.008

Gonçalves, M. L., Netto, M. L. A., Costa, J. A. F., & Zullo Junior, J. (2008). An unsupervised method of classifying remotely sensed images using Kohonen self-organizing maps and agglomerative hierarchical clustering methods. *International Journal of Remote Sensing*, *29*(11), 3171–3207. https://doi.org/10.1080/01431160701442146

Grace, K., Husak, G., & Bogle, S. (2014). Estimating agricultural production in marginal and food insecure areas in Kenya using very high resolution remotely sensed imagery. *Applied Geography*, *55*, 257–265. https://doi.org/10.1016/j.apgeog.2014.08.014

Grace, K., Husak, G. J., Harrison, L., Pedreros, D., & Michaelsen, J. (2012). Using high resolution satellite imagery to estimate cropped area in Guatemala and Haiti. *Applied Geography*, *32*(2), 433–440. https://doi.org/10.1016/j.apgeog.2011.05.014

Granados-Ramírez, R., Reyna-Trujillo, T., Gómez-Rodríguez, G., & Soria-Ruiz, J. (2004). Analysis of NOAA-AVHRR-NDVI images for crops monitoring. *International Journal of Remote Sensing*, *25*(9), 1615–1627. https://doi.org/10.1080/0143116031000156855

Griffiths, P., Nendel, C., & Hostert, P. (2019). Intra-annual reflectance composites from Sentinel-2 and Landsat for national-scale crop and land cover mapping. *Remote Sensing of Environment*, *220*(November 2018), 135–151. https://doi.org/10.1016/j.rse.2018.10.031

Gumma, M. K., Gauchan, D., Nelson, A., Pandey, S., & Rala, A. (2011). Temporal changes in rice-

growing area and their impact on livelihood over a decade: A case study of Nepal. *Agriculture, Ecosystems and Environment*, *142*(3–4), 382–392. https://doi.org/10.1016/j.agee.2011.06.010

Hanuschak, G., Hale, R., Craig, M., Mueller, R., & Hart, G. (2001). *The New Economics of Remote Sensing for Agricultural Statistics in the United States*. Retrieved from http://www.nass.usda.gov/research/Cropland/SARS1a.htm

Hastie, T., Tibshirani, R., Hastie, T., & Tibshirani, R. (2016). Generalized Additive Models : Some Applications Generalized Additive Models : Some Applications, *82*(398), 371–386.

Hazell, P., & Wood, S. (2008). Drivers of change in global agriculture. *Philosophical Transactions of the Royal Society B: Biological Sciences*, *363*(1491), 495–515. https://doi.org/10.1098/rstb.2007.2166

Hentze, K., Thonfeld, F., & Menz, G. (2016). Evaluating crop area mapping from modis time-series as an assessment tool for Zimbabwe's "fast track land reform programme." *PLoS ONE*, *11*(6), 1–22. https://doi.org/10.1371/journal.pone.0156630

Huang, C., Davis, L. S., & Townshend, J. R. G. (2002). An assessment of support vector machines for land cover classification. *International Journal of Remote Sensing*, *23*(4), 725–749. https://doi.org/10.1080/01431160110040323

Husak, G., & Grace, K. (2016). In search of a global model of cultivation: using remote sensing to examine the characteristics and constraints of agricultural production in the developing world. *Food Security*, *8*(1), 167–177. https://doi.org/10.1007/s12571-015-0538-6

Husak, G., Marshall, M., Michaelsen, J., Pedreros, D., Funk, C., & Galu, G. (2008). Crop area estimation using high and medium resolution satellite imagery in areas with complex topography. *Journal of Geophysical Research Atmospheres*, *113*(14). https://doi.org/10.1029/2007JD009175

Hussain, M., Chen, D., Cheng, A., Wei, H., & Stanley, D. (2013). Change detection from remotely sensed images: From pixel-based to object-based approaches. *ISPRS Journal of Photogrammetry and Remote Sensing*, *80*, 91–106. https://doi.org/10.1016/j.isprsjprs.2013.03.006

Iizumi, T., & Ramankutty, N. (2015). How do weather and climate influence cropping area and intensity? *Global Food Security*, *4*, 46–50. https://doi.org/10.1016/j.gfs.2014.11.003

Immitzer, M., Vuolo, F., & Atzberger, C. (2016). First experience with Sentinel-2 data for crop and tree species classifications in central Europe. *Remote Sensing*, *8*(3). https://doi.org/10.3390/rs8030166

Jain, M., Mondal, P., DeFries, R. S., Small, C., & Galford, G. L. (2013). Mapping cropping intensity of smallholder farms: A comparison of methods using multiple sensors. *Remote Sensing of Environment*, *134*, 210–223. https://doi.org/10.1016/j.rse.2013.02.029

Jeong, J. H., Resop, J. P., Mueller, N. D., Fleisher, D. H., Yun, K., Butler, E. E., … Kim, S. H. (2016). Random forests for global and regional crop yield predictions. *PLoS ONE*, *11*(6), 1–15. https://doi.org/10.1371/journal.pone.0156571

Jiao, X., Kovacs, J. M., Shang, J., McNairn, H., Walters, D., Ma, B., & Geng, X. (2014). Object-oriented crop mapping and monitoring using multi-temporal polarimetric RADARSAT-2 data. *ISPRS Journal of Photogrammetry and Remote Sensing*, *96*, 38–46. https://doi.org/https://doi.org/10.1016/j.isprsjprs.2014.06.014

Kaspar, T. C., Colvin, T. S., Jaynes, D. B., Karlen, D. L., James, D. E., Meek, D. W., … Butler, H. (2003). Relationship between six years of corn yields and terrain attributes. *Precision Agriculture*, *4*(1), 87–101. https://doi.org/10.1023/A:1021867123125

Kaufman, Y. J., Tanré, D., Markham, B., & Gitelson, A. A. (1992). Atmospheric Effects on the NDVI--Strategies for Its Removal. *Papers in Natural Resources*, 1238–1241. https://doi.org/10.1109/IGARSS.1992.578402.

Kerdiles, H., Dong, Q., Spyratos, S., & Gallego, F. J. (2014). Use of high resolution imagery and ground survey data for estimating crop areas in Mengcheng county, China. *IOP Conference Series: Earth and Environmental Science*, *17*, 12057. https://doi.org/10.1088/1755-1315/17/1/012057

Khan, M. R., de Bie, C. A. J. M., van Keulen, H., Smaling, E. M. A., & Real, R. (2010a). Disaggregating and mapping crop statistics using hypertemporal remote sensing. *International Journal of Applied Earth Observation and Geoinformation*, *12*(1), 36–46. https://doi.org/10.1016/j.jag.2009.09.010

Khan, M. R., de Bie, C. A. J. M., van Keulen, H., Smaling, E. M. A., & Real, R. (2010b). Disaggregating and mapping crop statistics using hypertemporal remote sensing. *International Journal of Applied Earth Observation and Geoinformation*, *12*(1), 36–46. https://doi.org/10.1016/j.jag.2009.09.010

Kumhálová, J., Matějková, Š., Fifernová, M., Lipavský, J., & Kumhála, F. (2008). Topography impact on nutrition content in soil and yield. *Plant, Soil and Environment*, *54*(6), 255–261.

Kussul, N., Skakun, S., Shelestov, A., Lavreniuk, M., Yailymov, B., & Kussul, O. (2015). Regional scale crop mapping using multi-temporal satellite imagery. *International Archives of the Photogrammetry, Remote*

Sensing and Spatial Information Sciences - ISPRS Archives, *40*(7W3), 45–52. https://doi.org/10.5194/isprsarchives-XL-7-W3-45-2015

Kuwata, K., & Shibasaki, R. (2015). Estimating crop yields with deep learning and remotely sensed data. *2015 IEEE International Geoscience and Remote Sensing Symposium (IGARSS)*, 858–861. https://doi.org/10.1109/IGARSS.2015.7325900

Lambert, M. J., Traoré, P. C. S., Blaes, X., Baret, P., & Defourny, P. (2018). Estimating smallholder crops production at village level from Sentinel-2 time series in Mali's cotton belt. *Remote Sensing of Environment*, *216*(September 2017), 647–657. https://doi.org/10.1016/j.rse.2018.06.036

Lambert, M. J., Waldner, F., & Defourny, P. (2016). Cropland mapping over Sahelian and Sudanian agrosystems: A Knowledge-based approach using PROBA-V time series at 100-m. *Remote Sensing*, *8*(3). https://doi.org/10.3390/rs8030232

Landgrebe, T. C. W., & Duin, R. P. W. (2007). Approximating the multiclass ROC by pairwise analysis. *Pattern Recognition Letters*, *28*(13), 1747–1758. https://doi.org/10.1016/j.patrec.2007.05.001

Langley, S. K., Cheshire, H. M., & Humes, K. S. (2001). A comparison of single date and multitemporal satellite image classifications in a semi-arid grassland. *Journal of Arid Environments*, *49*(2), 401–411. https://doi.org/10.1006/jare.2000.0771

Lebourgeois, V., Dupuy, S., Vintrou, É., Ameline, M., Butler, S., & Bégué, A. (2017). A Combined Random Forest and OBIA Classification Scheme for Mapping Smallholder Agriculture at Different Nomenclature Levels Using Multisource Data (Simulated Sentinel-2 Time Series, VHRS and DEM). *Remote Sensing* . https://doi.org/10.3390/rs9030259

Lefsky, M. A., & Cohen, W. B. (2003). SELECTION OF REMOTELY SENSED DATA. In M. A. Wulder & S. E. Franklin (Eds.), *Remote Sensing of Forest Environments: Concepts and case studies* (pp. 13–46). Boston: Kluwer Academic Publishers. Retrieved from https://andrewsforest.oregonstate.edu/sites/default/files/lter/pubs/pdf/pub3131.pdf

Li, D., Yang, F., & Wang, X. (2017). Study on Ensemble Crop Information Extraction of Remote Sensing Images Based on SVM and BPNN. *Journal of the Indian Society of Remote Sensing*, *45*(2), 229–237. https://doi.org/10.1007/s12524-016-0597-y

Liew, J., & Forkman, J. (2015). A guide to generalized additive models in crop science using SAS and R, 41–57.

Liu, D., & Xia, F. (2010). Assessing object-based classification: advantages and limitations AU - Liu, Desheng. *Remote Sensing Letters*, *1*(4), 187–194. https://doi.org/10.1080/01431161003743173

Liu, J., Liu, M., Tian, H., Zhuang, D., Zhang, Z., Zhang, W., … Deng, X. (2005). Spatial and temporal patterns of China's cropland during 1990-2000: An analysis based on Landsat TM data. *Remote Sensing of Environment*, *98*(4), 442–456. https://doi.org/10.1016/j.rse.2005.08.012

Lobell, D. B., & Asner, G. P. (2004). Cropland distributions from temporal unmixing of MODIS data. *Remote Sensing of Environment*, *93*(3), 412–422. https://doi.org/https://doi.org/10.1016/j.rse.2004.08.002

López, S. (2014). Modeling Agricultural Change through Logistic Regression and Cellular Automata: A Case Study on Shifting Cultivation. *Journal of Geographic Information System*, *6*(6), 220–235. https://doi.org/10.4236/jgis.2014.63021

Lu, D., & Weng, Q. (2007). A survey of image classification methods and techniques for improving classification performance. *International Journal of Remote Sensing*, *28*(5), 823–870. https://doi.org/10.1080/01431160600746456

Lunetta, R. S., Shao, Y., Ediriwickrema, J., & Lyon, J. G. (2010). Monitoring agricultural cropping patterns across the Laurentian Great Lakes Basin using MODIS-NDVI data. *International Journal of Applied Earth Observation and Geoinformation*, *12*(2), 81–88. https://doi.org/https://doi.org/10.1016/j.jag.2009.11.005

Malarvizhi, K., Kumar, S. V., & Porchelvan, P. (2016). Use of High Resolution Google Earth Satellite Imagery in Landuse Map Preparation for Urban Related Applications. *Procedia Technology*, *24*, 1835–1842. https://doi.org/10.1016/j.protcy.2016.05.231

Maloney, K. O., Schmid, M., & Weller, D. E. (2012). Applying additive modelling and gradient boosting to assess the effects of watershed and reach characteristics on riverine assemblages. *Methods in Ecology and Evolution*, *3*(1), 116–128. https://doi.org/10.1111/j.2041-210X.2011.00124.x

Marshall, M., Norton-Griffiths, M., Herr, H., Lamprey, R., Sheffield, J., Vagen, T., & Okotto-Okotto, J. (2017). Continuous and consistent land use/cover change estimates using socio-ecological data. *Earth System Dynamics*, *8*(1), 55–73. https://doi.org/10.5194/esd-8-55-2017

Marshall, M. T., Husak, G. J., Michaelsen, J., Funk, C., Pedreros, D., & Adoum, A. (2011). International

Journal of Remote Testing a high-resolution satellite interpretation technique for crop area monitoring in developing countries, (September), 37–41.

Martinez-Beltran, C., & Calera-Belmonte, A. (2001). Irrigated Crop Area Estimation Using Landsat TM Imagery in La Mancha, Spain. *PHOTOGRAMMETRIC ENGINEERING AND REMOTE SENSING*, *67*(10), 1177–1184. Retrieved from https://www.asprs.org/wp-content/uploads/pers/2001journal/october/2001_oct_1177-1184.pdf

Mas, J. F., & Flores, J. J. (2008). The application of artificial neural networks to the analysis of remotely sensed data. *International Journal of Remote Sensing*, *29*(3), 617–663. https://doi.org/10.1080/01431160701352154

McCarty, J. L., Neigh, C. S. R., Carroll, M. L., & Wooten, M. R. (2017). Extracting smallholder cropped area in Tigray, Ethiopia with wall-to-wall sub-meter WorldView and moderate resolution Landsat 8 imagery. *Remote Sensing of Environment*, *202*, 142–151. https://doi.org/10.1016/j.rse.2017.06.040

Mehnatkesh, A., Ayoubi, S., Jalalian, A., & Sahrawat, K. L. (2013). Relationships between soil depth and terrain attributes in a semi arid hilly region in western Iran. *Journal of Mountain Science*, *10*(1), 163–172. https://doi.org/10.1007/s11629-013-2427-9

Minet, J., Curnel, Y., Gobin, A., Goffart, J. P., Mélard, F., Tychon, B., … Defourny, P. (2017). Crowdsourcing for agricultural applications: A review of uses and opportunities for a farmsourcing approach. *Computers and Electronics in Agriculture*. https://doi.org/10.1016/j.compag.2017.08.026

Misra, A. K. (2014). Climate change and challenges of water and food security. *International Journal of Sustainable Built Environment*, *3*(1), 153–165. https://doi.org/10.1016/j.ijsbe.2014.04.006

Moigne, J. Le, & Tilton, J. C. (1995). Refining image segmentation by integration of edge and region data. *IEEE Transactions on Geoscience and Remote Sensing*, *33*(3), 605–615. https://doi.org/10.1109/36.387576

Mondal, A., Kundu, S., Chandniha, S. K., Shukla, R., & Mishra, P. K. (2012). Comparison of Support Vector Machine and Maximum Likelihood Classification Technique using Satellite Imagery. *International Journal of Remote Sensing and GIS*, *1*(2), 116–123.

Mountrakis, G., Im, J., & Ogole, C. (2011). Support vector machines in remote sensing: A review. *ISPRS Journal of Photogrammetry and Remote Sensing*, *66*(3), 247–259. https://doi.org/https://doi.org/10.1016/j.isprsjprs.2010.11.001

Mu, W., Yu, F., Li, C., Xie, Y., Tian, J., Liu, J., & Zhao, N. (2015). Effects of Rainfall Intensity and Slope Gradient on Runoff and Soil Moisture Content on Different Growing Stages of Spring Maize. *Water*. https://doi.org/10.3390/w7062990

Mukashema, A., Veldkamp, A., & Vrieling, A. (2014). Automated high resolution mapping of coffee in Rwanda using an expert Bayesian network. *International Journal of Applied Earth Observation and Geoinformation*, *33*(1), 331–340. https://doi.org/10.1016/j.jag.2014.05.005

Murmu, S., & Biswas, S. (2015). Application of Fuzzy Logic and Neural Network in Crop Classification: A Review. *Aquatic Procedia*, *4*(Icwrcoe), 1203–1210. https://doi.org/10.1016/j.aqpro.2015.02.153

Musande, V., Kumar, A., & Kale, K. (2012). Cotton Crop Discrimination Using Fuzzy Classification Approach. *Journal of the Indian Society of Remote Sensing*, *40*(4), 589–597. https://doi.org/10.1007/s12524-012-0201-z

Mutanga, O., Odindi, J., & Abdel-Rahman, E. M. (2014). Land-use/cover classification in a heterogeneous coastal landscape using RapidEye imagery: evaluating the performance of random forest and support vector machines classifiers AU - Adam, Elhadi. *International Journal of Remote Sensing*, *35*(10), 3440–3458. https://doi.org/10.1080/01431161.2014.903435

NASA. (2000, August 30). Measuring Vegetation (NDVI & EVI). Retrieved August 12, 2018, from https://earthobservatory.nasa.gov/Features/MeasuringVegetation/measuring_vegetation_2.php

Neigh, C. S. R., Carroll, M. L., Wooten, M. R., McCarty, J. L., Powell, B. F., Husak, G. J., … Hain, C. R. (2018). Smallholder crop area mapped with wall-to-wall WorldView sub-meter panchromatic image texture: A test case for Tigray, Ethiopia. *Remote Sensing of Environment*, *212*(January), 8–20. https://doi.org/10.1016/j.rse.2018.04.025

Nitze, I., Schulthess, U., & Asche, H. (2012). Comparison of machine learning algorithms random forest, artificial neuronal network and support vector machine to maximum likelihood for supervised crop type classification. *Proceedings of the 4th Conference on GEographic Object-Based Image Analysis – GEOBIA 2012*, 35–40.

Ok, A. O., Akar, O., & Gungor, O. (2012). Evaluation of random forest method for agricultural crop classification. *European Journal of Remote Sensing*, *45*(1), 421–432. https://doi.org/10.5721/EuJRS20124535

Ormerod, S. J., Manel, S., & Williams, H. C. (2001). Evaluating presence-absence models in ecology: the need to account for prevalence. *Journal of Applied Ecology*, *38*(5), 921–931. Retrieved from https://besjournals.onlinelibrary.wiley.com/doi/pdf/10.1046/j.1365-2664.2001.00647.x

Ozdogan, M., Yang, Y., Allez, G., & Cervantes, C. (2010). Remote sensing of irrigated agriculture: Opportunities and challenges. *Remote Sensing*, *2*(9), 2274–2304. https://doi.org/10.3390/rs2092274

Pal, M. (2005). Random forest classifier for remote sensing classification. *International Journal of Remote Sensing*, *26*(1), 217–222. https://doi.org/10.1080/01431160412331269698

Pandey, S., & Bright, C. L. (2008). What Are Degrees of Freedom? *Social Work Research*, *32*(2), 119–128. Retrieved from http://www.montefiore.ulg.ac.be/~kvansteen/MATH0008-2/ac20122013/Class11Dec/Supplementary info_AppendixD_DegreesOfFreedom.pdf

Peña-Barragán, J. M., Ngugi, M. K., Plant, R. E., & Six, J. (2011). Object-based crop identification using multiple vegetation indices, textural features and crop phenology. *Remote Sensing of Environment*, *115*(6), 1301–1316. https://doi.org/10.1016/j.rse.2011.01.009

Petitjean, F., Inglada, J., & Gancarski, P. (2012). Satellite Image Time Series Analysis Under Time Warping. *Geoscience and Remote Sensing, IEEE Transactions On*, *50*(8), 3081–3095. https://doi.org/10.1109/TGRS.2011.2179050

Potere, D. (2008). Horizontal positional accuracy of google earth's high-resolution imagery archive. *Sensors*, *8*(12), 7973–7981. https://doi.org/10.3390/s8127973

Pradhan, S. (2001). Crop Area Estimation Using GIS, Remote Sensing and Area Frame Sampling. *International Journal of Applied Earth Observation and Geoinformation*, *3*(1), 86–92. https://doi.org/10.1016/S0303-2434(01)85025-X

Quiroz, R., Zorogastúa, P., Baigorria, G., Barreda, C., Valdivia, R., & Cruz, M. (2000). Toward A Dynamic Definition of Agroecological Zones Using Modern Information Technology Tools. *Program*, 361–370. Retrieved from www.esri.com/software

Rahman, R., & Saha, S. K. (2008). Multi-resolution Segmentation for Object-based Classifi cation and assessment of accuracy for land cover _IRS.pdf. *Journal of Indian Society of Remote Sensing*, *36*(June), 189–201. Retrieved from https://link.springer.com/content/pdf/10.1007/s12524-008-0020-4.pdf

Rao, K. Y., Stephen, M. J., & Phanindra, D. S. (2012). Classification Based Image Segmentation Approach. *Ijcst*, *3*(1), 685–660.

Recio, J. A., Hermosilla, T., Ruiz, L. A., & Fernández-Sarría, A. (2010). Addition of geographic ancillary data for updating geo-spatial databases. *International Archives of the Photogrammetry, Remote Sensing and Spatial Information Sciences - ISPRS Archives*, *38*, 46–51. Retrieved from http://www.scopus.com/inward/record.url?eid=2-s2.0-79960376376&partnerID=tZOtx3y1

Reed, B. C., Brown, J. F., Vanderzee, D., Loveland, T. R., Merchant, J. W., & Ohlen, D. O. (1994). Measuring phenological variability from satellite imagery. *Journal of Vegetation Science*, *5*(5), 703–714. Retrieved from http://pubs.er.usgs.gov/publication/70187023

Reiche, J., Verbesselt, J., Hoekman, D., & Herold, M. (2015). Fusing Landsat and SAR time series to detect deforestation in the tropics. https://doi.org/10.1016/j.rse.2014.10.001

Richards, J. A. (2012). *Remote Sensing Digital Image Analysis: An Introduction* (5th ed.). Springer Publishing Company, Incorporated.

Rogan, J., & Chen, D. (2004). Remote sensing technology for mapping and monitoring land-cover and land-use change. *Progress in Planning*, *61*(4), 301–325. https://doi.org/https://doi.org/10.1016/S0305-9006(03)00066-7

Rydberg, A., & Borgefors, G. (2001). Integrated method for boundary delineation of agricultural fields in multispectral satellite images. *IEEE Transactions on Geoscience and Remote Sensing*, *39*(11), 1678–1680. https://doi.org/10.1109/36.964989

Sakamoto, T., Yokozawa, M., Toritani, H., Shibayama, M., Ishitsuka, N., & Ohno, H. (2005). A crop phenology detection method using time-series MODIS data. *Remote Sensing of Environment*, *96*(3–4), 366–374. https://doi.org/10.1016/j.rse.2005.03.008

Savitzky, A., & Golay, M. (1964). Smoothing and Differentiation of Data by Simplified Least Squares Pro,cedures. *Analytical Chemistry*, *36*(8), 1627–1639. Retrieved from https://pubs.acs.org/sharingguidelines

Schiewe, J. (2002). SEGMENTATION OF HIGH-RESOLUTION REMOTELY SENSED DATA - CONCEPTS , APPLICATIONS AND PROBLEMS. In *Symposium on Geospatial Theory , Processing and Applications*. Ottawa. Retrieved from http://test.ecognition.com/sites/default/files/383_358.pdf

See, L., Fritz, S., You, L., Ramankutty, N., Herrero, M., Justice, C., … Obersteiner, M. (2015). Improved global cropland data as an essential ingredient for food security. *Global Food Security*, *4*, 37–45.

https://doi.org/10.1016/j.gfs.2014.10.004

See, L., McCallum, I., Fritz, S., Perger, C., Kraxner, F., Obersteiner, M., … Ram Kalita, N. (2013). Mapping Cropland in Ethiopia Using Crowdsourcing. *International Journal of Geosciences*, *4*, 6–13. https://doi.org/10.4236/ijg.2013.46A1002

Seetha, M., Sunitha, K. V. N., & Devi, G. M. (2012). Performance Assessment of Neural Network and K-Nearest Neighbour Classification with Random Subwindows. *International Journal of Machine Learning and Computing*, *2*(6), 844–847. https://doi.org/10.7763/IJMLC.2012.V2.250

Selassie, Y. G., Anemut, F., & Addisu, S. (2015). The effects of land use types, management practices and slope classes on selected soil physico-chemical properties in Zikre watershed, North-Western Ethiopia. *Environmental Systems Research*, *4*(1), 3. https://doi.org/10.1186/s40068-015-0027-0

Shao, Y., & Lunetta, R. S. (2012). Comparison of support vector machine, neural network, and CART algorithms for the land-cover classification using limited training data points. *ISPRS Journal of Photogrammetry and Remote Sensing*, *70*, 78–87. https://doi.org/https://doi.org/10.1016/j.isprsjprs.2012.04.001

Sharma, R., Ghosh, A., & Joshi, P. K. (2013). Decision tree approach for classification of remotely sensed satellite data using open source support. *Journal of Earth System Science*, *122*(5), 1237–1247. https://doi.org/10.1007/s12040-013-0339-2

Shen, K., Li, W., Pei, Z., Fei, W., Sun, G., Zhang, X., … Ma, S. (2015). Crop Area Estimation from UAV Transect and MSR Image Data Using Spatial Sampling Method. *Procedia Environmental Sciences*, *26*(41301506), 95–100. https://doi.org/10.1016/j.proenv.2015.05.007

SINGH, R., SIDHU, S. S., NARANG, R. S., DADHWAL, V. K., PARIHAR, J. S., & SHARMA, A. K. (1993). Pre-harvest state level wheat acreage estimation using IRS-IA LISS-I data in Punjab (India) AU - MAHEY, R. K. *International Journal of Remote Sensing*, *14*(6), 1099–1106. https://doi.org/10.1080/01431169308904398

Smith, G. M., & Fuller, R. M. (2001). An integrated approach to land cover classification: An example in the Island of Jersey. *International Journal of Remote Sensing*, *22*(16), 3123–3142. https://doi.org/10.1080/014311601152558288

Sonobe, R., Yamaya, Y., Tani, H., Wang, X., Kobayashi, N., & Mochizuki, K. (2018). Crop classification from Sentinel-2-derived vegetation indices using ensemble learning. *Journal of Applied Remote Sensing*, *12*(2), 1–17. Retrieved from https://doi.org/10.1117/1.JRS.12.026019

Soudani, K., Hmimina, G., Delpierre, N., Pontailler, J. Y., Aubinet, M., Bonal, D., … Dufrêne, E. (2012). Ground-based Network of NDVI measurements for tracking temporal dynamics of canopy structure and vegetation phenology in different biomes. *Remote Sensing of Environment*, *123*(December), 234–245. https://doi.org/10.1016/j.rse.2012.03.012

Steele-Dunne, S. C., McNairn, H., Monsivais-Huertero, A., Judge, J., Liu, P., & Papathanassiou, K. (2017). Radar Remote Sensing of Agricultural Canopies: A Review. *IEEE Journal of Selected Topics in Applied Earth Observations and Remote Sensing*, *10*(5), 2249–2273. https://doi.org/10.1109/JSTARS.2016.2639043

Swinnen, E., Verbeiren, S., Deronde, B., & Henry, P. (2014). Assessment of the impact of the orbital drift of SPOT-VGT1 by comparison with SPOT-VGT2 data. *International Journal of Remote Sensing*, *35*(7), 2421–2439. https://doi.org/10.1080/01431161.2014.883100

Tatsumi, K., Yamashiki, Y., Canales Torres, M. A., & Taipe, C. L. R. (2015). Crop classification of upland fields using Random forest of time-series Landsat 7 ETM+ data. *Computers and Electronics in Agriculture*, *115*, 171–179. https://doi.org/10.1016/j.compag.2015.05.001

Teshome, M. (2014). Population Growth and Cultivated Land in Rural Ethiopia: Land Use Dynamics, Access, Farm Size, and Fragmentation. *Resources and Environment*, *4*(3), 148–161. https://doi.org/10.5923/j.re.20140403.03

The World Bank. (2011). *GLOBAL STRATEGY TO IMPROVE AGRICULTURAL AND RURAL STATISTICS United Nations*. Retrieved from www.worldbank.org/rural

Toté, C., Swinnen, E., Sterckx, S., Clarijs, D., Quang, C., & Maes, R. (2017). Evaluation of the SPOT/VEGETATION Collection 3 reprocessed dataset: Surface reflectances and NDVI. *Remote Sensing of Environment*, *201*(September), 219–233. https://doi.org/10.1016/j.rse.2017.09.010

Tran, V. T., Julian, P. J., & De Beurs, M. K. (2014). Land Cover Heterogeneity Effects on Sub-Pixel and Per-Pixel Classifications. *ISPRS International Journal of Geo-Information*. https://doi.org/10.3390/ijgi3020540

Tumlisan, G. Y. (2017). *Monitoring Growth Development and Yield Estimation of Maize Using Very High-Resolution Uav- Images in Gronau, Germany*. Faculty of Geo-Information Science and Earth Observation (ITC),

University of Twente, Enschede, Netherlands. Retrieved from
http://www.itc.nl/library/papers_2017/msc/nrm/tumlisan.pdf

U.S. Geological Survey. (2018). SLC-off Products: Background | Landsat Missions. Retrieved December
8, 2018, from https://landsat.usgs.gov/slc-products-background

USGS. (2014). MOD13Q1 V006 | LP DAAC :: NASA Land Data Products and Services. Retrieved
August 28, 2018, from
https://lpdaac.usgs.gov/dataset_discovery/modis/modis_products_table/mod13q1_v006

Veloso, A., Mermoz, S., Bouvet, A., Le Toan, T., Planells, M., Dejoux, J.-F., & Ceschia, E. (2017).
Understanding the temporal behavior of crops using Sentinel-1 and Sentinel-2-like data for
agricultural applications. *Remote Sensing of Environment*, *199*, 415–426.
https://doi.org/https://doi.org/10.1016/j.rse.2017.07.015

Verbeiren, S., Eerens, H., Piccard, I., Bauwens, I., & Van Orshoven, J. (2008). Sub-pixel classification of
SPOT-VEGETATION time series for the assessment of regional crop areas in Belgium. *International
Journal of Applied Earth Observation and Geoinformation*, *10*(4), 486–497.
https://doi.org/10.1016/j.jag.2006.12.003

Verdin, J., Lietzow, R., Rowland, J., Klaver, R., Reed, B., Falls, S., … Lee, F. (2000). A comparison of
methods for estimating start-of-season from operational remote sensing products: first results. *Sioux
Falls*. Retrieved from
http://citeseerx.ist.psu.edu/viewdoc/download?doi=10.1.1.510.1255&rep=rep1&type=pdf

Victoria, D. C., da Paz, A. R., Coutinho, A. C., Kastens, J. H., & Brown, J. C. (2012). Cropland area
estimates using MODIS NDVI time series in the state of Mato Grosso, Brazil. *Pequisa Agropecuaria
Brasileira*, *47*(9), 1270–1278. https://doi.org/10.1590/S0100-204X2012000900012

Viña, A., Gitelson, A. A., Rundquist, D. C., Keydan, G., Leavitt, B., & Schepers, J. (2004). Monitoring
maize (Zea mays L.) phenology with remote sensing. *Agronomy Journal*, *96*(4), 1139–1147. Retrieved
from https://www.scopus.com/inward/record.uri?eid=2-s2.0-
4043166894&partnerID=40&md5=83507b6231350cee6169182600c8afc1

Vintrou, E., Desbrosse, A., Bégué, A., Traoré, S., Baron, C., & Lo Seen, D. (2012). Crop area mapping in
West Africa using landscape stratification of MODIS time series and comparison with existing global
land products. *International Journal of Applied Earth Observation and Geoinformation*, *14*(1), 83–93.
https://doi.org/10.1016/j.jag.2011.06.010

Vogels, M. F. A., de Jong, S. M., Sterk, G., & Addink, E. A. (2017). Agricultural cropland mapping using
black-and-white aerial photography, Object-Based Image Analysis and Random Forests. *International
Journal of Applied Earth Observation and Geoinformation*, *54*, 114–123.
https://doi.org/10.1016/j.jag.2016.09.003

Vogels, M. F. A., de Jong, S. M., Sterk, G., & Addink, E. A. (2019). Mapping irrigated agriculture in
complex landscapes using SPOT6 imagery and object-based image analysis – A case study in the
Central Rift Valley, Ethiopia –. *International Journal of Applied Earth Observation and Geoinformation*, *75*,
118–129. https://doi.org/https://doi.org/10.1016/j.jag.2018.07.019

Waine, T. W., Taylor, J. C., & Juniper, G. R. (2014). The application of time-series MODIS NDVI profiles
for the acquisition of crop information across Afghanistan AU - Simms, Daniel M. *International
Journal of Remote Sensing*, *35*(16), 6234–6254. https://doi.org/10.1080/01431161.2014.951099

Wang, F. (1990). Improving remote sensing image analysis through fuzzy information representation.
Photogrammetric Engineering and Remote Sensing, *56*(8), 1163–1169. Retrieved from
https://www.asprs.org/wp-content/uploads/pers/1990journal/aug/1990_aug_1163-1169.pdf

Wang, L., & Uchida, S. (2008). Use of Linear Spectral Mixture Model to Estimate Rice Planted Area Based
on MODIS Data. *Rice Science*, *15*(2), 131–136. https://doi.org/https://doi.org/10.1016/S1672-
6308(08)60031-1

Wardlow, B. D., Egbert, S. L., & Kastens, J. H. (2007). Analysis of time-series MODIS 250 m vegetation
index data for crop classification in the U.S. Central Great Plains. *Remote Sensing of Environment*,
108(3), 290–310. https://doi.org/10.1016/j.rse.2006.11.021

Wolters, E., Dierckx, W., Dries, J., & Swinnen, E. (2015). *PROBA-V Products User Manual*. Retrieved from
http://lps16.esa.int/posterfiles/paper1213/[RD15]_PROBAV-Products_User_Manual_v1.2.pdf

Wood, S. (2013). *Package 'mgcv', Version 1.8-23*. https://doi.org/10.1186/1471-2105-11-11.Bioconductor

WU, W., YANG, P., TANG, H., ZHOU, Q., CHEN, Z., & Shibasaki, R. (2010). Characterizing Spatial
Patterns of Phenology in Cropland of China Based on Remotely Sensed Data. *Agricultural Sciences in
China*, *9*(1), 101–112. https://doi.org/https://doi.org/10.1016/S1671-2927(09)60073-0

Wulder, M. A., White, J. C., Hay, G. J., & Castilla, G. (2008). Towards automated segmentation of forest

inventory polygons on high spatial resolution satellite imagery. *The Forestry Chronicle*, *84*(2), 221–230. https://doi.org/10.5558/tfc84221-2

Xie, Y., Sha, Z., & Yu, M. (2008). Remote sensing imagery in vegetation mapping: a review. *Journal of Plant Ecology*, *1*(1), 9–23. https://doi.org/10.1093/jpe/rtm005

Xiong, J., Thenkabail, P. S., Gumma, M. K., Teluguntla, P., Poehnelt, J., Congalton, R. G., … Thau, D. (2017). Automated cropland mapping of continental Africa using Google Earth Engine cloud computing. *ISPRS Journal of Photogrammetry and Remote Sensing*, *126*, 225–244. https://doi.org/https://doi.org/10.1016/j.isprsjprs.2017.01.019

Xiong, J., Thenkabail, P., Tilton, J., Gumma, M., Teluguntla, P., Oliphant, A., … Gorelick, N. (2017). Nominal 30-m Cropland Extent Map of Continental Africa by Integrating Pixel-Based and Object-Based Algorithms Using Sentinel-2 and Landsat-8 Data on Google Earth Engine. *Remote Sensing*, *9*(10), 1065. https://doi.org/10.3390/rs9101065

Yang, J., Yang, R., Li, S., Yin, S.-J., & Qin, Q. (2008). *A Novel Edge-Detection Based Segmentation Algorithm for Polarimetric SAR Images* (Vol. 37). https://doi.org/10.1007/978-3-540-78630-6_12

Yeom, J.-M. (2014). Effect of red-edge and texture features for object-based paddy rice crop classification using RapidEye multi-spectral satellite image data AU - Kim, Hyun-Ok. *International Journal of Remote Sensing*, *35*(19), 7046–7068. https://doi.org/10.1080/01431161.2014.965285

Yin, H., Udelhoven, T., Fensholt, R., Pflugmacher, D., & Hostert, P. (2012). How normalized difference vegetation index (NDVI) trends from advanced very high resolution radiometer (AVHRR) and système probatoire d'observation de la terre vegetation (SPOT VGT) time series differ in agricultural areas: An inner mongolian case study. *Remote Sensing*, *4*(11), 3364–3389. https://doi.org/10.5829/idosi.mejsr.2012.12.3.64113

Zhang, J., & Foody, G. M. (1998). A fuzzy classification of sub-urban land cover from remotely sensed imagery. *International Journal of Remote Sensing*, *19*(14), 2721–2738. https://doi.org/10.1080/014311698214479

Zhang, X., Zhang, M., Zheng, Y., & Wu, B. (2016). Crop mapping using PROBA-V time series data at the Yucheng and hongxing farm in China. *Remote Sensing*, *8*(11), 1–18. https://doi.org/10.3390/rs8110915

Zhong, L., Gong, P., & Biging, G. S. (2014). Efficient corn and soybean mapping with temporal extendability: A multi-year experiment using Landsat imagery. *Remote Sensing of Environment*, *140*, 1–13. https://doi.org/https://doi.org/10.1016/j.rse.2013.08.023